SUPERCONDUCTIVITY IN

Mn - DOPED Ca-Y-Ba-Cu-OXIDE CERAMICS

A dissertation submitted to the
Quaid-i-Azam University
in the partial fulfilment to the
requirement for the degree of

MASTER OF PHILOSOPHY

IN

PHYSICAL CHEMISTRY

BY

KHIZAR HAYAT

DEPARTMENT OF CHEMISTRY
QUAID-I-AZAM UNIVERSITY
ISLAMABAD

1991

DEDICATION

WITH HUMILITY AND TRUE SINCERITY I DEDICATE

THIS MEAGRE SCIENTIFIC INVESTIGATION

TO MY

AFFECTIONATE PARENTS WHOSE CONSTANT PRAYS, LOVE,

ENCOURAGEMENT AND ASSISTANCE INVARIABLY BUOYED ME UP

AND COVER NOT TRUTH WITH

FALSEHOOD NOR HIDE THE

TRUTH WHEN YOU KNOW

(QURAN)

CERTIFICATE

This dissertation submitted by KHIZAR HAYAT is accepted in its present form by the Department of Chemistry as satisfying the thesis requirements for the Degree of MASTER OF PHILOSOPHY in Physical Chemistry.

Supervisor:

Dr. A. Y. Khan
Associate Professor
Department of Chemistry
Quaid-i-Azam University
Islamabad

Chairperson:

Professor
Department of Chemistry
Quaid-i-Azam University
Islamabad

External Examiner:

"ACKNOWLEDGEMENT"

All glories be to Allah, the omniscient, the omnipresent and the omnipotent and His Benediction be upon His Prophet, The Saviour of mankind from the darkness of ignorance and a Symbol to be and to do right.

I wish to express my sincere gratitude, heartiest obligation and appreciation to my worthy supervisor, Dr. A.Y. Khan, Associate Professor, Department of Chemistry, Quaid-i-Azam University, Islamabad, for his guidance valuable suggestions, sincere and sympathetic attitude, especially for his politness throughout the study. His kind attitude has an unforgettable impression on my mind and memory.

I express sincere thanks to Dr. Mahboob Mohammad, Professor and Dr. S. Subhani, Assistant Professor, Department of Chemistry, for giving valuable suggestions.

Thanks are also extended to Dr.(Mrs.) Mashooda Hasan, Professor and Chairperson, Department of Chemistry, Quaid-i-Azam University, Islamabad, for providing laboratory facilities.

I avail this opportunity to pay my compliments in respect of all teachers of the Chemistry Department for being a source of inspiration and enlightment for me throughout my stay here.

I am also grateful to Dr. Jamil and Dr. C.A. Majid, Principal Scientific Officer, PINSTECH, Nilore, Islamabad for resistivity and X-ray diffraction measurements.

I express my gratitudes to my group fellows and friends, especially Mohammad Asghar, Abaid-ur-Rehman, Abdul Razzaq, Arshad Ali, Janbaz Khan, Yousaf Nazir and Javed Asghar Janjua for their moral help and co-operation at the times of need.

I am thankful to Maqsood Ahmed for his help in indexing X-ray diffractograms.

I am also thankful to Mr. Liaquat Ali, Computer Centre, Quaid-i-Azam University, Islamabad, for data entry of entire manuscript very carefully.

Last but not least heartfelt thanks to my parents, brothers and sister, without their cooperation and prayers this work would have never been materialized.

KHIZAR HAYAT

C O N T E N T S

LIST OF FIGURES

A B S T R A C T

The Mn-doped $Y_{0.3}Ba_{0.5-x}Mn_xCa_{0.2}CuO_{3-z}$ superconducting ceramics for $0 < x \leq 0.15$ were prepared under different heat treatments and sintering conditions. Electrical resistance and X-ray diffraction measurements from ambient temperature to 77K show that samples are either nonsuperconducting (for $x > 0.07$) or multiphase systems. The high temperature superconducting phase shows Tc^{onset} $85^{o}K$. The resistance does not approach to zero value up to $77^{o}K$. Results indicate that likely occupancy sites for Mn are Ba and/or Ca-sites rather than Cu(1) or Cu(2) sites. Somewhat gross "structural modifications" in the neighbourhood of Mn-sites is responsible for depression of Tc and the appearance of low Tc phase (below 77K). The effect of increased Mn content is adverse on the superconducting properties of the samples. ESR studies of Mn-doped samples in dil. HCl are also reported.

INTRODUCTION

CHAPTER - 1

INTRODUCTION

The transition temperature of a superconductor, defined as the temperature at which superconductor loses resistance, is affected by the presence of impurities.[1] There is a large body of literature dealing with the effect of magnetic and non-magnetic impurities of the properties of superconductors.[2-10] Small concentrations of non-magnetic impurities remove the crystalline anisotropy of the energy gap and thereby reduce the transition temperature.[11-13] For larger impurity concentrations, numerous other effects such as shifts of valence electron concentration, electron and phonon band structure, electron-phonon interaction become important.[14]

Magnetic impurities[15,16] generally have a tendency to lower the transition temperature because the exchange interaction between valence electrons and spinning impurity atoms leads to non-conservation of the electron spin, which may affect the formation of Cooper pairs. There are examples,[3] however, where no localized moment occurs and Tc is increased. In addition, magnetic impurities can lead to gapless superconductivity within a limited range of

concentration[17,18]. This important effect was predicted by Abrikosov and Gor'kov[19] and observed by Reif and Wolf[20].

Interest in the study of superconducting materials has increased largely after the discovery of high T_c superconductor La - Ba - Cu - O by Bednorz and Muller[21] because these materials have a variety of technological applications such as computer switching elements, bolometers and superconducting electromagnets[22]. The effect of chemical doping (Ag, Li, Pt, Zn, Al, Cr, Mn, Fe, Co and Ni)[23-25] at cu sites, on physical properties of high T_c superconductors, has been investigated.

It has been found that all rare earth can be substituted for yttrium in Y-Ba-Cu-O[26] without much change in T_c. The substitution at cu site by transition metals (Mn, Fe, Ni,)[27,28] in a small amount ($\leq$ 20%) decreases T_c drastically. Substitution of strontium[29] and calcium[30] on the Ba sites in Y-Ba-Cu-O have also been investigated Strontium doped compositions show depression of T_c which has attributed to structural changes[29]. Though Ba, Sr and Ca have identical valence states, Ca has less effect on T_c reduction[30]. No attempt has been made to study the effect of transition metal atoms (Ti, V, Cr, Fe, Mn and Zn) substitution, on structure and superconducting properties,

at Ba sites in Y-Ba-Ca-Cu-O. In the present work, the effect of Mn (an antiferromagnetic element) substitution on Ba sites in Y-Ba-Ca-Cu-O has been studied.

It is more interesting to study the effect of Mn substitution at Ba sites,on structure and superconducting properties of Y-Ba-Ca-Cu-O. It may be helpful in explaining the mechanism of superconductivity and the effect of Mn substitution on some other physical properties such as transition temperature, structure and magnetic susceptibility.

All superconducting materials are extensively studied in order to know the mechanism of superconductivity. Various theories are formulated to explain this novel phenomena. One of the theory is due to Bardeen, Cooper and Schrieffer[1] which states that at low temperature in certain metals and alloys, interactions among electrons and phonons can result in paired electrons, called Cooper pairs. The formation of paired electrons in singlet state is responsible for the superconductivity. Anything that destroys the Cooper pairs will destroy the superconductivity.

Several experimental studies have been made to

investigate the mechanism of superconductivity and these include ESR studies in $YBa_2Cu_3O_{7-\delta}$[31-35] as well as raman studies in $YBa_2Cu_3O_{7-\delta}$[36]. In order to elucidate the influence of the magnetic moment at Cu sites, Cu ions were substituted with other ions such as Fe, Co, Cr, Ni and Mn[37,38].

In the present work an attempt is made to substitute Mn at Ba sites in Y-Ba-Ca-Cu-Oxide superconductor with a view to study its effect on superconducting characteristics. Moreover, Mn is also used as a microscopic probe to investigate the effect of Mn substitution by measuring ESR spectra. It is known that $YBa_2Cu_3O_{7-x}$ or the calcium substituted ceramic oxide show no ESR spectra in solid state. ESR spectra of Mn-doped Y-Ba-Ca-Cu-O have been studied in dilute HCl (6M) solution.

HISTORICAL REVIEW

CHAPTER - 2

2.1 HISTORICAL REVIEW

Superconductivity was discovered in 1911 by Kamerlingh Onnes[22]. He found that mercury lost its resistance below $4.15^{o}K$ within a fraction of a degree temperature change and the resistance became effectively zero. Onnes declared," No doubt is left of a new state of mercury in which its resistance has practically vanished". Mercury has passed into a new state which is called the superconducting state.

After the discovery of Onnes, most of the properties of superconducting state were established and a number of other superconducting materials discovered. Among these superconductors subsequently discovered are lead, Tin and Aluminium. In 1935, the number of known superconductors was about eighty. In 1933, Meisner[1] discovered the flux expulsion, called the Meisner effect. In 1950, the number of superconductors was slightly over one hundred.[22]

In 1957, J. Bardeen, L.N. Cooper and J. Schrieffer[1] presented the general quantum theory of superconductivity, called BCS theory. The BCS theory states

that the electrons are paired due to the interactions between electrons and phonons at low temperature, so that the momentum of each pair is zero. If impurities are added, the electrons are still paired but the total momentum of each pair is not zero. The same year during the studies of magnetic properties, type II superconductors were discovered.

In 1964, superconductivity in certain semiconductors was predicted by M.L. Cohen[39]. Upto 1976, the highest critical temperature was $\sim 23^{o}K$ (of Nb_3Ge compound)[40]. The temperatue at which there is a phase transition from a state of normal electrical resistivity to zero is called the critical temperature of superconductor (Tc).

Over the years, though several attempts were made but not much success was achieved in raising the Tc. However, some useful rules[22] were deducted by researchers working on supercnductivity. Some of these are the following:-

1. Only metals are superconductors.
2. No ferromagnetic or antiferromagnetic materials are superconductors.
3. In metallic elements, superconductivity is only

found when the number of valence electrons per atom lies between two and eight.

4. In transition metal elements, the critical temperature varies in a periodic manner with the number of valence electrons per atom and exhibit sharp maxima. In non-transition elements, the critical temperature increases as the number of valence electrons per atom increases.

2.2 IMPURITIES IN SUPERCONDUCTORS

It was observed that addition of impurities in already known metallic superconductors caused striking changes in their superconducting properties. Addition of impurities[41] led to enhanced and drastic changes such as lack of precision in superconductive transition (broadening of line width), disorder in structure, change in mean free path (smaller mean free path), and change in scattering life time τ. Thus a collision time of $\tau = 10^{-14}$sec. implies an uncertainity in energy of the order of $h\tau^{-1}$ that is about 0.1eV which is well above the usual energy gap of a few meV. Thus one should expect an increase in the energy gap on adding impurities, whereas experimentally little change is observed, provided the impurities are non-magnetic. The impurity concentration in the pure substance also depressed

the critical temperature Tc. For instance in $La_{1-x}Gd_x$ system 0.8% Gd concentration reduces Tc from 6^oK to 1^oK[42].

Clean and dirty superconductors can be distinguished on the basis of Ginzberg-Landau[1] constant K, $K = \xi/l$. In clean superconductors, the electron mean free path is much larger than the coherence length "ξ" and in dirty superconductors, the $l << \xi$. Clean superconductors, often referred to as pure superconductors, are metals and other pure substances and dirty superconductors are alloys and metals containing impurities.

We can classify impurities in the superconductors into two main groups non-magnetic impurities and magnetic impurities:

2.3. EFFECT OF NON-MAGNETIC IMPURITIES

The addition of non-magnetic impurities[22] has various quantitative effects on their properties in the superconductive state. Low concentraion of non-magnetic impurities, of the order of 0.5%, decreases the critical temperature of the superconducting material irrespective of the nature of impurity. For higher concentration, the critical temperature begins to increase if the valence of

the impurity atoms is larger than that of the atoms of the host metal and decreases if the valence of the impurity atom is less than that of the host atom (as shown in Fig. 2.1)[22].

Lynton, Serin and Zucker[43] found that initial reduction in Tc seemed to be a universal function of the residual resistance of the specimen. However as the concentration is increased, other effects rapidly became dominant. The critical concentration above which this behaviour occured was extremely small (< 0.1%).

In second order perturbation theory[43] the free energies of both the normal and the superconducting state are depressed. The decrease of energy is slightly greater for the normal than for the superconducting state. Consequently, the transition from the superconducting to the normal state will occur at a lower temperature than in the absence of impurity. In second order perturbation, the scattering of electrons from one plane wave state to another (with or without possible spin reversal according to whether the interaction is spin dependent or not) contributes to the lowering of free energy. For electrons whose initial and final energies are remote from the Fermi energy, the reduction in free energy is about the same in the normal and superconducting states. When both initial and final states

are within a neighbourhood ε_o (the energy gap) of the Fermi surface, the reduction of the free energy is greater for the normal state. Because in the normal condition, the energy denominator can go to zero, it cannot become smaller than $2\varepsilon_o$ in the superconducting state.

Let $\xi = N_I/N$ be the impurity concentration. In order to relate the value of ξ required to reduce the transition temperature from Tc to T_c^*, one may calculate the free energies $F_n(T_c^*) - \xi\,\delta F_n(T_c^*)$ of the normal and $F_s(T_c^*) - \xi\,\delta F_s(T_c^*)$ of the superconducting state, and equate the two, giving

$$\xi = \frac{F_n(T_c^*) - F_s(T_c^*)}{\delta F_n(T_c^*) - \delta F_s(T_c^*)}$$

This formula fails to predict the linear behaviour for the initial decline of Tc versus ξ in the case of no-magnetic scattering. It predicts $\frac{dT}{d\xi} \to 0$ as $\xi \to 0$.

The reason for this difficulty[43] is that when the impure superconductors behave in the same way as a pure superconductor then its energy gap must go to zero at T_c^*. There are two ways to solve this problem.

i) To determine the effect of impurities on

electron-phonon interaction which leads to modification in the effective electron-electron interaction.

ii) To calculate the change in temperature "from a safe distance" assuming the impure substance to obey the law of corresponding states. This law gives universal proportionality between the energy gap at absolute zero and the transition temperature.

The final equation is

$$\frac{d\varepsilon_0}{d\xi} = \frac{\delta F_n(\xi, 0) - \delta F_s(\xi, 0)}{N_{(0)}\,\varepsilon_0(\xi, 0)}.$$

δF_n is not dependent on concentration, while δF_s depends on it only through ε_o. $N_{(0)}$ is the number of states per unit energy range near the Fermi surface, and $\varepsilon_0(\xi,0)$, the energy gap at concentration ξ and temperature zero.

For non-magnetic scattering, Tc versus ξ is initially linear but T_c^* approaches zero with steadily diminishing slope.

2.4. EFFECT OF MAGNETIC IMPURITIES (ABRIKOSOV AND GOR'KOV THEORY)[44,41]

Addition of magnetic impurities causes striking changes in the properties of a superconductor, for instance,

a rapid decrease of the transition temperature with increasing impurity concentration. This problem was studied theoretically by Abrikosov and Gorkov[44] on the basis of s-d exchange model. In this model the interaction between the conduction electron and the magnetic impurity atom is described by the Hamiltonian.

$$H = V - JS.\sigma$$

Where V is the ordinary impurity potential, J is the s-d (s-f in case of rare earth impurities) exchange integral, S is the impurity spin and σ is the conduction electron spin. The second term of this Hamiltonian gives the s-d exchange scattering of electrons by localized spins.

Abrikosov and Gorkov[44] made the following assumptions and approximations while developing their theory.

1. The order parameter is assumed to be spatially constant. This required that the spin impurities be randomly distributed on the host lattice.
2. The impurity spins are assumed to be unpolarized and uncorrelated. This implies the absence of magnetic ordering effects and spin fluctuations which involve more than impurity spins.
3. The effect of impurities on the Green's function is treated only in the first Born approximation.

The essential feature of the effect of the s-d exchange scattering upon the superconductors according to AG theory, is as follows:

The zero field superconducting normal transition is second order and the zero field coexistance curve which separates the superconducting and normal phases is given by the simple relation

$$\ln\left(\frac{Tc}{Tc_o}\right) + \psi\,(1/2 + \rho) - \psi\,(1/2) = 0$$

Where $\rho = \dfrac{1}{2\pi\ Tc\ \tau_{ex}}$ and

$$(\tau_{ex})^{-1} = n\pi\ N_{(o)}\ J_{ex}^2\ S(S+1).$$

$$\psi_{(z)} = \Gamma'_{(z)} / \Gamma_{(z)}$$

$\Gamma_{(z)}$ is simply gamma function, Tc and Tc_o are the transition temperatures in the presence and absence of magnetic impurities respectively. τ_{ex} is the scattering time associated with the exchange scattering (of strength J_{ex})from the magnatic impurities. $N_{(O)}$ The density of states at the fermi energy for both spins and S the total spin of the impurity atom. If the spin-impurity has non-zero orbital momentum and complete spin orbit coupling, the factor S(S+1) must be replaced by $(J.S)^2 / J(J+1)$, since the conduction electrons see only the time averaged projection of S on J (J is the total angular momentum).

The s-d exchange scattering[41], also, makes the life time of the Cooper pairs finite in contrast to ordinary potential scattering where the life time remains infinite. Due to this depairing effect, Tc decreases. The finite life time of the pairs causes an energy spread potential to the inverse life time and this broadens the BCS density of states curve. As a result the superconductor becomes gapless at high impurity concentration.

In addition to this, Abrikosov-Gorkov[44] predicted a linear temperature dependence of the electronic specific heat. The AG theory has been successful in explaining the epxeriments on the electron tunneling the critical field and the specific heat.

2.4.1 ELECTRON TUNNELING

The first really convincing verification of the AG theory was provided by the electron tunneling experiments of Woolf and Reif[20]. The experiments were carried out in a He calorimeter with thin film samples which were evaporated onto cryogenic substrates. Various samples were studied (e.g $Pb_{1-x}Gd_x$, $In_{1-x}Fe_x$, $Pb_{1-x}Mn_x$)[20] all of which exhibited at least qualitative agreement between theory and the experiments. The best agreement was obtained with the

$Pb_{1-x}Gd_x$ system.

2.4.2 SPECIFIC HEAT STUDIES

Philips and Mathias[45] attempted to determine whether superconductivity extended throughout a sample in presence and absence of magnetic order by measuring the specific heat in the presence and absence of a magnetic field large enough to quench the superconductivity. The entropy differences between the normal and superconducting states determined in this way were of the right order of magnitude for the $La_{1-x}Gd_x$ system. However, because of lack of knowledge about the nature of ordered magnetism in the $La_{1-x}Gd_x$[45], they could not verify that the change in entropy upon the application of magnetic field could be attributed solely to the superconducting and normal states. The application of a magnetic field produces a decrease in entropy in paramagnetic system, an increase in entropy in antiferromagnetic system, and essentially no change in entropy in a ferromagnetic system with long range order.

2.4.3 CRITICAL TEMPERATURE

Crow and Parks[42] undertook a study of the intermetallic $InLa_{3-x}Gd_x$ system. This system was chosen

because of its high critical temperature, and expectation that the system would exhibit homogenous, monophase, solid solutions at least for small Gd concentrations, thereby allowing one to avoid the two-crystal phase problems inherent in the $La_{1-x}Gd_x$ studies.

As with the La_{1-x} Gd_x system an anomalous departure from the AG curve is oobserved for higher Gd concentrations. However, the results are qualitatively different from those of the In La_{3-x} Gd_x system which are shown in Fig. 2.2.

2.4.4. DEFECTS OF ABRIKOSOV AND GROKOV THEORY:

The defects of AG theory seem to be due to the terms which are not considered in the theory. They are:

i) The spatial variation of the order parameter in the vicinity of impurity atom.
Abrikosov and Gorkov considered the order parameter to be constant, while in actual superconductors the order parameter is expected to be zero in the vicinity of impurity atom due to the strong depairing effect of the exchange interaction. Tsuzuki and Tsuneto[57] calculated the

order parameter as a function of the distance from impurity atom and found that the order parameter increases with increasing distance with oscillation. According to their analysis, the effect raises slightly the critical temperature given by AG theory. This correction amounts to 1% at the most. Similar small deviation from AG theory is expected for other bulk properties of a superconductor.

ii) Effect of the anomalous exchange scattering i.e. the Kondo effect[41].

In the AG theory the effect of the exchange interaction was treated only in the first Born approximation. This fact raised several questions concerning the influence of higher terms. Such terms are, in fact, responsible for the anomalous behaviour of the normal metal as was pointed out at first by Kondo.[41] He calculated the scattering matrix of the s-d exchange interaction upto the second Born approximation and found that a temperature dependent term like log T appears in the resistivity as a consequence of the sharpness of the Fermi surface.

iii) Effect of interaction betwen the impurity spins and of magnetic ordering[41] was neglected by AG

theory. But, in fact, the impurity S is a quantum mechamical operator and has 25+1 possible orientations relative to some axis of quantization. Thus it is quite different from the impurity potential, which is essentially an external field. This means AG treated the components of S as commuting operators, whereas, in truth, they obey angular momentum commutation relations i.e.

$$\left[\hat{S}_x , \hat{S}_y = i \hat{S}_z \right]$$

Thus in general, the effect of magnetic impurities, was considered to be detrimental to superconductivity and this situation has persisted till the discovery of new high Tc superconductors. Due to the absence of an understanding of the pair formation mechanisms, it remains to be seen whether the AG theory remains applicable for these systems, or has to be replaced by some other formulation.

2.5. HIGH T_C SUPERCONDUCTORS AND EFFECT OF DOPING

Superconductivity above 30K was first reported in the mixed phase La-Ba-Cu-O compound system.[21] With the steady improvements in sample conditions and application of

pressure, the superconducting transition temperature Tc raised to above 40K at ambient pressure and 57K under pressure[21].

By substituting Y at La sites, Tc is increased. The Y-Ba-Cu-O system became a target of material scientists and many laboratories rushed into this fascinating field. Later the two phases in the Y-Ba-Cu-O compound were separated and identified orthorhombic ($Y Ba_2Cu_3O_{7-\delta}$) with $0 < \delta \leq 0.5$ and tetragonal ($Y Ba_2Cu_3O_{7-y}$) with $0.5 \leq y < 1$. The two structures have very similar lattice parameters but differ in oxygen stoichiometry and ordering of oxygen atoms. The orthorhombic phase shows a Tc of about 91K. While the tetragonal is non-superconducting down to 4.2 K[47].

2.5.1 ROLE OF SUBSTITUTION ON "Y" SITES:

To determine the role of "Y" in the high Tc superconductivity, Hor, Meng and their workers[48] synthesized and examined the $ABa_2 Cu_3 O_{6+x}$ compound systems with A = La, Nd, Sm, Eu, Gd, Ho, Er, Lu in addition to Y. They found superconductivity in the 90K range in the system. Their results suggested that the unique square planar Cu atoms, each surrounded by four or six oxygen atoms, are crucial to the superconductivity of oxides in general. In

particular, they attributed the high superconducting transition temperature of $ABa_2Cu_3O_{6+x}$ mainly to the quasi-two-dimensional assembly of CuO_2-Ba-CuO_{2+x}-Ba-CuO_2 layers sandwiched between two "A" layers. They lay emphasis on the CuO_{2+x} layers because the doping on "A" defined above sites does not affect the high T_c superconductivity of 1:2:3 compounds as the substitutions do not enter into CuO_2 planes.

In 1989, Gasnier et al[49] crystrallized $Pb_2Sr_2Y_{1-x}Ca_xCu_3O_{8+\delta}$ (x = 0.5, 0.25)in an orthorhombic structure. Resistivity measurements show a two step transition with distinct onset at 86K and 4K with zero resistivity at 15K. The resistivity increases as T decreases shows a maximum at around 86K, and decreases slowly showing another maximum at 45K. This is followed by a further decrease and the zero resistivity is reached only at 15K.

In 1990, Kanai et al[50] have prepared $Bi_2Sr_2(Ca_{1-x}Y_x)Cu_2O_8$ based superlattices by stacking two different unit cell layers containing different yttrium concentrations. One unit layer contains lower "Y" concentration (x = 0.15) to be a superconductor and the other contains higher concentration (x = 0.5) was found to be a semiconductor, and these layers are periodically

stacked with appropriate ratios. This variation is due to the decrease of carrier concentration in Bismuth Strontium Calcium Copper Oxide unit layer with the increase of trivalent y^{3+} ion at the divalent Ca^{2+} sites.

Morris and his coworkers[51] substituted calcium in the Y-Ba-Cu-O system at elevated oxygen pressure $P(O_2)$ which resulted in superconducting compounds with novel and enhanced properties tetragonal $Ca_xY_{1-x}Ba_2Cu_3O_y$ with Tc = 86K for x = 0.2 prepared at $P(O_2)$ = 16 bars, and $Ca_xY_{1-x}Ba_2Cu_4O_y$ (1:2:4) with Tc = 89K for x = 0.1 prepared at 50-200 bars. Calcium substitution shifts the phase stability boundary between 1:2:3, 2:4:7, and 1:2:4 phases to higher $P(O_2)$, and stabilizes a tetragonal 1:2:3 structure at moderately elevated pressure $P(O_2)$ with substantial decrease in Tc. The T_c of 1:2:4 increases with Ca substitution upto x = 0.1 and then decreases gradually for larger x, possibly because of excessive hole concentration.

Akira ONO and Uchida[52] identified and prepared a single phase system ($Sr_2Y_{0.7}Ca_{0.3}Cu_{2.35}Pb_{0.65}O_y$). The Tc was 17K for the sample quenched from 86°C to 77°K. According to a previous report, a multiphase sample of the nominal composition $Sr_2Y_{0.5}Ca_{0.5}Cu_2PbO_y$ exhibited zero electrical resistivity at 16K, while $Sr_2Y_{0.85}Ca_{0.15}Cu_{2.31}Pb_{0.69}O_{6.8}$

and $(Pb_{0.71}, Cu_{0.29})\ Sr_2(Y_{0.3}, Ca_{0.27})Cu_2O_7$ are non superconductors. The absence of superconductivity might be due to the lower Y/Ca ratios of these samples as compared with the above sample.

2.5.2 SUBSTITUTION IN THE $Cu-O_2$ PLANES OF 1:2:3 SUPERCONDUCTING COMPOUNDS:

In 1987, Felner and Nowik[53] reported the studies on the effect of substitution at the oxygen sites by sulphur and in copper site by Iron. In both cases the superconductivity features were strongly affected; by iron for the worse, by sulphur for the better. Substitution of Cu by trivalent ions sharply decreased Tc monotonically with iron concentration. On the other hand, the substitution of oxygen by sulphur ($YBa_2Cu_3O_6S$) did not change Tc, but the phase transition was much sharper and Meisner effect was complete. Both their samples had the single-phase orthorhombic structure.

Mehbod and Wyder[54] studied the influence of Fe impurities in the high temperature superconductors of the type $Y_{1.2}Ba_{0.8}CuO_{4-\delta}$ and $YBa_2Cu_3O_{7-\delta}$ on the critical temperature as measured by the resistance measurements using four-probe method. They observed that for

low concentration (upto 10% Fe), two important phases were present. The semiconducting phase Y_2BaCuO_5 and superconducting phase $YBa_2Cu_3O_{7-\delta}$. The critical temperature Tc decreases linearly with the concentration of Fe (upto 10%). Above certain concentration of Fe_2O_3 (12%), the superconductivity in $YBa_2Cu_3O_{7-\delta}$ is completely destroyed.

The effect of substitution for Cu by aluminium nickel and zinc in Y-Ba-Cu-O was studied by Ruth Jones and coworkers[23]. They found that all three metals lower the Tc value and make the transition width broader. However, the strength of the effect varies with the metal, and this is attributed to their different reactivities and site preferences. The most dramatic effect is with zinc. Which completely quenches the superconductivity when as small as 10% of the Cu sites are replaced. It is postulated[23] that under these synthetic conditions zinc prefers the five coordinated "Cu(2)" site, which is presumed to be in the main superconducting pathway. Nickel has a stronger affinity for the four coordinated "Cu(1)" site, Aluminium prefers the four coordinated "Cu (1)" site for initial substitution. It was suggested that substitution of Cu(1) sites eliminates their contribution to the superconductivity.

Yang et al[55] determined several important parameters of $YBa_2(Cu_{1-x}Mx)O_{7-\delta}$ (M = Fe , Co, Ni, Zn) i.e. the location of dopants, the valence of dopants, structural changes, modifications of electronic densities of states and the distribution of holes. They found that Fe and Co preferentially substitute for the Cu(1) atom at the linear chain site, while Ni resides in both Cu(1) and Cu(2) sites Zn occupies only the plane position Cu(2). In all cases, the metal oxygen bond lengths (Fe-O, Co - O, Ni-O and Zn-O) and valence states of dopants (mainly Fe^{3+},Co^{3+},Ni^{2+} and Zn^{2+})[55] show little dependence on dopant concentration. However, each dopant affects to a different degree the oxygen 2P states. The changes of the oxygen 2P states for Fe, Co, and Ni doped samples may be related to reduction of some oxygen hole states. This reduction is attributed to a redistribution of charge carriers in the chain layer and possibly an inhibition of charge transfer from the chain to the planes. However, Zn substitution show no observable change in its valence and oxygen hole states, but the presence of Zn in the structure leads to breakdown of hole pairs[56]. The pair breaking can occur due to weakened coulomb interaction or magnetic interactions on Cu(2) plane site by substitution of Zn on Cu(2) site. The lack of hybridization between Zn(3d) and O(2P) orbitals certainly affects the conduction band and thus the effective hole concentration

may increase by doping of Zn. Although the hole conentration increases in the Zn-doping, other killing factors are sufficient to suppress superconductivity.

It has been previously obsered that the superconductivity of $YBa_2Cu_3O_{7-\delta}$ is not significantly affected by the magnetic character of the rare earth elements when they are substituted at "Y" sites . On the other hand, because the superconductivity is associated with the conduction in the $Cu-O_4$ planes coupled by chains of $Cu-O_4$ squares. It is thus dependent both on oxygen contents and the substitution of Cu by other elements.

Gama and his coworkers[56] studied the effect of Mn substitution for Cu in $YBa_2Cu_3O_{7-x}$. They observed that the onset in resistive transition is little affected by Mn concentration. An analysis of the magnitude of the diamagnetic signal shows that the relative superconducting fraction decreases linearly with the Mn content. X-ray diffraction analysis[56] shows that the orthorhombic structure is preserved for all samples, in spite of the occurence of additional phases, whose amounts increase with the Mn content.

2.5.3 SUBSTITUTION ON "B_a" SITES

In 1987, Veal, and coworkers [29] doped $YBa_2Cu_3O_{7-\delta}$ with Sr and synthesized $YBa_{2-x}Sr_xCu_3O_{7-\delta}$ for $0 < x < 2$. They found a systematic depression of Tc and contraction of unit cell volume with increasing x. They also observed that the resistivity above Tc generally increased with increasing Sr contents. They discussed two possibilities for explaining the decrease in Tc: a change in the phonon or electronic structure due to the direct substitution of Ba with Sr or change in the environment of the Sr site due to local strains or oxygen vacancies.

They have negated the first idea arguing that the Ba and Sr ions are both doubly ionised with comparable electronegativities and therefore present the same coulomb field to the crystal potential and contribute the same number of electrons to the conduction bands. They have stressed that the depression of Tc by Sr substitution must be indirectly caused by a local perturbation of the structure in the neighbourhood of the Sr sites. They argued that the perturbation could involve a slight collapse of the surrounding Cu-O planes or the introduction of additional oxygen vacancies.

Suzuki and workers[57] have reported the influence of composition of 36 metallic elements on the Tc of the superconductor ($Y Ba_{2-x}M_x Cu_3O_y$). Furthermore, some combinations of two species were tried as heterovalent ion dopant. They found that for $x \leq 0.4$, the samples containing (M - Mg, Co, Te, V, Cr, Mn, Fe, Co, Ni, Zn, Ga, Ce, Zr, Nb, Mo, B, Al, Si, P, Sb, Bi, La, Ta, W)[57] exhibited residual resistance above 80K and were not superconductors. The specimens (M = Sr, Sn, Pb) showed a higher Tc, than 87K, but their resistance no longer fell to zero at x = 0.6. Similarly M = In specimen with $x \leq 0.6$ showed a T_c greater than 86K. The remaining M = Yb was a superconductor above about 80K at x = 0.8. Generally, the ratio of the superconducting orthorhombic phase decreases as the amount of dopant increased.

The effect of heterovalent ion-doping of K-In and K-La is that $YBa_{2-x}K_{0.5x}Cu_3O_y$[57] exhibited superconductivity at temperature higher than 82K upto the composition of 1.0. The most interesting behaviour was observed in $YBa_{2-x}K_{0.5x}La_{0.5x}Cu_3O_y$. For the sample (x=0.4), the first trial showing negative electrical resistance below 160 and 210K, may be arising from a temperature gradient induced at the surface. For the second time with different sintering time, a little residual resistance always persists, there is

a steep drop in resistance around 200K. This drop was found to be unstable.

T. Bjornholm et al[58] studied the effect of Ca substitution on "Y" sites and La for Ba^{2+}. These studies suggest that two phases coexist in (Ca, Ba, La) $CuO_{7-\delta}$, a superconducting phase in which La^{3+} ions occupy Y^{3+} sites, and a second non superconducting phase where Ca^{2+} ions occupy Y sites.

The effect of Ca substitution at Ba sites was studied by Mahboob et al [30]. The observed Tc of the calcium doped sample is slightly lower than the parent compound ($Y-Ba_2Cu_3O_{7-\delta}$). The lower Tc in strontium-doped sample is explained in terms of structural changes caused by local distortions of the lattice in the vicinity of strontium sites and the additional oxygen vacancies. It is likely that similar "local distortions" are operating in the case of Ca substitution which leads to depression of Tc.

2.6. APPLICATIONS OF SUPERCONDUCTORS[59,22]

The discovery of superconductivity opened the prospect of practical application of superconductors. But due to low current densities and low Tc's, the commercial as

well as the military and industrial applications were slow. The discovery of high Tc superconductors with Tc > 77K by Wu et al set off a flurry of research activities on these ceramic superconductors. Some applications by employing conventional low Tc superconductors are described below:-

By using superconductors, almost 100% transmission efficiency could be achieved.

These are used to shield space vehicles against radiations, in accelerators and in fusion reactions etc.

The levitation property of the superconductor could be used in designing the magnetically levitating trans.

Cryotron is a switch based on superconductivity. Simplest form consists of a coil of wire of one superconducting material would round a length of another superconductor, all immersed in a bath of liquid helium. A control current passed through the coil produces a magnetic field strong enough to destroy the superconductivity of the central wire but not of the coil. Thus the current in the coil controls the resistance of the wire, switching it from zero to a finite value.

The ability of specimens with holes through them to carry a persistent current with its accompanying magnetic field can be used to produce intense magnetic fields by compressig together the flux lines of the field. Consider the arrangement as shown in Fig.12.

The cylinder with the "figure of eight" hole through it is brought into the superconductive state in the presence of an applied field which is then removed. This produces a persistent current flowing round the hole and this current is accompanied by its magnetic field. The flux of this field is now intensified in the following way. A solid superconductive cylinder, which fits tightly, is now inserted into the larger hole of "figure of eight". Since this solid cylinder is in the superconductive state, the flux lines which were in this hole cannot penetrate the solid cylinder due to Meisner effect. They are forced into the smaller hole to join the flux lines there. So the flux lines in the smaller hole are ;now much closer and denser and flux density greater (by a factor $\frac{R_1^2 + R_2^2}{R_2^2}$).Fields of strength 5×10^5 A/m have been produced by this apparatus.

Superconductive heat valves are widely used devices to control the flow of heat. The basic superconductive heat valve is simply a long, thick, cylindrical wire of typeI material connnecting the two systems, A and B, between which the heat has to be controlled (Fig. 2.2)

If the wire is made of lead and kept at tempertures press than 1K, then its thermal conductivity in the superconductive state is very small and about 200 times less than that in the normal state. When the wire is in the normal state, heat can flow between A and B and if the wire is in the superconductive state then almost no heat flows. To switch the valve open, the valve is taken from the superconducting state to the normal state by the application of a sufficiently strong magnetic field. To close the valve, the field is removed and the value returns to the superconductived state.

EXPERIMENTAL

CHAPTER - 3

"EXPERIMENTAL"

Superconducting cermacis of general compositions $Y_{0.3}$ $(Ba_{0.5-x}Mn_x)$ $Ca_{0.2}$ CuO_{3-z} (x = 0.03, 0.05, 0.07, 0.1, 0.15) were prepared by heating the starting materials mixed in appropriate ratio at high temperature in a furnace. The ceramics were then characterized by X-ray diffraction and resistivity measurements. Some ESR studies at ambient temperature of the ceramics were also carried out.

The starting materials used for the preparation of the ceramics are given below:

		Punity	Supplier
1.	Y_2O_3	99.9%	Fluka
2.	$BaCO_3$	> 99%	Prepared in the laboratory
3.	$CaCO_3$	99.5%	"
4.	$MnCO_3$	> 99%	E-Merk.
5.	CuO	> 98%	Fluka

3.1 SAMPLE PREPARATION:

The sample I of nominal composition $Y_{0.3}(Ba_{0.47}Mn_{0.03})\ Ca_{0.2}CuO_{3-z}$ was prepared by using appropriate amounts of Y_2O_3, $BaCO_3$, $CaCO_3$ $MnCO_3$ and CuO. The required amounts of the respective compounds were calculated by the formula,

$$\text{Weight required} = \frac{\text{Molecular Weight} \times \text{Molar ratio} \times 1.04}{25}$$

The amounts of the various starting materials required are shown in the last column.

COMPOUND	MOLECULAR WEIGHT	MOLAR RATIO	AMOUNT REQUIRED
Y_2O_3	225.82	0.15	1.4091g
$BaCO_3$	197.34	0.47	3.8584g
$CaCO_3$	100.00	0.2	0.832g
$MnCO_3$	114.97	0.03	0.1435g
CuO	79.55	1.0	0.3093g

Total weight = 9.5523g

The sequence of operations involved in the preparation of the ceramic is (a) Calcination (b)pelletization and (c) Sintering.

a) CALCINATION:

The weighed amounts of the starting materials Y_2O_3, $BaCO_3$, $CaCO_3$, $MnCO_3$ and CuO (all of high purity) were thoroughly mixed by grinding in an agate mortar and pestle. The initial colour of the mixture was grey. The finely ground powder was then heated in a furnace (range from ambient temperature to 1400^{o}C) at 800^{o}C for several hours. The furnace was calibrated using copper-constantan thermocouple. The variation between the set temperature and the actual temperature in the furnace was not more than 5^{o}C. Calcintion procedure was carried out for a total period of 67 hours in an atmosphere of air. During this step, the calcined product was furnace cooled, reground and heated at least four times. The calcined product was further processed in five steps. First of all, a portion of the calcined product was separated for sintering. The remainder of the powder was treated in four steps (B1, C1, D1, E1) as shown in Table.1. The well ground product was heated at 820^{o}C in air for 12 hours (step B1). The powder was furnace cooled to 300^{o}C and allowed to soak in air for 7 hours. It was then cooled slowly to room temperature in the furnace. The resultant product was reground, heated at 820^{o}C in air, furnace cooled to 300^{o}C, soaked in air for further 7 hours and then slowly cooled to room

temperature. The pellet was pressed at 6000 Kg/cm^2 pressure. Its resistance was measured by a digital multimeter and the Meisner effect was tested without sintering. The powder was then treated as in step C1, followed by steps D1 and E1 as shown in Table I.

(b) PELLETIZATION:

The dark black granular powder obtained after calcination at 800^oC was powdered thoroughly. A drop of 2% polyvinyl alcohal was added to it as binder and grinding was carried out again. Two pellets (diameter=13mm, thickness $\sim$2mm) were pressed at 6000Kg/Sq cm pressure using D-01 die (diameter 13 mm) and 25 ton RIIC hydraulic press. The pellets were then sintered.

(c) SINTERING:-

The two pellets were sintered in air at 800^oC for 24.0 hours and furnace cooled to room temperature. The resistance of the pellet was found to be $\sim$200 ohms and it showed positive Meisner effect.

The nominal composition and the amounts of the starting materials for the sample II, III, IV and V corresponding to x = 0.05, 0.07, 0.1, 0.15 respectively are given below:-

	COMPOUND	MOLECULAR WEIGHT	MOLAR RATIO	AMOUNT REQUIRED
II.	Y_2O_3	225.82	0.15	1.084
	$BaCO_3$	197.34	0.45	2.842
	$CaCO_3$	100.00	0.2	0.64
	$MnCO_3$	114.97	0.05	0.184
	CuO	79.55	1.00	2.546
		Total Weight = 7.296g		
III.	Y_2O_3	225.82	0.15	1.4091
	$BaCO_3$	197.34	0.43	3.530
	$CaCO_3$	100.00	0.2	0.832
	$MnCO_3$	114.97	0.07	0.3348
	CuO	79.55	1.0	3.3093
		Total weight = 9.4152g		
IV.	Y_2O_3	225.82	0.15	1.4091
	$BaCO_3$	197.34	0.45	3.6946
	$CaCO_3$	100.00	0.2	0.832
	$MnCO_3$	114.97	0.1	0.4784
	CuO	79.54	1.0	3.3093
		Total weight = 9.7234g		
V.	Y_2O_3	225.82	0.15	1.4091
	$BaCO_3$	197.34	0.35	2.8732
	$CaCO_3$	100.00	0.2	0.832
	$MnCO_3$	114.97	0.15	0.7174
	CuO	79.55	1.0	3.3093

The basic heat treatment and sintering procedure followed for samples II, III, IV and V are essentially the same as detailed for sample I. Heat treatment conditions and sintering parameters for these samples are shown in Table II to VI.

3.2 RESISTIVITY MEASUREMENT:

3.2.1 INSTRUMENTATION:-

The resistivity measurements were made using the customary four-probe method. The contacts on the pellet were made using silver paint which is conducting.

The circuit diagram used for the resistivity measurements is shown in Fig. 3.1.

(a) Ministat Model 251 (H.B. Thomson).

Ministat was employed as a Galvanostat to obtain constant currents across contacts a and d. Usually the current value ranged between 0.1 to 1.0mA. The potential across the contacts b and c was measured using a high precision system multimeter, M 2534 by Philips. A heating element is also fixed to the base of the mount through a piece of asbestos sheet.

3.2.2 CRYOSTAT AND CONTACTS:

The cryostat consisted of a pellet mount contained in a hollow metallic cylinder. The four-probe contact leads together with the copper constantan thermocouple lead pass through a long cylindrical handle. The pellet is mounted on the base and the contacts are fixed. The thermocouple tip is also fixed on the pellet. The whole assembly is airtight. Before measurement, the apparatus is evacuated. The assembly is then placed in liquid nitrogen contained in a dewar vessel (half filled). Fig. 3.1 shows the pellet connection to the ministat and the system multimeter. The thermocouple lead is connected to the digital thermometer (Digi Sense).

It was found that if the silver paint was slightly thinned with acetone for fixing contacts, the quality of contact is improved. Essentially noise free contacts result if the area under the contacts is small. It was also found that fresh contacts were necessary for the noise free output from the multimeter. On many occasions contacts were loosened or detached from the base. In such a case, the contacts are removed from the pellet and the silver paint remove by rubbing with fine sand paper. After resintering the contacts are refixed.

The resistance of the ceramic element was measured by the four-probe method as described earlier. The voltage V across the element corresponding to the applied current I is measured with precision multimeter. The temperature is measured with the thermocouple attached to the digital thermometer. Using Ohm's law, the resistance R is calculated

$$R = V/I$$

A plot of temperature (^{o}K) against resistance gives the temperature-resistance curves.

The resistance values can be converted into resistivity ρ,

$$\rho = \frac{RA}{L}$$

(the area A and length of the element L)

3.3 X-RAY DIFFRACTION[60,61]

X-ray diffraction measurements of the samples were made at room temperature using a D-Max series 3 Rigaku diffractometer with Cu Kα (λ = 1.5418A^{o}) radiation. The Cu Kα radiations were diffracted from the sample surface. The tube voltage was kept at 40Kv and the current at 20mA. The alignment of diffractometer was carried out and test runs for standard silicon was obtained before getting the diffraction pattern (intensity vs 2θ) of the samples.

Methods usually employed in X-ray diffraction measurements are (a) Laue (variable λ, fixed θ) (b) Rotating crystal (Fixed λ, variable θ) and (c) Powder (Fixed λ variable θ). These various methods differ in the type of radiation used and sample employed. The powder method is the only method that can be employed when a single crystal specimen is not available. This method is suited for determining lattice parameters and for the identification of phases, whether they occur alone or as polyphase alloys. There are two main powder methods:-

a) Debye-Scherrer powder method

b) Diffractometer powder method

X-ray diffraction method is commonly used for structure determination since X-rays have a wavelength of the same order of the magnitude as the distance separating the atoms in solids. When x-rays are directed at the crystalline materials, they are diffracted by the planes of atoms in the crystal at certain angles depending on internuclear distances. The characteristic features of an x-ray powder spectrum are the angle at which reflections occur and relative intersities of reflection. The dependence of the reflection angle on the wavelength and interplanar distance (d_{hkl}) is given by Bragg's Law.

$$n\lambda = 2\, d_{hkl} \mathrm{Sin}\theta$$

The spacing (d_{hkl}) depends upon the dimension of the unit

cell, which for different systems are:-

System	d_{hkl}
Cubic	$a/(h^2+k^2+l^2)$
Tetragonal	$\left[\frac{h^2+k^2}{a^2}+\frac{l^2}{c^2}\right]^{1/2}$
Orthorhombic	$\left[\frac{h^2}{a^2}+\frac{k^2}{b^2}+\frac{l^2}{c^2}\right]^{-1/2}$

The relative intensities of the reflections depend on the kind of the atoms and their arrangements between lattice planes. Following are the factors affecting the relative intensities of diffraction lines:-

a) Polarization (P)

b) Structure factor (F_{hkl})

c) Multiplicity factor (M)

d) Lorentz factor L,

e) Absorption factor A,

f) Temperature factor T,

Relative intensities are given by relation

$$I_{hkl} \alpha \left(\frac{1+\text{Cos}^2 2\theta}{2}\right) |F_{hkl}|TLP$$

The unit cell parameters (a, b, c, α, β, γ) can be

expressed either as a function of the interplanar spacing, d or the miller indices. The unit cell of cubic, tetragonal and hexagonal systems can be determined with graphical methods. However, monoclinic, triclinic and orthorhombic systems present difficulties in indexing by graphical methods. The cell of such systems are characterized by three (orthorhombic), four (Monoclinic) and six (Triclinic) lattice constants depending on the complexity of the system in terms of symmetry.

After recording the diffractogram of the sample, the stored data in comprising of the diffraction angle, spacing and intensity of each reflection is printed out.The unit cell dimensions of the unknown samples were calculated by using a computer program. The program requires the estimated values of the lattice constants, space group, wavelength and the total scanning width (2θ) as input data. The output of the program gives us the total possible reflections in this 2θ range along with the multiplicities for the estimated values of lattice constants. Hence by hit and trial method, a set of values are obtained which are in agreement with the observed ones and the corresponding values of the lattice constants are assumed to be the approximate lattice constants for the particular space group of the sample. The approximate values of the lattice

constants are then fed into another program for refinment purpose. The respective space group number gives the crystal structure, the space group and all other symmetry conditions.

3.4 ELECTRON SPIN RESONANCE SPECTROSCOPY

3.4.1 BASIC PRINCIPLE:-[66,68]

An electron has an intrinsic angular momentum $\hbar$ with half integral spin (S=1/2), S is the electron spin quantum number. A component of electron spin along a given axis, z axis, is expressed by $M_S\hbar$ ($M_S = \pm 1/2$). The electron spin is associated with a magnetic moment given by

$$\mu = - g \frac{e}{2mc} S\hbar$$

Where e, m and c are the electronic charge, the mass of electron and velocity of light respectively.

Substituting β, Bohr Magneton, for $\frac{e}{2mc}\hbar$, we get $\mu = - g\beta S$

Because the angular momentum and the magnetic moment are vector quantities, the magnitude of angular momentum vector for an electron is $\hbar\sqrt{S(S+1)}$ and its magnetic moment is $g\beta\sqrt{S(S+1)}$. The component of the magnetic moment along z axis is $\mu_z = g\beta M_S$.

When an electron is placed in a uniform magnetic field H, the magnetic moment of the electron might be expected to interact with the electric component of the field. The energy of the electron due to interaction will be

$$E = - \mu_z H$$

By substituting μ_z

$$E_+ = \frac{1}{2} g\beta H,$$

$$E_- = - \frac{1}{2} g\beta H$$

The electron may be excited from lower energy level to higher energy level by absorption of radiation energy ($h\nu$). Two conditions are necessary for absorption.

i) Ther energy of a quantum must be equal to the separation between energy levels i.e.

$$E_+ - E_- = h\nu = g\beta H$$

ii) The oscillating electric field component must be able to stimulate an oscillating electric dipole in the molecule.

When these conditions are satisfied, the ESR spectra is obtained.

The g values can be calculated by

$$g = \frac{h\nu}{\beta H}$$

3.4.2 INSTRUMENTATION[67]

All measurements were performed on Jeol JES-FEIXG instrument using 100 KH_z field modulation. The instrument

consisted of various units.

a) Spectrometer:

Comprising the following:-

i) Magnetic field control unit.

Field sweep intensity could be varied upto maximum 6500 G.

ii) Mod width/Amplitude ($100KH_z/80\ KH_z$) unit

Modulation rate could be varied from 0.002 G to 20 G and fieldwidth could be varied upto ± 2500 G.

iii) Oscilloscope

Concluding mode checks, ESR signal, malfunction checks etc. could be observed on this screen.

iv) Recorder:-

D-YT recorder type was used to record the ESR signal.

b) Microwave unit:-

c) Cavity Resonator

d) Electromagnet and Excitation Power Supply.

For other details see manual for ESR instrument[67].

3.4.3 PROCEDURE:

0.01 M solutions of the samples $Y_{0.3}(Ba_{0.5-x}Mn_x)\ Ca_{0.2}CuO_{3-z}$ with (x = 0.03, 0.05, 0.07, 0.1, 0.15) were prepared by dissolving 0.0153g, 0.0935g,

0.0646g, 0.0448 and 0.0293g of the ceramics per 2ml of the solvent (dil. HCl). The spectra of the solution were recorded in capillaries (diameter = 1mm). The tube was screwed in the microwave cavity between the poles of a strong electromagnet. The field of the strong magnet was varied gradually until a setting is reached at which the natural precession frequency of the resultant paramagnetic ion just maches the microwave magnetic field frequency. This is the condition of resonance at which energy is absorbed from the microwave field by the spin system. Generally, the Klystron operates at 9.44 GHz. At resonance, a quantum of microwave radiation just equals the spacing between two energy levels of the spin system. g value can be calculated by

$$g = \frac{h\nu}{\beta H}$$

RESULTS AND DISCUSSION

CHAPTER - 4

RESULTS AND DISCUSSION

4.1 RESISTIVITY MEASUREMENTS:

The ceramics of nominal composition $Y_{0.3}Ba_{0.5-x}Mn_xCa_{0.2}CuO_{3-z}$ (x = 0.03, 0.05, 0.07, 0.1 and 0.15) were prepared by the solid state reaction. Pellets of 13mm diameter and of ~1mm thickness were prepared from the finely ground calcined powder and sintered. The heat treatment conditions and sintering parameters are given in Table I to VI. The unsintered pellets showed high resistance in the range of kilo and mega ohms at ambient temperature. However sintering of the pellets reduced the resistance to within few hundreds ohms. All samples were sintered for a total duration of 24-hours in air. In the case of sample D_3'', resistance of the pellet was observed at several steps during the 24 hour sintering cycle at 900°C. After six hours its resistance was found to be 60-90kilo-ohm.Further sintering for 6 hours reduced the resistance to 5-10kilo-ohm.At the end of the 24 hour sintering the resistance of the pellet reduced to 150-600 ohm. Generally, majority of the samples studied showed continual decrease in resistance when the sintering duration was prolonged. The sample D_5' was also sintered at 900°C and its resistance was

measured at intervals of nine hours. First the resistance of this sample reduced from ~20 M ohm to about 1K ohm and the end of 9 hour sintering period. Further sintering for additional nine hours increased the resistance to ~15K ohm. All samples (A_1', A_1'', D_2', E_2', D_3', D_3'', C_4', D_4', E_4', C_5', D_5') were subjected to Meisner test to check the presence of superconductivity. Only those samples which showed +ve Meisner effect were chosen for resistivity and x-ray diffraction measurements.

As is clear from Table - VI the samples with x=0.1 and x = 0.15 are not superconducting. Three samples corresponding to x = 0.1 were sintered at 870^{o}C, 875^{o}C and 890^{o}C. The first two samples showed resistance of ~800 to 1000 ohm but at highest temperature the resistance increased to > 20 M ohm.

It appears that the heat treatment and in particular the sintering parameters are quite critical in stability of the superconducting phase. A change of sintering atmosphere from air to N_2 in the case of sample A_1'' leads to the formation of a ceramic which is non-superconducting.Forsamples containing low concentration of Mn (x=0.03, 0.05 and 0.07) variation of sintering temperature in the 800 - 900^{o}C range does not destroy the

superconducting phase altogether. The presence of higher amounts of Mn (samples with x = 0.1 and 0.15) produces a ceramic material which is essentially insulating.

Resistance of Mn-substituted samples as a function of temperature was made using the usual four-probe method. Figs 4.1 to 4.4 present the resistance-temperature data of the samples studied.

The D_3' sample shows metallic behaviour from ambient temperature (290K) down to about 90K. In this temperature range the resistance of the sample falls from 97m ohm to 77m ohm. At 77K the resistance is $\sim$62m ohm. Thus there is an indication of the onset of a super conducting transition around 95K. The D_3'' sample having the same composition as D_3' sample but sintered at 900^{o}C clearly shows the onset of superconducting transition at 85K since there is a sharp fall of resistance. In the range 225-85K, this sample shows metallic behaviour (gradual decreaseof resistance with temperature). However between 290-225K there is a significant drop in resistance which indicates that there is another superconducting phase above 225K. The D_2' and E_2' samples show an onset transition around 87K. Above this temperature both samples show a mixed metallic/semi conducting behaviour. The A_1' sample having the lowest

concentration of Mn (x = 0.03) and also sintered at lowest temperature (800^{o}C) shows a marked decrease in resistance with decreasing temperature in the range 230 - 210 K. The resistance drops from 70m ohm to 33m ohm. This change in resistance may be attributed to the presence of a metastable superconducting transition state. The resistance of this sample does not show any significant change in the temperature range 210-90K. At about 88K resistance temperature curves show a short fall in resistance indicating the onset of a superconducting transition. The D_4' sample shows essentially metallic and semiconducting behaviour from ambient to liquid nitrogen temperature. The resistance change R (Tc^{onset}) - R(77K) of the samples A_1', D_2', E_2' and D_3'' is 18, 38, 25.5 and 33 m ohm respectively. None of these samples shows zero resistance in the liquid nitrogen temperature range. The existance of residual resistance indicates that there is another phase below 77K. Resistivity measurements below 77K could not be made to verify this suggestion due to experimental limitations.

The parent compound Y-Ba-Cu-O system has been extensively studied.[65] The superconductivity in this system has been attributed to the quasi--two-dimensional assembly of CuO_2-Ba-CuO_2-Ba-CuO_2 layers sandwiched between the layers of Y atoms. Several modifications of the basic structure

have been attempted by substitution at Y sites by other rare earth atoms and at Ba sites by Sr[29] and Ca[30]. Such substitutions have shown littleinfluence on the superconducting behaviour of the parent compound. Other likely sites for substitutions are the Cu(1) and Cu(2) sites in the one dimensional Cu-O chains along the b axis and two-dimensional Cu-O sheets in the a-b plane respectively. Substitution of Cu by metallic elements has been carried out in the light of different pairing mechanisms recently discussed. Substitution of Cu by Ag to a transition onset of 50K and a transition width of $\sim$30K.[24] Copper has also been substituted by 3d transition metals (A) in the nominal composition $YBa_2(Cu_{1-x}A_x)_3O_{7-\delta}$ .In the case of Mn (antiferromagnetic element) substitution[63], onset and T_c^o,remained practically unchanged in the range $0< x < 0.1$ which suggests that Mn substitution does not cause a measurable change in Tc. It was also observed that Mn-substituted samples in the range $0< x < 0.1$ contained very small amount of additional phases (below 1%). For $x \geq 0.1$ not only the superconducting characteristics changed but also the amount of additional phases increased. The occurence of non-superconducting additional phases broadened the transition width. The normal state resistivity also increased with Mn content probably due to the enhancement of carriers scattering by dispersed amounts of the intragrain

additional phases. The resistivity results suggest that the Cu(2) sites in the Cu-O planes are preferntially occupied by the Mn ion.

Strobel et al[24] studied $YBa_2Cu_{3(1-x)}Mn_{3x}O_{7-\delta}$, (M=Ag, Li, Pt, Zn, Cr, Mn, Fe, Co, Ni) compositions for x=5 or 10%. For 10% Mn substitution, 60-70K phase is dominant while the high temperature phase with Tc^{onset} above 80K is present as minor phase. This behaviour is attributed to preferential substitution on particular sites. The oxygen content of the samples (annealed in O_2) varies with M and this provides an alternate explanation of the observed effect.

Substitution at Ba sites by a variety of metal atoms has been attempted by Suzuki and coworker[57]. They studied $YBa_{2-x}M_xCu_3O_{7-\delta}$ compositions for 36 metals with x=0.4, 0.6, 0.8, 1.0. Their results show that iron group metals in general exhibit residual electrical resistance. Also the ratio of the superconducting orthorhombic phase decreases as the amount of dopant increased.

Substituation of Mn at Ba sites in presence of Ca has not been attempted in Y-Ba-Cu-O system. Mahboob and coworkers[30] have studied Ca- substituted compound,

$Ca_{0.2}Y_{0.3}Ba_{0.5}CuO_{3-z}$ prepared under different heat treatment and sintering conditions. All their samples were single phase with Tc in the range 83-85K and To ~77K. This Ca-substituted sample showed a depression of Tc in comparison to the parent Y-Ba-Cu-O compound. Veal's studies[29] of Y $Ba_{2-x}Sr_xCu_3O_{7-\delta}$ compositions show similar results for Sr-substitution. The depression of Tc caused by Sr or Ca substitution are attributed to "local distortions".

The resistivity measurements of Mn substituted samples under investigation show that the substitution of Mn at Ba sites in suppressing the usual superconductivity orthorhmbic phase observed in Y-Ba-Cu-O or Y-Ba-Ca-Cu-O systems. The existence of another phase below 77K is indicated by the presence of the residual resistance at 77K. With increased Mn content the proportion of the high Tc phase (Tc ~85K) is decreasing since samples with x = 0.1 and 0.15 are found to be non-superconducting. These results are in agreement with Suzuki[57] . The occupancy sites for Mn in the unit cell need to be rationalized on the basis of resistivity and x-ray diffraction data. The likely position which Mn can occupy in the unit cell are Cu-sites and Ba-sites. If Mn occupies Cu(2) sites in the Cu-O planes or the Cu(1) sites in the Cu-O chains, little influence is expected on the superconducting behaviour, Tc^{onset} and

T_c^o values of the Y-Ba-Ca-Cu-O system on Mn substitution corresponding to x=0.03, 0.05 and 0.075 in the light of Jardim's[63] result. The resistivity results in the present study do not substantiate the possibility of Mn occupancy of Cu(1) or Cu(2) sites. The presence of minor additional phases which increase with Mn content ($x \geq 0.1$) appear to be responsible for suppressing T_c^{onset} and T_c^o and indicative of the ultimate transition of the high Tc phase to low Tc phase. Strobel[24] finds that 60-70K phase is dominant while the phase with onset transition above 80K is the minor phase in samples containing 10% Mn substitution. Therefore the presence of low Tc phase in our sample is not surprising.The other likely occupancy sites for Mn are Ba and Ca-sites. Substitution of Ca or Sr at Ba sites leads to a depression of Tc of the parent Y-Ba-Cu-O compound due to 'local perturbations'. Manganese is lighter than Ba or Sr and its ionic radius (80ppm) is smaller than the ionic radii of Ba(134 ppm), Sr (112ppm) or Ca(99ppm). Substitution of Mn at Ba-sites will increase the phonon frequencies associated with these sites. An increase in phonon frequencies will tend to raise the Tc, if these phonons are involved in the electron pairing interactions. The observed T_c^{onset} of the higher temperature phase is lower than in the parent compound. This suggests that change in phonon frequencies is not significant in affecting Tc. It is likely that Mn with

smaller ionic size and larger electronegativity than Ba or Ca might cause a gross modification of the crystal field potential. The 'local perturbations appear to be stronger in the neighbourhood of Mn in comparison to Ba or Ca. The O_4atoms are the nearest neighbourto Ba atoms. However, since O_4 atoms are strongly bonded to Cu(1) atoms, Mn substitution is not expected to affect 0.4 site occupancies. The next nearest neighbours of Ba atoms are O_1 atoms which are less strongly bonded to Cu(1). Possibly Mn substitution affects O1 site occupancies leading to depression of Tc and additional O_1 vacancies.

It is worth noticing that resistivity measurements of $A_3^{'}$ and $D_3^{''}$ show the existence of a phase above 200K. Such a phase has not been observed in previous studies of Mn doped samples whether this phase is genuine or it is just metastable state during transition superconducting state with $T_c \sim 85$ K is yet to be investigated.

4.2 X-RAY DIFFRACTION MEASUREMENTS:-

The results of x-ray diffraction measurements of samples showing positive Meisner effect are presented in figs 4.7 - 4.10. The XRD measurements of a nonsuperconducting sample are also presented in fig 4.10 .

Table VII - X contains the lattice parameters computed on the basis of Pmmm symmetry of the orthorhombic unit cell. Tables VIII- XI presented the 2θ, d and I/I_o (where I_o = intensity of the strongest peak) values of the main reflection in the XRD spectra of the samples. The h, k, l values have been assigned to mains peaks in the diffractograms.

In the case of A_1' sample, major peaks occur at 2θ values of 22.77, 27.55, 32.64, 38.51, 40.28, 46.58 and 58.18 corresponding to d-values of 3.901, 3.235, 2.741, 2.335, 2.236, 1.948 and 1.584 A^o respectively. The corresponding peaks for the Y-Ba-Cu-Oxide system appear at d-values of 3.893, 3.235, 2.726, 2.336, 2.232, 1.946 and 1.584 A^o. Thus the A_1' sample has orthorhombic structure of the $YBa_2Cu_3O_{7-\delta}$ type[64]. Some additional weaker peaks in the region of $2\theta=28.3^o$ to 31.6^o of the spectrum arise from copper. In this region x-rays lines due to copper occur at 2θ values of 28.3, 29.2, 29.9, 30.5, 30.9 and 31.6.[24] The last four peaks have been observed in Mn-doped sample by Suzuki[57]. Lines due to $BaCuO_2$ and Y_2BaCuO_5 are frequently present in the XRD spectrum of the parent compound[24]. Particularly lines due to $BaCuO_2$ and $Y_2Cu_2O_5$ phases would be present if the Ba:Y ratio differs from 2:1[64]. Hence the remaining peaks observed for sampe A_1' may be attributed to the presence of these phases.

The x-ray diffraction patterns of samples in which Mn content is 1.0 and 2.5 mole percent (x = 0.01 and 0.025) are essentially similar to Y-Ba-Cu-O. However, $x \geq 0.05$ new phases appear. According to Jardim,[63] the Y_2BaCuO_5 phase accounts for most of the extra peaks.

The x-ray pattern of A_1' sample is also similar to those of $Y_{0.3}Ba_{0.5}Ca_{0.2}CuO_{3-z}$ samples[30] sintered at different temperature in the 870 - 910°C range. For the Ca-substituted sample, the peak at $2\theta \sim 33^{o}$ adjacent to the strongest peak is well resolved and intense in comparison to other samples. The sample sintered at 920°C is non-superconducting in the liquid N_2 temperature range. This peak is most likely the strongest peak of the low Tc phase (Tc < 77 K). The presence of this peak in the XRD pattern of the A_1' sample is indicative of the existence of this low Tc phase in the sample. The XRD patterns of D_2' and E_2' samples are similar to that of A_1'. The peaks due to impurity phases and copper are also present. The main peak of the low Tc phase is also present in the x-ray diffraction spectra of the samples.

The XRD patterns of D_3' and D_3'' or markedly different in comparison to that of A_1', particularly in the 2θ region of 20^{o}- 45^{o}. In addition to peak due to

orthorhombic structure impurity phases and copper, other peaks are also present. The peak at $2\theta \sim 33^{o}$ is the strongest in D_3' sample indicating large proportion of the low Tc phase. Anohter striking feature common to spectra of all samples is the presence of a peak at $2\theta \sim 43.5^{o}$ (d 2.08). This peak is weak in A_1', D_2' and E_2' samples but strong in D_3' and D_3'' samples. In addition, D_3'' sample also shows a peak at $2\theta \sim 42.9^{o}$ which is not observed in other samples. The XRD patterns of the non-superconducting samples C_4' and D_4' appear to be a mixture of several phases. The main features have already been discussed. A comparison of the structural parameters reported in table VII shows that b and c constants have nearly the same value as observerd in $Y_{0.3}Ba_{0.5}Ca_{0.2}CuO_{3-z}$ [30], $YBa_2Cu_3O_{7-\delta}$ [64], $YBa_2(Cu_{1-x}Mn_x)_3O_{7-\delta}$ [24], $YBa_{2-x}Sr_xCu_3O_{7-\delta}$ [64] and $Y_{1/3}Ba_{2/3}CuO_{3-z}$. [65]

The c-value of the E_2' sample is somewhat smaller but comparable with the Sr-doped sample. The b-value of D_3'' sample is also somewhat smaller. As for a-value is concerned, it is larger for A_1', D_2' and E_2' samples but of the same order of magnitude of D_3' and D_3'' as in the parent compound. In the case of A_1', D_2' and E_2' samples a-value is comparable with the a-value in the tetragonal phase. For some samples, c-value is also close to that for tetragonal

phase. These changes in lattice parameters suggest structural modification resulting from Mn substitution at Ba-sites.

4.3 ESR STUDIES

If a free paramegnetic ion of total angular momentum characterized by J is subjected to a magnetic field, H_o, the energy of interaction is given by $g_l \beta H_o M_J$

where $M_J = J, (J-1), ..., -J$

M_J is magnetic quantum

g_l = Lande 'g' factor

β = Bohr magneton

In a magnetic resonance experiment on the free ion, transitions may be induced between various M_J levels according to the selection rule $\Delta M_J = \pm 1$.

In practice ions are situated in a crystal lattice and therefore it is necessary to consider their environment. For example, a paramagnetic ion placed at a normal lattice site in the crystal is surrounded by a regular array of diamagnetic ions. It is considered to be separated from other paramagnetic ions by a distance enough to reduce magnetic interaction to a negligible proportion. Such a

situation is found when small concentration of magnetic ions (< 0.1%) are present as impurities in diamagnetic crystals.

Since pure high Tc superconductors do not show ESR spectra, Mn doping is of interest. Mn^{2+} ions may be used as microscopic probes for ESR spectra. Effect of Mn substitution on ESR spectra has been studied in La-based system. Another such study is due to Akihiro Moto et al[38].

Unfortunately ESR signal of the powder samples cold not be recorded at ambient temperature in the present study. Measurements at low temperature were also not possible due to experimental limitations. All ESR measurements made by dissolving the ceramic material in dilute HCl. Hence it is not possible to draw conclusion about lattice environment.

The ESR spectra of the samples $Y_{0.3}(Ba_{0.5-x}Mn_x)Ca_{0.2}CuO_{3-z}$ sintered at different temperaturesrecorded in dil. HCl (6M) solution. Because the manganese has the electronic configuration $(4s^2 3d^5)$[69], the half filled shell of the high spin $3d^5$ implies that the ground state will be an orbital singlet $^6S_{5/2}$.In lower field, generally six lines are observed. The outer lines correspond to transitions $\pm 3/2 \leftrightarrow \pm 1/2$, the intermediate

lines ± 5/2 ↔ ± 3/2 and the central lines to + 1/2 ↔ 1/2. Theoretically, the intensity ratio is 8:5:9, but experimental results do not agree with this ratio. The peak positions, line width and intensity of the lines are important for the chemists[70]. Since not only the different frequencies are used in different spectrophotometers, but the frequency of each spectrophotometer need to be varried somewhat in different samples. That is why line positions are stated in terms of g values. The g value of all the samples at different temperatures are given in Table XIII-XVII. The g value for $CuSO_4$ in dil.HCl is 2.1603 and g values for $MnCO_3$ in dil.HCl are 2.155, 2.089, 2.036, 1.960, 1.920 and 1.866 respectively (Table - III). The g value for Mn^{2+} ion is different as compared to the free electron 2.002319. Due to hyperfine structure, g value varies. The different value of g may be due to interactions. There are two types of interactions[70] which determine the magnetic energy level that are separated by $g\mu_o Hz$. The first interaction is the interaction of the spin with external magnetic field. The other interaction is the hyperfine interaction. The magnetic interactions involving the orbital angular momentum of the unpaired electrons are the cause of the deviation of g values from 2.002319. Since the orbital angular momentum depend upon the chemical environment in an atom or molecule, therefore, g values also depend on the

chemical environment.

Peak position or g-values are affected by temperature[68]. The g-values are given in Table XII-XVII. But the effect of temperature is quite unusual, shift is not constant. A broad peak is observed for Cu, but the first peak of Mn merge into the broader Cu peak. The reason may be that the concentration of copper is 20 times more as compared to Mn^{2+} concentration. The intensity of the lines is affected by the concentration of the paramagnetic ion. As the dopant concentration of Mn increases, the Ist peak of Mn become prominent and at concentration (x=0.15), it becomes more prominent, copper peak is diminished. The other factors which affect the intensity are[70].

i) The intensity of the signal decreases with increasing frequency.

ii) Power of applied resonance

iii) Temperature (inversly proportional to temperature)

Both concentration and temperature affect the Cu-Mn signal. Mn could be used as a probe but change in signal shape does not correlate with resistance. Since XRD measurements of the powdered samples before sintering are not available, only we can say that the environment of Cu changes. Hence the concentration of Cu giving signal changes, either Cu^{2+} going to Cu^{3+} or Cu^{1+}.

SUGGESTIONS FOR FURTHER WORK

In the present study, the Mn-doped samples of nominal composition $Y_{0.3}Ba_{0.5-x}Mn_xCa_{0.2}CuO_{3-z}$ with dopant concentration $0 < x \leq 0.15$ were prepared. Resistivity and XRD measurements show that these samples are multiphase systems with transition temperature both above and below 77K.

The present study has shown the existence of a phase for $0 < x \leq 0.07$ samples above $200^{o}K$. A through study of conditions in relation to stability of this phase is required. Further the presence of low Tc phase (Tc < 77K) even for small concentrations of Mn in the samples shows that substitution at Ba-sites and/or Ca-sites is relatively more critical in modifying the crystal structure than substitution at Cu1 and Cu2 sites. In this regard more elaborate x-ray diffraction experiments are required to throw light on structural changes accompanying Mn substitution. Rāman and IR spectral data in the low frequency region will also be helpful to draw conclusion about phonon frequencies and their relationship to structure. Moreover, it will be interesting to find the minimum concentration of Mn dopant required in the host crystal necessary for observing ESR signal at ambient and

liquid N_2 temperatures. ESR spectral studies of powder samples will provide information about the environment of Mn sites in the crystal lattice. Studies of magnetic properties of the samples will also be of interest.

TABLES AND FIGURES

TABLE - I

SAMPLE NO.I

Preparation of $Y_{0.3}(Ba_{0.47}Mn_{0.03})Cu_{0.2}CuO_{3-z}$

Heat treatment:-

STEP	TEMPERATURE	TIME	ATMOSPHERE
A_1	$800^{o}C$	67 hours	Air
	a		
B_1	$820^{o}C$	12 hours	Air
	$300^{o}C$	7 hours	
	b		
C_1	$850^{o}C$	24 hours	-do-
	$300^{o}C$	7 hours	
	b		
D_1	$875^{o}C$	24 hours.	-do-
	$300^{o}C$	7 hours	
	b		
E_1	$890^{o}C$	24 hours	-do-
	$300^{o}C$	7 hours.	
	b		

a = Furnace cooled to room temperature, repeated grindings.

b = Furnance cooled to room temperature.

TABLE - I (B)

SAMPLE NO.I (B)

STEP	TEMPERATURE	TIME	ATMOSPHERE
A_1'	$800^{o}C$	67 hours	N_2
	Repeated grindings. Furnance cooled to room temperature		

TABLE - II

SAMPLE NO. II

Preparation of $Y_{0.3}(Ba_{0.45}Mn_{0.05})Ca_{0.2}CuO_{3-z}$

Heat treatment:-

STEPS	TEMPERATURE	TIME	ATMOSPHERE
A_2	800^oC	67 hours	Air
	a		
B_2	850^oC	24 hours	Air
	300^oC	7 hours	
C_2	870^oC	24 horus	Air
	300^oC	7 hours	
	b		
D_2	875^oC	24 hours	Air
	300^oC	7 hours	
	b		
E_2	890^oC	24 hours	Air
	300^oC	7 hours	
	b		

a = Furnace cooled to room temperature' repeated grindings.

b = Furnace cooled to room temperature.

TABLE - III

SAMPLE NO.III

Preparation of $Y_{0.3}(Ba_{0.43}Mn_{0.07})Cu_{3-z}$

Heat treatment:-

STEPS	TEMPERATURE	TIME	ATMOSPHERE
A_3	800^oC	67 hours	Air
	a		
B_3	850^oC	24 hours	Air
	300^oC	7 hours	
	b		
D_3	880^oC	24 hours	Air
	300^oC	7 hours	
	b		

a = Furnace cooled to room temperature,
Repeated grindings

b = Furnace cooled to room temperature.

TABLE - IV

SAMPLE NO. - IV

Preparation of $Y_{0.3}(Ba_{0.45}Mn_{0.1})Ca_{0.2}CuO_{3-z}$

Heat treatment:-

STEPS	TEMPERATURE	TIME	ATMOSPHERE
A_4	$800^{o}C$	67 hours	Air
	a		
B_4	$850^{o}C$	24 hours	Air
	$300^{o}C$	7 hours	
	b		
C_4	$870^{o}C$	24 hours	Air
	300^{o} C	7 hours	
	b		
D_4	$875^{o}C$	24 hours	Air
	$300^{o}C$	7 hours	
	b		
E_4	$890^{o}C$	24 hours	Air
	$300^{o}C$	7 hours	
	b		

a = Furnace cooled to room temperature

Repeated grindings

b = Furnace cooled to room temperature.

TABLE - V

SAMPLE NO. - V

Preparation of $Y_{0.3}(Ba_{0.35}Mn_{0.15})Ca_{0.2}CuO_{3-z}$

Heat treatment:-

STEPS	TEMPERATURE	TIME	ATMOSPHERE
A_5	$800^{o}C$	67 hours	Air
	a		
B_5	$850^{o}C$	24 hours	Air
	$300^{o}C$	7 hours	
	b		
C_5	$870^{o}C$	24 hours	Air
	$300^{o}C$	7 hours	
	b		
D_5	$890^{o}C$	24 hours	Air
	$300^{o}C$	7 hours	
	b		

a = Furnace cooled to room temperature

Repeated grindings.

b = Furnace cooled to room temperature.

TABLE - VI

	Composition	Sample	Sintering Parameters			Resistance	Meisner Effect Test
			Temp.	Time	Atmosphere	(Sintered Pellet)	
	$Y_{0.3}Ba_{0.5-x}Mn_xCa_{0.2}CuO_{3-z}$						
1.	$Y_{0.3}Ba_{0.47}Mn_{0.03}Ca_{0.2}CuO_{3-z}$	A_1'	800°C	24 hrs	air	300-900 Ω	+ve
	(x=0.03)	A_1''	800°C	24 hrs	N_2	1-4 M Ω	-ve
2.	$Y_{0.3}Ba_{0.45}Mn_{0.05}Ca_{0.2}CuO_{3-z}$	D_2'	875°C	24 hrs	air	300-500 Ω	+ve
	(x=0.05)	E_2'	880°C	24 hrs	air	300-600 Ω	+ve
3.	$Y_{0.3}Ba_{0.43}Mn_{0.07}Ca_{0.2}CuO_{3-z}$	D_3'	880°C	24 hrs	air	250-700 Ω	+ve
	(x=0.07)	D_3''	900°C	24 hrs	air	150-600 Ω	+ve
4.	$Y_{0.3}Ba_{0.45}Mn_{0.10}Ca_{0.2}CuO_{3-z}$	C_4'	870°C	24 hrs	air	800-1000 Ω	-ve
	(x=0.10)	D_4'	875°C	24 hrs	air	900-1200 Ω	-ve
		E_4'	890°C	24 hrs	air	> 20 M Ω	-ve
5.	$Y_{0.3}Ba_{0.35}Mn_{0.15}Ca_{0.2}CuO_{3-z}$	C_5'	880°C	24 hrs	air	∿ 12-18M Ω	-ve
	(x=0.15)	D_5'	890°C	24 hrs	air	> 20 M Ω	-ve

TABLE - VII

Sample	T_c^{onset} (K)	Lattice Parameters (A°) a	b	c	Crystal System	Composition
A_1'	88	3.862	3.874	11.695	orthorhombic	$Y_{0.3}Ba_{0.47}Mn_{0.03}Ca_{0.2}CuO_{3-}$
D_2'	87	3.872	3.885	11.725	orthorhombic	$Y_{0.3}Ba_{0.45}Mn_{0.05}Ca_{0.2}CuO_{3-}$
E_2'	87	3.876	3.876	11.600	tetragonal	-do-
D_3'	~ 95	3.826	3.867	11.717	orthorhombic	$Y_{0.3}Ba_{0.43}Mn_{0.05}Ca_{0.2}CuO_{3-}$
D_3''	85	3.820	3.790	11.698	orthorhombic	-do-
C_4'	-	3.928	3.882	11.725	orthorhombic	$Y_{0.3}Ba_{0.45}Mn_{0.10}Ca_{0.2}CuO_{3-}$
D_4'	-	3.800	3.882	11.702	orthorhombic	-do-
-	-	3.839	3.886	11.707	orthorhombic	$Y_{0.3}Ba_{0.5}Ca_{0.2}CuO_{3-z}$
		3.823	3.886	11.681	orthorhombic	$YBa_2Cu_3O_{7-\delta}$
		3.828	3.889	11.673	orthorhombic	$YBa_2(Cu_{1-x}Mn_x)_3O_{7-\delta}$
		3.822	3.839	11.531	orthorhombic	$YBa_{2-x}Sr_xCu_3O_{7-x}$
		3.820	3.895	11.69	orthohombic (R.T to 710K)	$Y_{1/3}Ba_{2/3}CuO_{3-z}$
		3.829	3.884	11.69	orthohombic (710K-820K)	-do-
		3.873	3.873	11.76	tetragonal (above 820K)	-do-

TABLE - VIII

SAMPLE NO. - A_1'

XRD measurements of $Y_{0.3}(Ba_{0.47}Mn_{.03})Ca_{0.2}CuO_{3-z}$

ANGLE (2θ)	INTENSITY	I/I_o	D-VALUE
15.07	121	0.123	5.873
22.768	201	0.204	3.901
27.547	139	0.141	3.235
30.970	111	0.113	2.884
32.643	983	1	2.741
33.354	215	0.219	2.684
38.510	206	0.210	2.335
40.280	191	0.194	2.236
43.472	99	0.100	2.079
46.582	184	0.187	1.948
58.175	238	0.242	1.584
68.705	170	0.173	1.364

TABLE - IX (A)

SAMPLE NO. D_2'

XRD Measurements of $Y_{0.3}(Ba_{0.45}Mn_{0.05})Ca_{0.2}CuO_{3-z}$

ANGLE (2θ)	INTENSITY	I/I_0	D-VALUE
27.388	130	0.245	3.253
30.925	105	0.198	2.889
32.493	530	1	2.753
33.271	255	0.48	2.691
38.380	170	0.321	2.342
40.160	118	0.226	2.242
43.371	83	0.156	2.084
46.460	138	0.260	1.953
68.480	135	0.254	1.368.

TABLE - IX (B)

SAMPLE NO - E_2'

XRD Measurements of $Y_{0.3}(Ba_{0.45}Mn_{0.05})Ca_{0.2}CuO_{3-z}$

ANGLE (2θ)	INTENSITY	I/I_o	D-VALUE
22.958	154	0.159	3.870
22.675	214	0.222	3.221
31.150	158	0.164	2.868
32.715	966	1	2.735
35.916	125	0.129	2.498
38.677	222	0.230	2.326
40.520	191	0.198	2.224
43.641	174	0.180	2.072
46.876	181	0.187	1.936
58.417	257	0.266	1.578
68.783	159	0.165	1.363

TABLE - X (A)

SAMPLE NO. - D_3'

XRD Measurements of $Y_{0.3}(Ba_{0.43}Mn_{0.07})\ Ca_{0.2}CuO_{3-z}$

ANGLE (2θ)	INTENSITY	I/I_o	D-VALUE
25.614	121	0.25	3.475
29.172	185	0.382	3.058
29.750	125	0.258	3.000
30.535	208	0.430	2.925
32.584	465	0.961	2.746
33.387	484	1	2.681
35.850	111	0.229	2.502
37.504	111	0.229	2.396
38.400	129	0.267	2.342
40.410	113	0.233	2.230
43.497	198	0.409	
52.435	88	0.182	1.743
56.226	111	0.229	1.634
58.310	112	0.231	1.581
60.283	83	0.171	1.534
70.300	79	0.163	1.337

TABLE - X (B)

SAMPLE NO. - D_3''

XRD Measurements of $Y_{0.3}(Ba_{0.43}Mn_{0.07})CuO_{3-z}$

ANGLES (2θ)	INTENSITY	I/I_o	D.VALUE
22.800	162	0.388	3.895
25.880	237	0.568	3.439
27.012	122	0.293	3.297
28.875	290	0.695	3.089
31.500	110	0.264	2.837
32.812	417	1	2.727
38.775	157	0.376	2.320
40.738	76	0.182	2.212
42.864	256	0.614	2.108
54.862	79	0.189	1.671
58.150	88	0.211	1.585
60.466	79	0.189	1.529
65.600	90	0.216	1.421
75.483	83	0.199	1.258

TABLE - XI (A)

SAMPLE NO. - C_4'

XRD Measurements of $Y_{0.3}(Ba_{0.45}Mn_{0.1})Ca_{0.2}CuO_{3-z}$

ANGLE (2θ)	INTENSITY	I/I_o	D-VALUE
15.060	108	0.141	5.876
22.775	98	0.128	3.900
25.686	130	0.170	3.465
27.462	250	0.327	3.245
29.175	155	0.203	3.058
30.875	223	0.292	2.893
32.583	765	1	2.746
33.385	435	0.569	2.681
35.946	115	0.150	2.496
38.375	198	0.259	2.343
41.816	128	0.167	2.158
43.500	168	0.220	2.078
45.310	83	0.108	1.999
46.462	130	0.170	1.953
58.366	185	0.242	1.579
62.352	98	0.128	1.487
66.352	95	0.124	1.398
77.220	80	0.1045	1.234

TABLE - XI (B)

SAMPLE NO. - D_4'

XRD Measurements of $Y_{0.3}(Ba_{0.45}Mn_{0.1})Ca_{0.2}CuO_{3-z}$

ANGLE (2θ)	INTENSITY	I/I_o	D.VALUE
15.11	105	0.125	5.857
22.805	128	0.152	3.895
25.666	95	0.113	3.468
27.466	265	0.314	3.244
28.720	115	0.136	3.105
29.208	220	0.261	3.055
29.958	80	0.095	2.980
30.951	230	0.273	2.886
32.628	843	1	2.742
33.393	518	0.614	2.681
38.507	198	0.235	2.335
40.476	128	0.152	2.226
43.525	178	0.211	2.077
46.528	208	0.247	1.950
53.480	120	0.142	1.711
58.414	235	0.279	1.578
62.364	125	0.148	1.487
68.652	113	0.134	1.365
70.315	103	0.122	1.337

1) SAMPLE - TABLE - XII (A)

g values of $CuSO_4$ + Dil.$HCl_{(6M)}$

0.1M

g = 2.1602836

SAMPLE TABLE - XII (B)

Sample

g values of $MnCo_3$ + Dil.HCl (6M)

0.01M

$$\frac{g = 6748.941963^{C}}{H}$$

1. 2.154628

2. 2.0890029

3. 2.0336425

4. 1.95975

5. 1.9201441

6. 1.866463

$$c = \frac{h\nu}{\beta}$$

TABLE - XIII

g values of $Y_{0.3}(Ba_{0.47}Mn_{0.03})Ca_{0.2}CuO_{3-z}$

	Sintering Tmep = 800°C $g=\frac{6747.512406}{H}$	Sintering Temp = 800°C Airatmosphere $g=\frac{6748.227184}{H}$	Sintering Temp = 850°C Air $g=\frac{6748.941963}{H}$	Sintering Temp = 875°C $g=\frac{6748.941963}{H}$	Sintering Temp = 890°C $g=\frac{6748.941963}{H}$
1	2.167374	2.170155	2.162173	2.169778	2.165969
2	2.053812	2.089376	2.085504	2.096127	2.090802
3	2.026846	2.029292	2.028976	2.025659	2.022331
4	1.970249	1.974320	1.973848	1.973361	1.969126
5	1.915242	1.908074	1.923137	1.927671	1.915680
6	1.863223	1.863899	1.863648	1.872122	1.863643

$$c = \frac{h\nu}{\beta}$$

TABLE - XIV

g values of $Y_{0.3}(Ba_{0.45}Mn_{0.05})Ca_{0.2}CuO_{3-z}$

	Sintering temp = 850°C $g = \frac{6747.512406}{H}$ c	Sinteromg temp = 875°C $g = \frac{6747.512406}{H}$ c	Sintering temp = 890°C $g = \frac{6747.512406}{H}$ c
1	2.159826	2.178887	2.157940
2	2.090359	2.093901	2.090359
3	2.035228	2.043654	2.031881
4	1.9781741	1.986128	1.970284
5	1.925726	1.929139	1.919737
6	1.8703086	1.875992	1.864659

$$c = \frac{h\nu}{\beta}$$

TABLE - XV

g values of $Y_{0.3}(Ba_{0.43}Mn_{0.07})Ca_{0.2}CuO_{3-z}$

	Sintering temp = 850°C $g = \frac{6748.227184^{C}}{H}$	Heating temp = 870°C $g = \frac{6748.227184^{C}}{H}$	Firing temp = 880°C $g = \frac{6748.227184^{C}}{H}$
1	2.161944	2.152524	2.160062
2	2.095898	2.078264	2.088808
3	2.031268	2.025430	2.035449
4	1.9831453	1.973639	1.981556
5	1.925929	1.919941	1.922928
6	1.8733419	1.867675	1.867680

$$c = \frac{h\nu}{\beta}$$

TABLE - XVI

$Y_{0.3}(Ba_{0.45}Mn_{0.1})Ca_{0.2}CuO_{3-z}$

	S.T = 850°C $g=\frac{h\nu}{\beta H}\ \frac{6.626\times10^{-27}\times9.44\times10^{9}}{0.927\times10^{-27}\times H} = \frac{6747.512406}{H}$	Sintering temp = 875°C $g = \frac{6748.941963}{H}$	Sintering temp = 890°C $g = \frac{6748.941963}{H}$
1	2.156058	2.150879	2.154628
2	2.090359	2.0890289	2.090802
3	2.026877	2.027306	2.025645
4	1.973430	1.9691257	1.972273
5	1.919737	1.918654	1.920144
6	1.859044	1.866463	1.866463

TABLE - XVII

g values of $Y_{0.3}(Ba_{0.35}Mn_{0.15})\ CaO_2CuO_{3-z}$

Sintering temp = 850°C $g = \frac{6748.941963^{c}}{H}$	Sintering temp = 880°C $g = \frac{6748.941963^{c}}{H}$	Sintering temp = 890°C $g = \frac{6748.941963^{c}}{H}$
1	2.197300	2.2066038	2.200704
2	2.152800	2.149009	2.147142
3	2.085504	2.080233	2.081991
4	2.019021	2.030643	2.022331
5	1.975425	1.973848	1.955425
6	1.918490	1.915680	1.918654
7	1.867873	1.862239	1.863643

$$c = \frac{h\nu}{\beta}$$

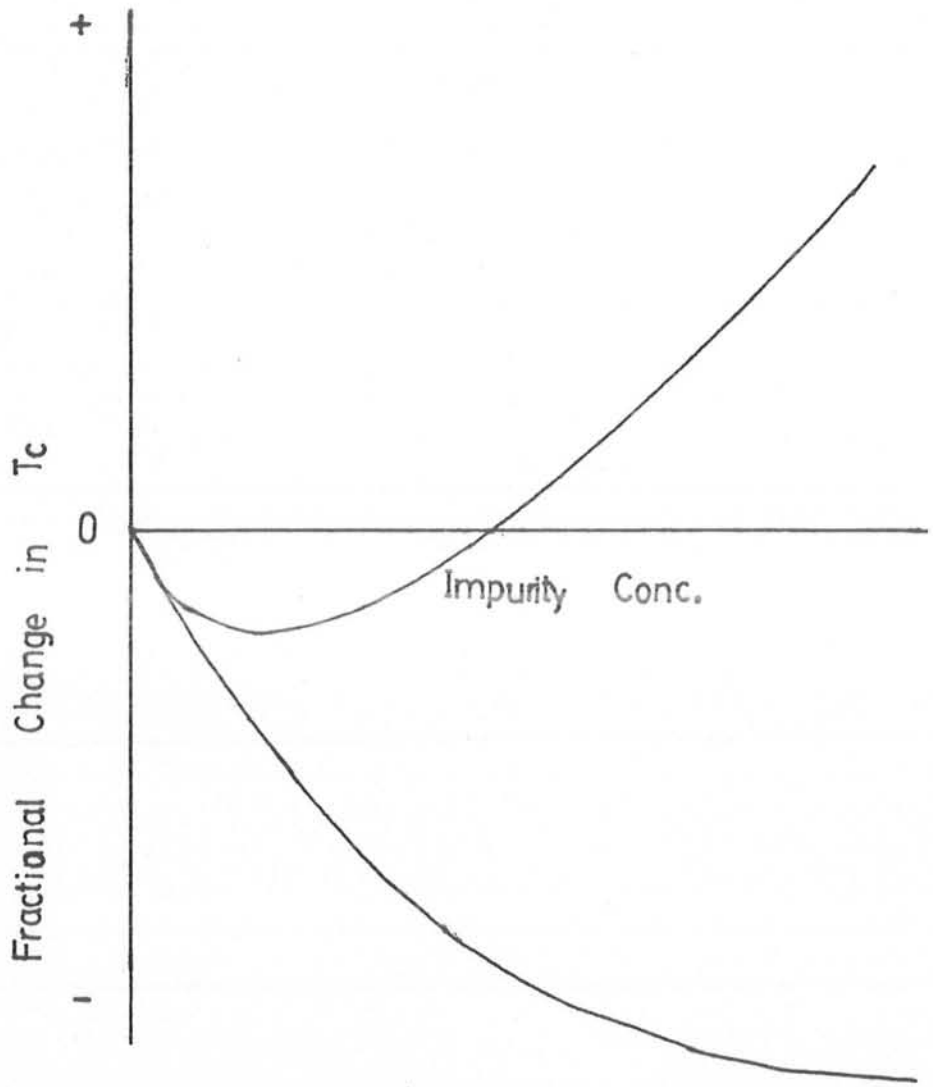

FIG. 2.1

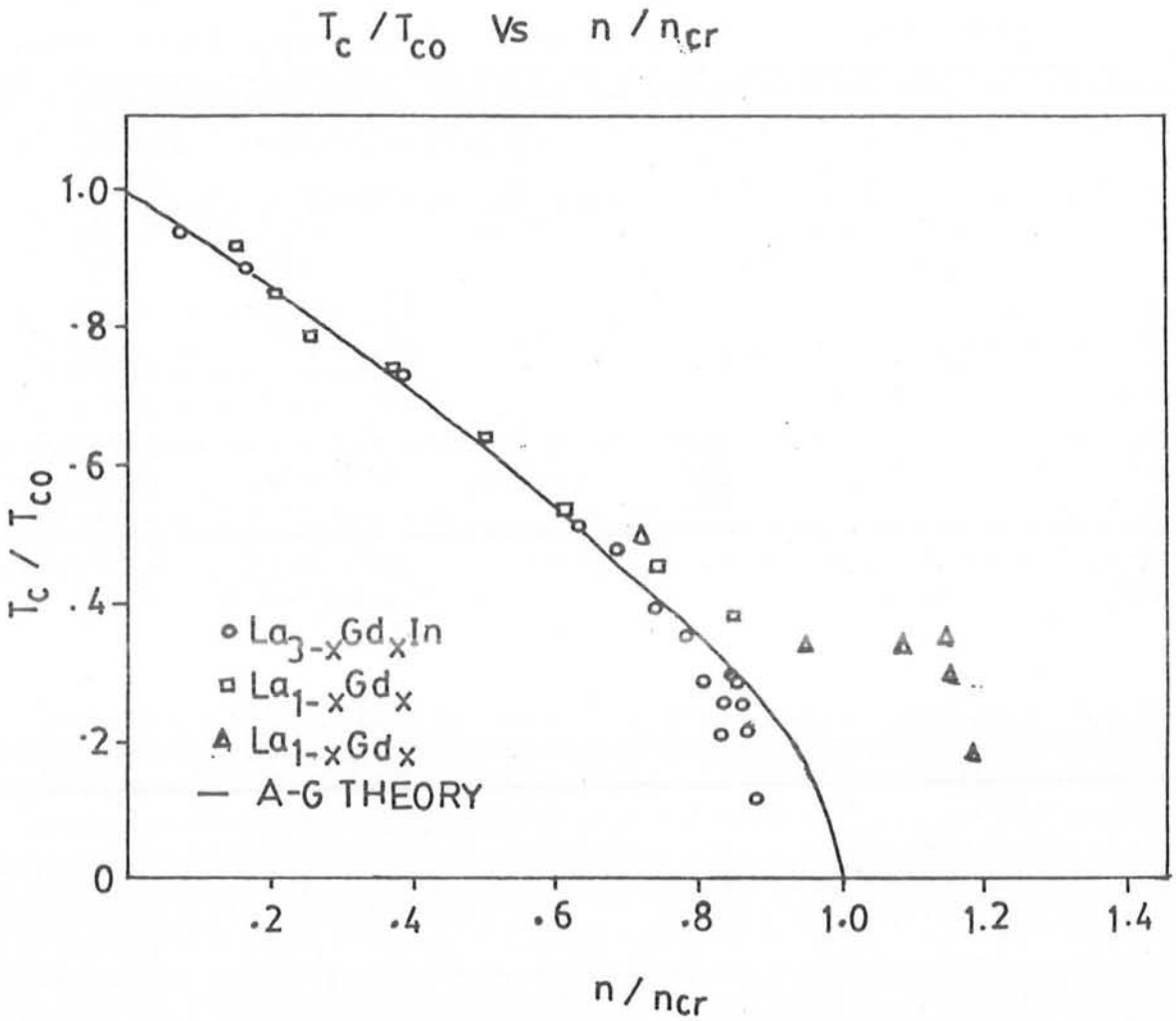
T_c / T_{co} Vs n / n_{cr}
1·0
·8
·6
·4
·2
0
T_c / T_{co}
.2
.4
.6
.8
1·0
1.2
1.4
n / n_{cr}
$La_{3-x}Gd_xIn$
$La_{1-x}Gd_x$
$La_{1-x}Gd_x$
A-G THEORY

FIG. 2.2

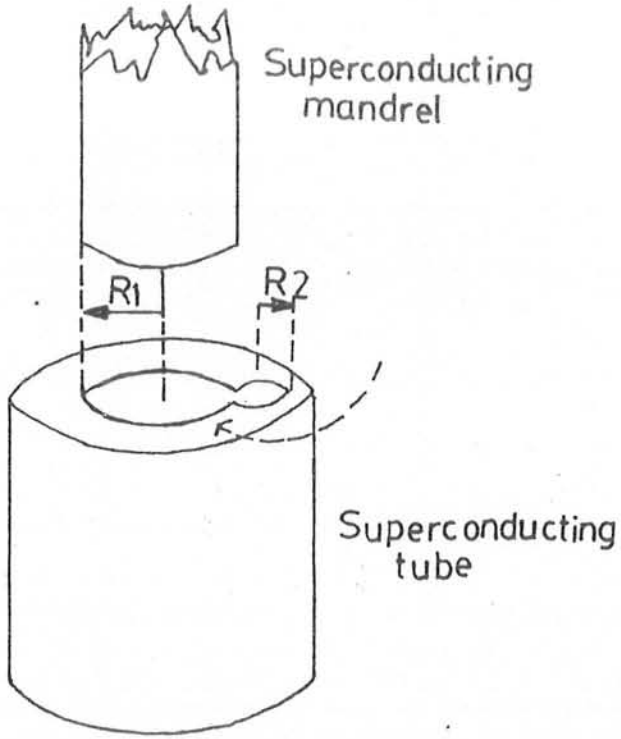

A FLUX COMPRESSOR

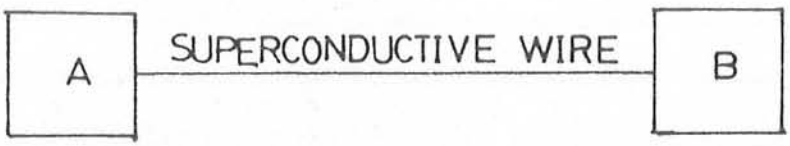

HEAT VALVE

FIG. 2.3

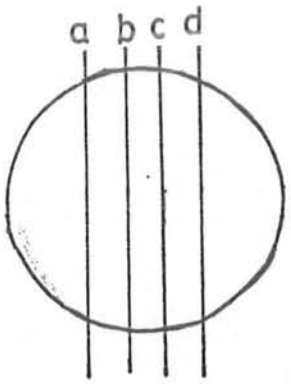

Contacts for the four-probemethod

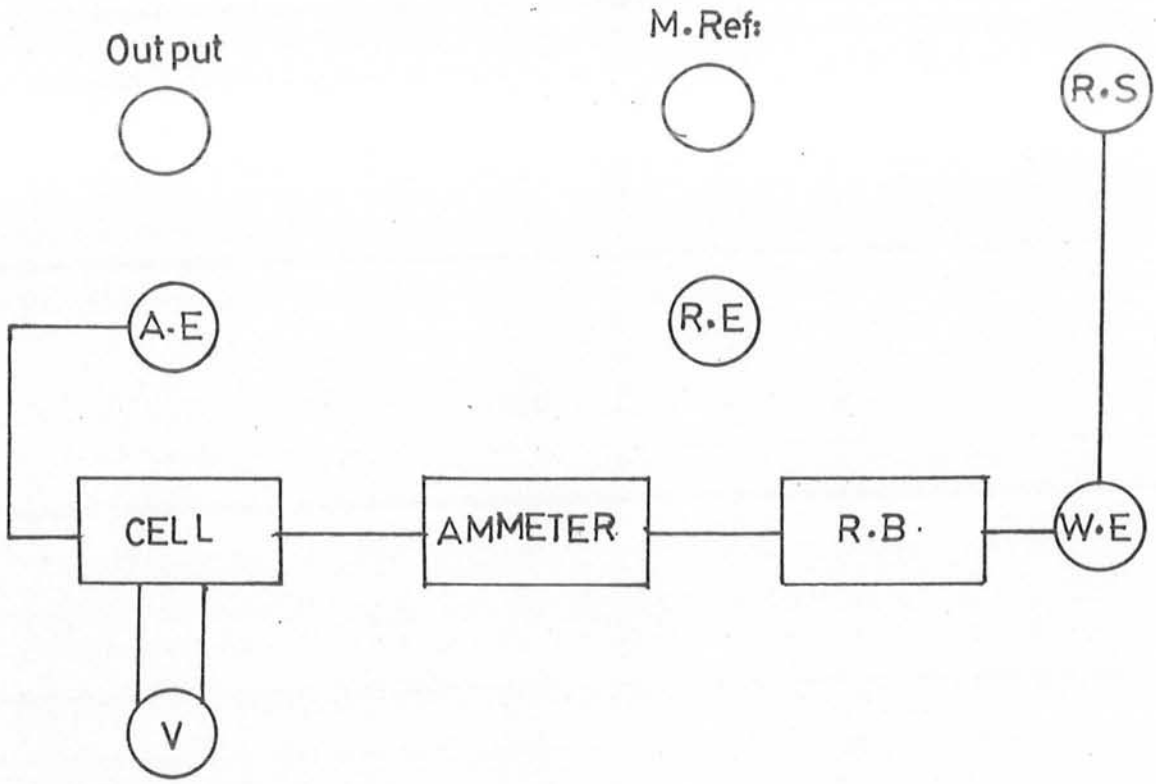

W.E=Working Electrode , R.E=Ref. Electrode, A.E=Auxiliary Electrode

M.Ref:=Measuring Ref:, R.B=Resistance Box, V=Voltmeter

Cell containing four leads. FIG. 3.1

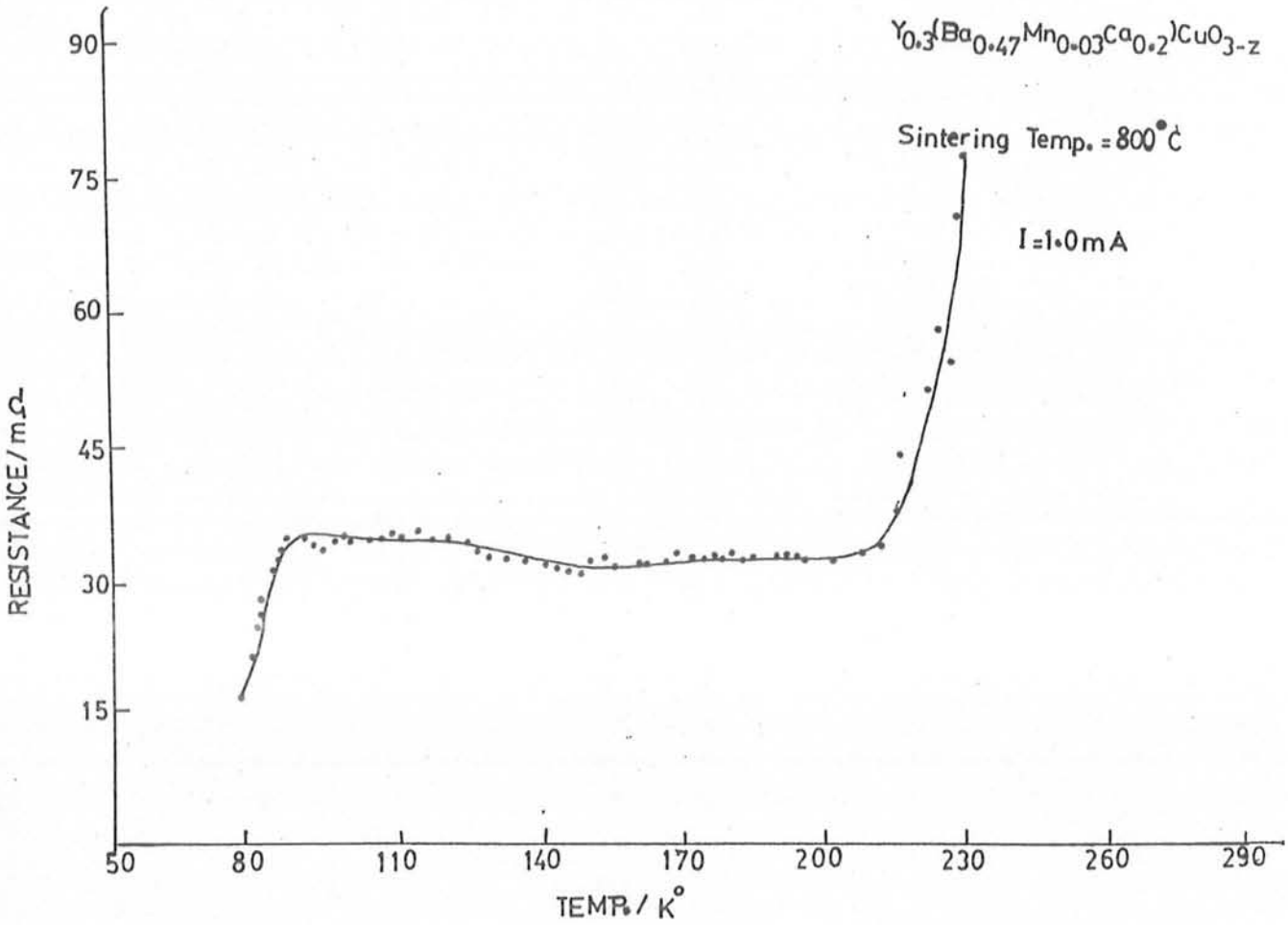
$Y_{0.3}(Ba_{0.47}Mn_{0.03}Ca_{0.2})CuO_{3-z}$
Sintering Temp. = 800°C
I = 1.0 mA
RESISTANCE / mΩ
90
75
60
45
30
15
50
80
110
140
170
200
230
260
290
TEMP. / K°

FIG. 4.1

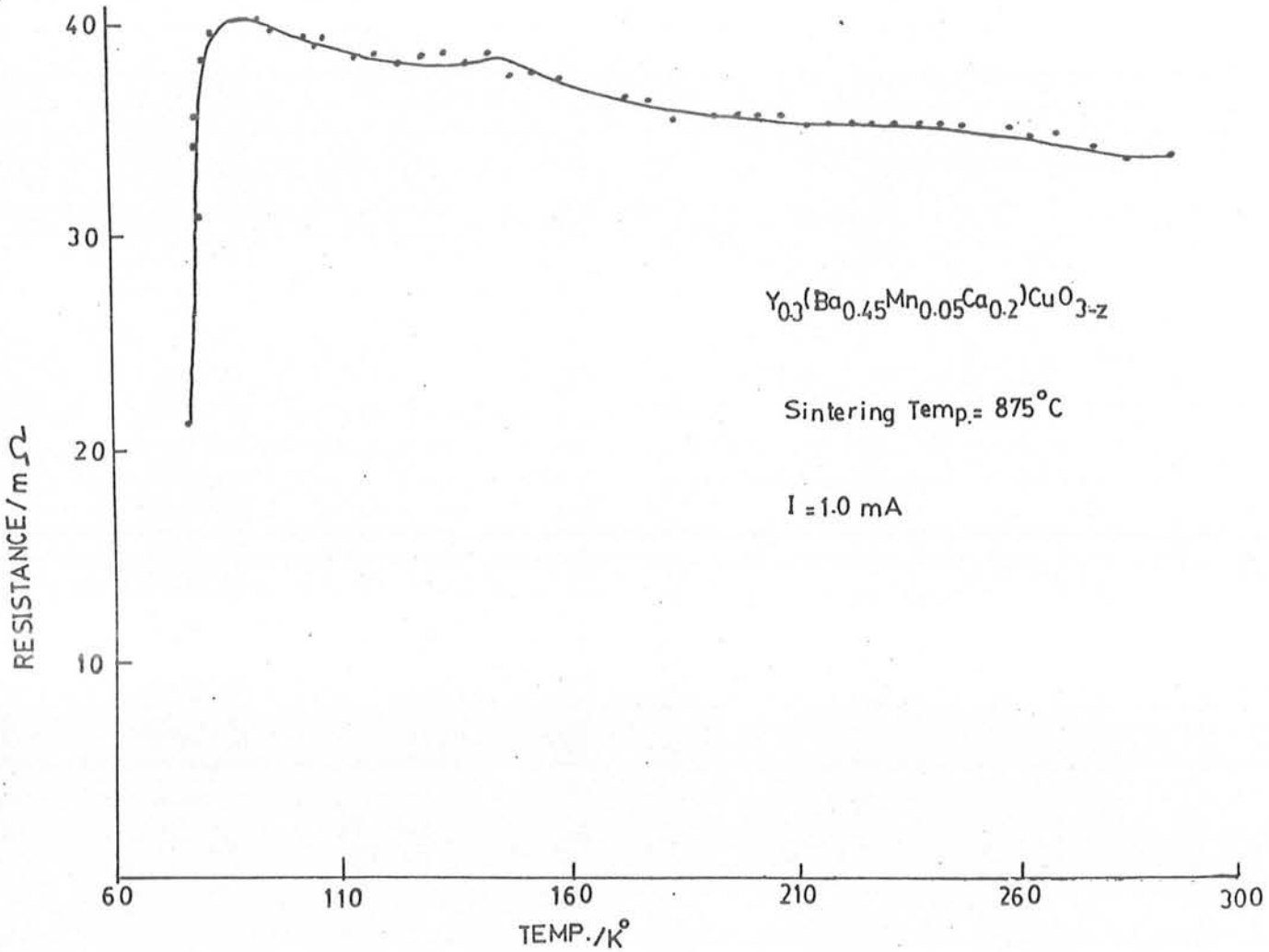
40
30
20
10
RESISTANCE/mΩ
60
110
160
210
260
300
TEMP./K°
$Y_{0.3}(Ba_{0.45}Mn_{0.05}Ca_{0.2})CuO_{3-z}$
Sintering Temp.= 875°C
I = 1.0 mA

FIG. 4.2-A

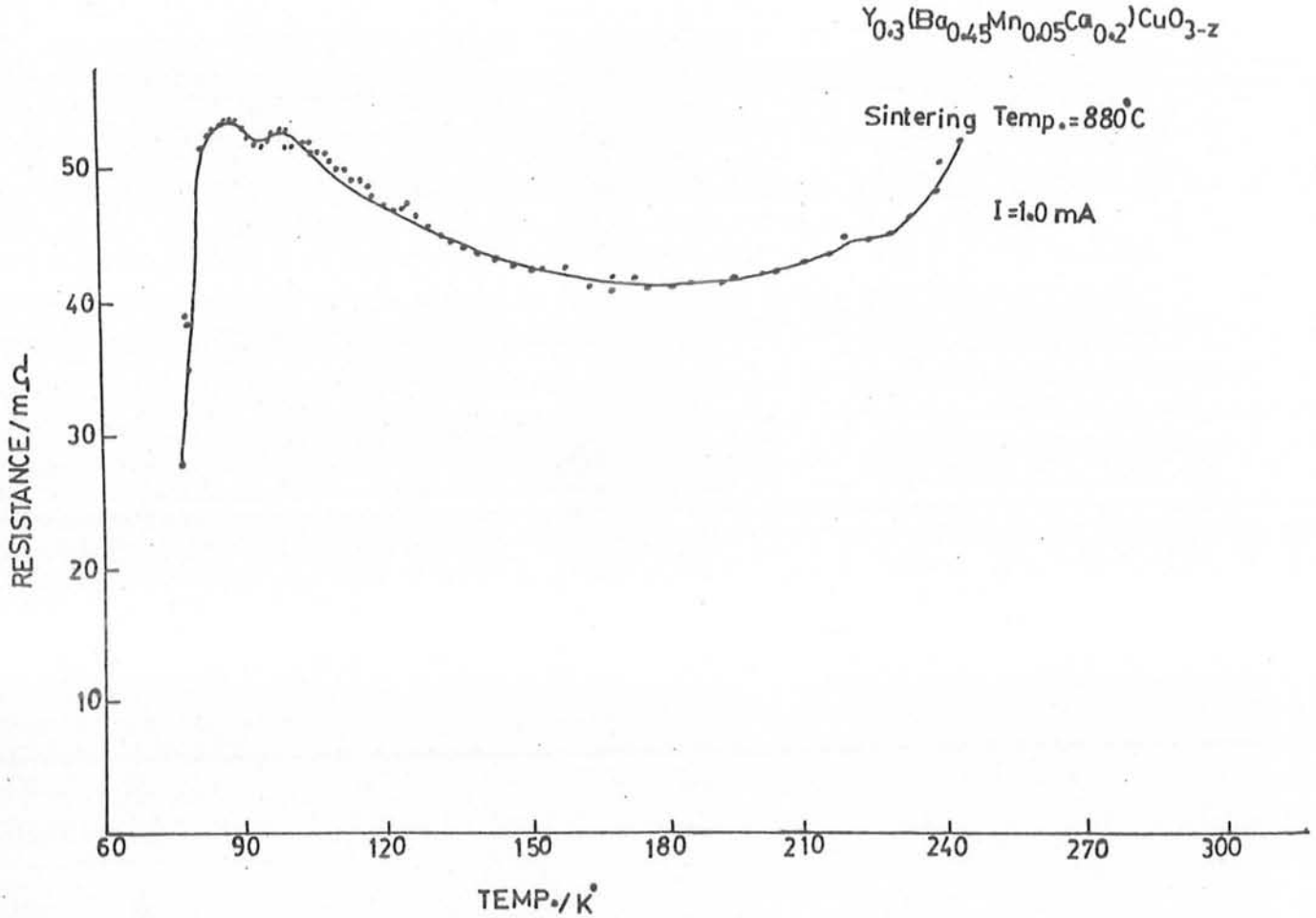
$Y_{0.3}(Ba_{0.45}Mn_{0.05}Ca_{0.2})CuO_{3-z}$
Sintering Temp.=880°C
I=1.0 mA
RESISTANCE/mΩ
50
40
30
20
10
60
90
120
150
180
210
240
270
300
TEMP./K°

FIG. 4.2-B

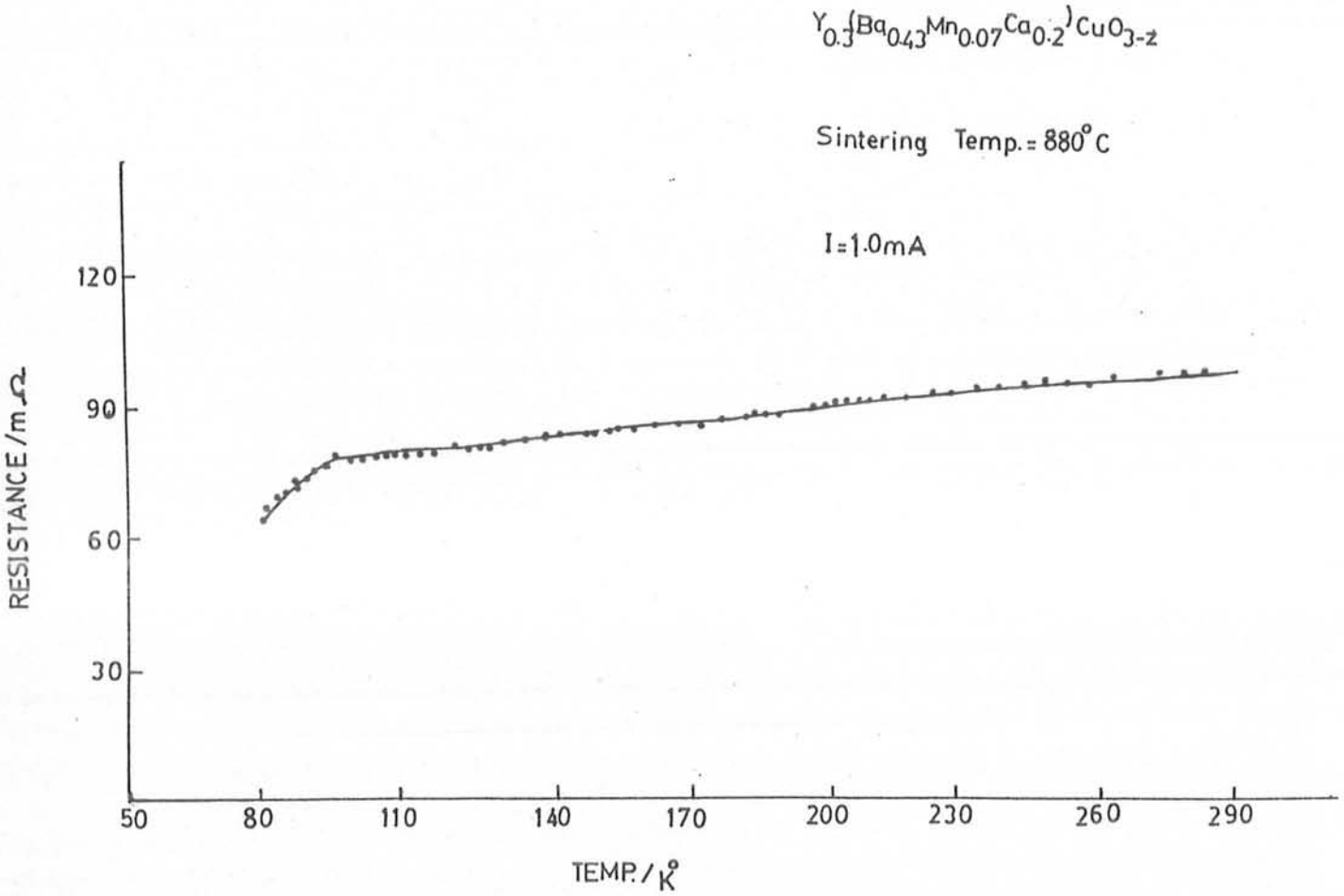
$Y_{0.3}\{Ba_{0.43}Mn_{0.07}Ca_{0.2}\}CuO_{3-z}$
Sintering Temp. = 880°C
I = 1.0mA
RESISTANCE / mΩ
120
90
60
30
50
80
110
140
170
200
230
260
290
TEMP. / K°

FIG. 4.3-A

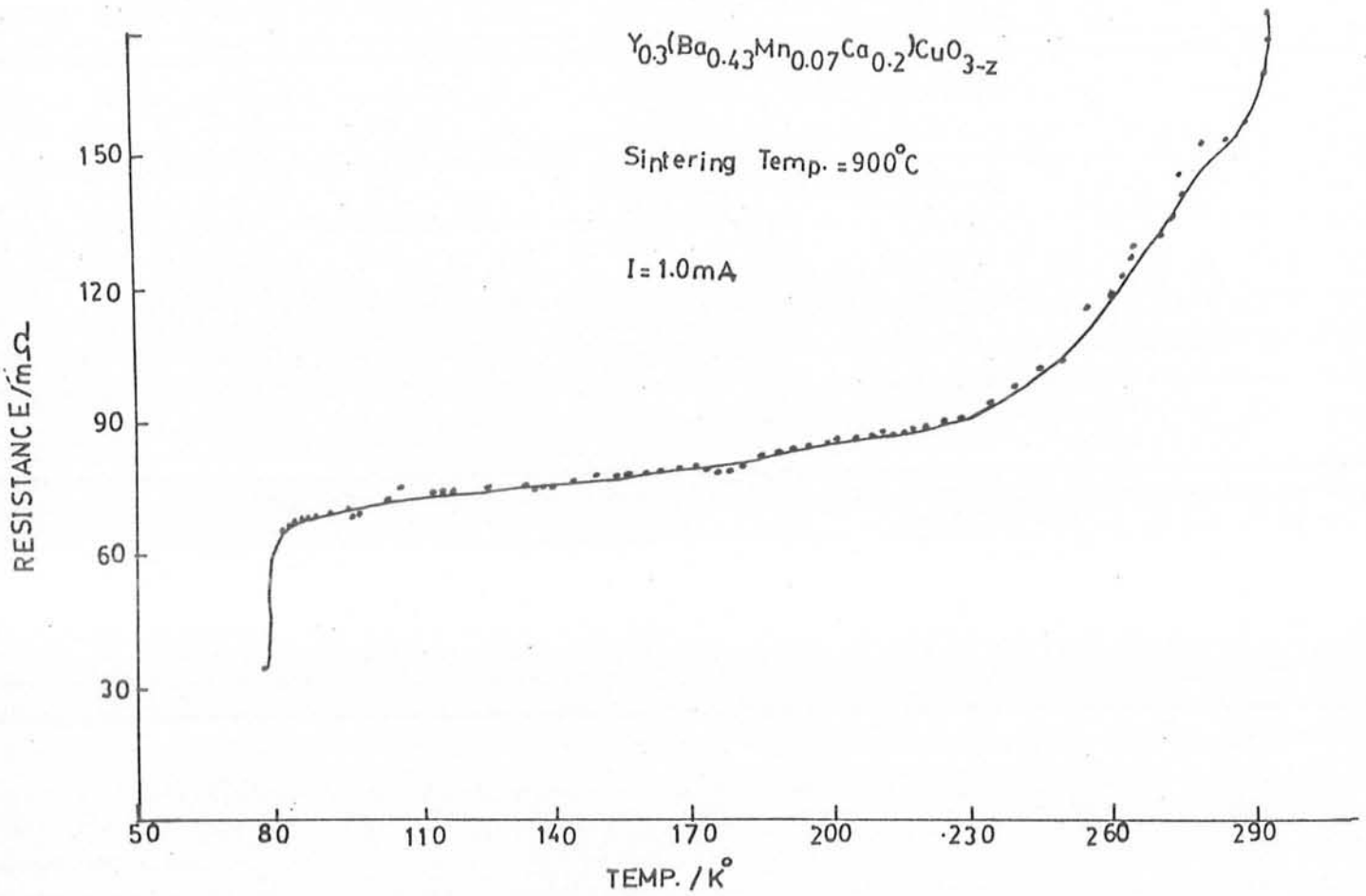
$Y_{0.3}(Ba_{0.43}Mn_{0.07}Ca_{0.2})CuO_{3-z}$
Sintering Temp. = 900°C
I = 1.0mA
RESISTANCE/mΩ
150
120
90
60
30
50
80
110
140
170
200
230
260
290
TEMP. / K°

FIG. 4.3-B

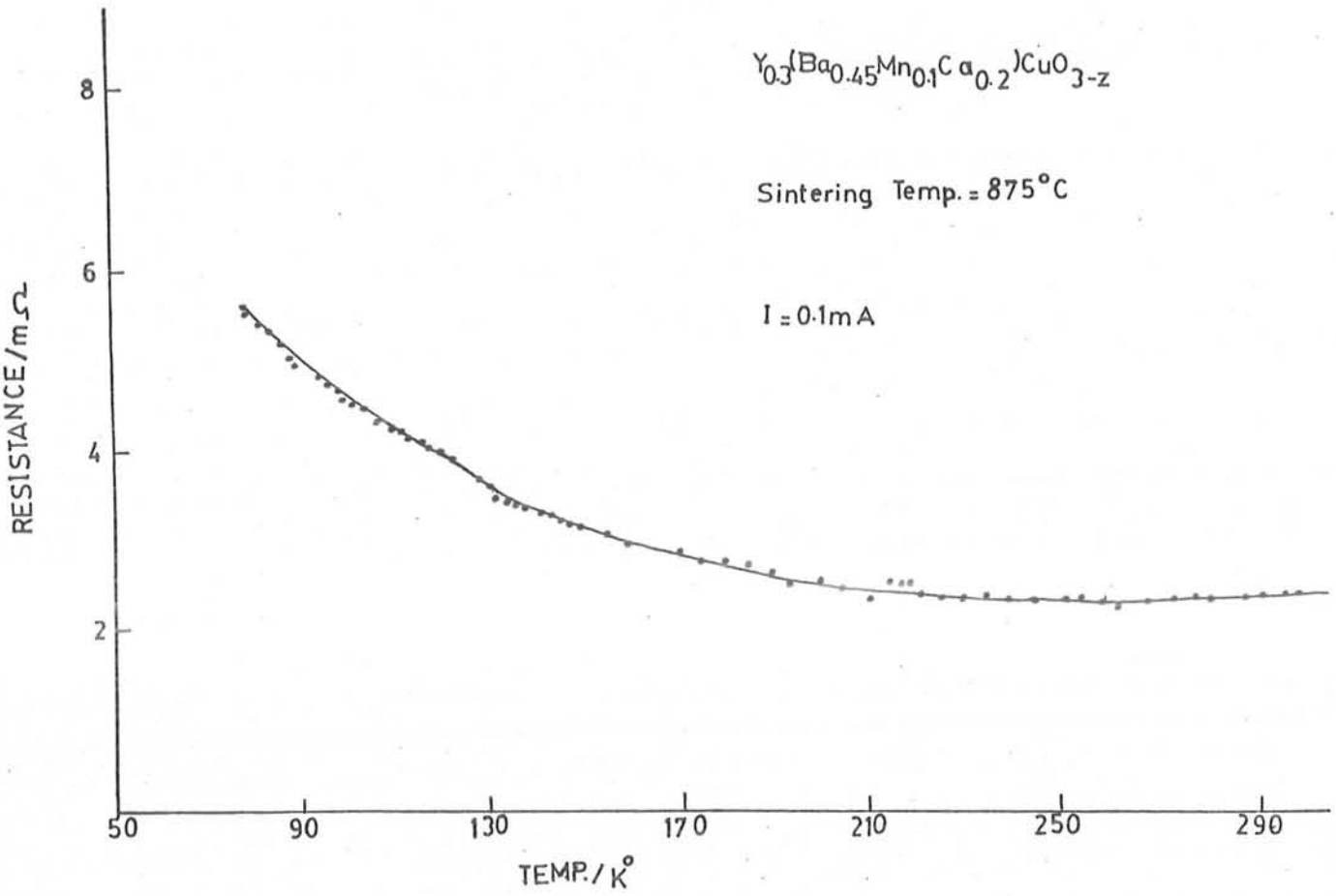
$Y_{0.3}(Ba_{0.45}Mn_{0.1}Ca_{0.2})CuO_{3-z}$
Sintering Temp. = 875°C
I = 0.1mA
RESISTANCE/mΩ
8
6
4
2
50
90
130
170
210
250
290
TEMP./K°

FIG. 4.4

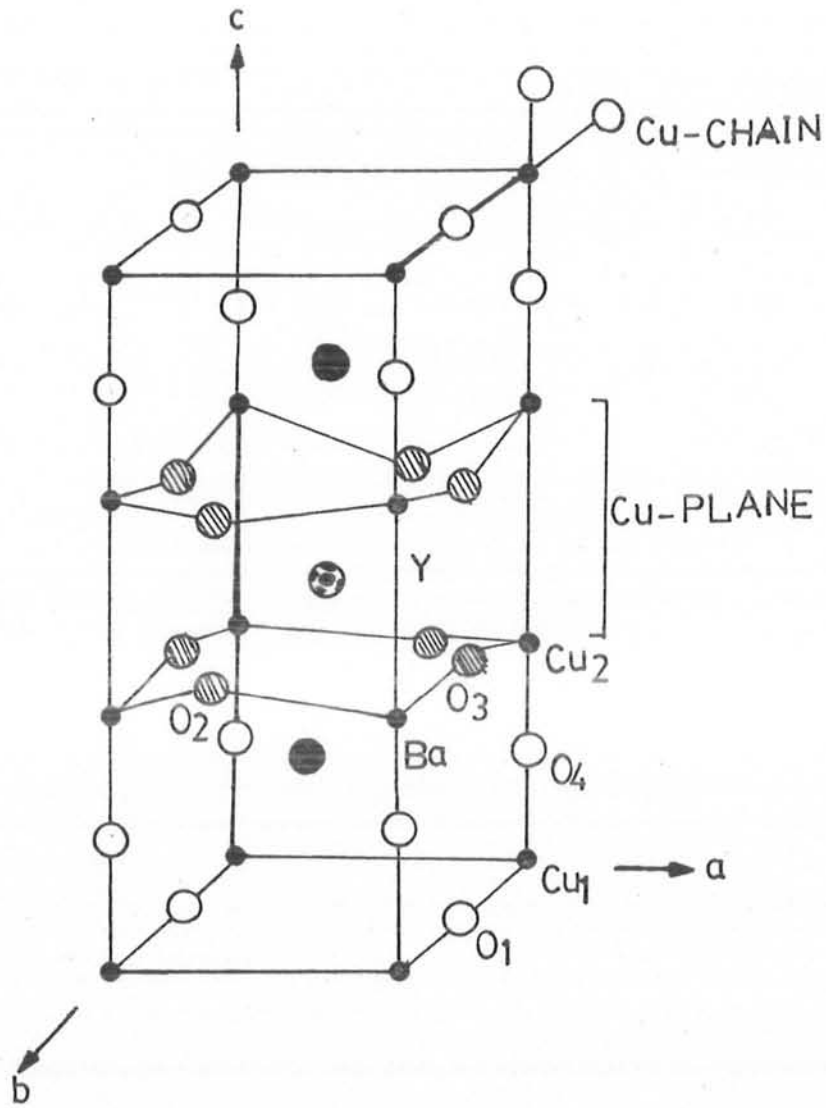

The Crystal Structure of $YBa_2Cu_3O_{7-\delta}$

FIG. 4.5

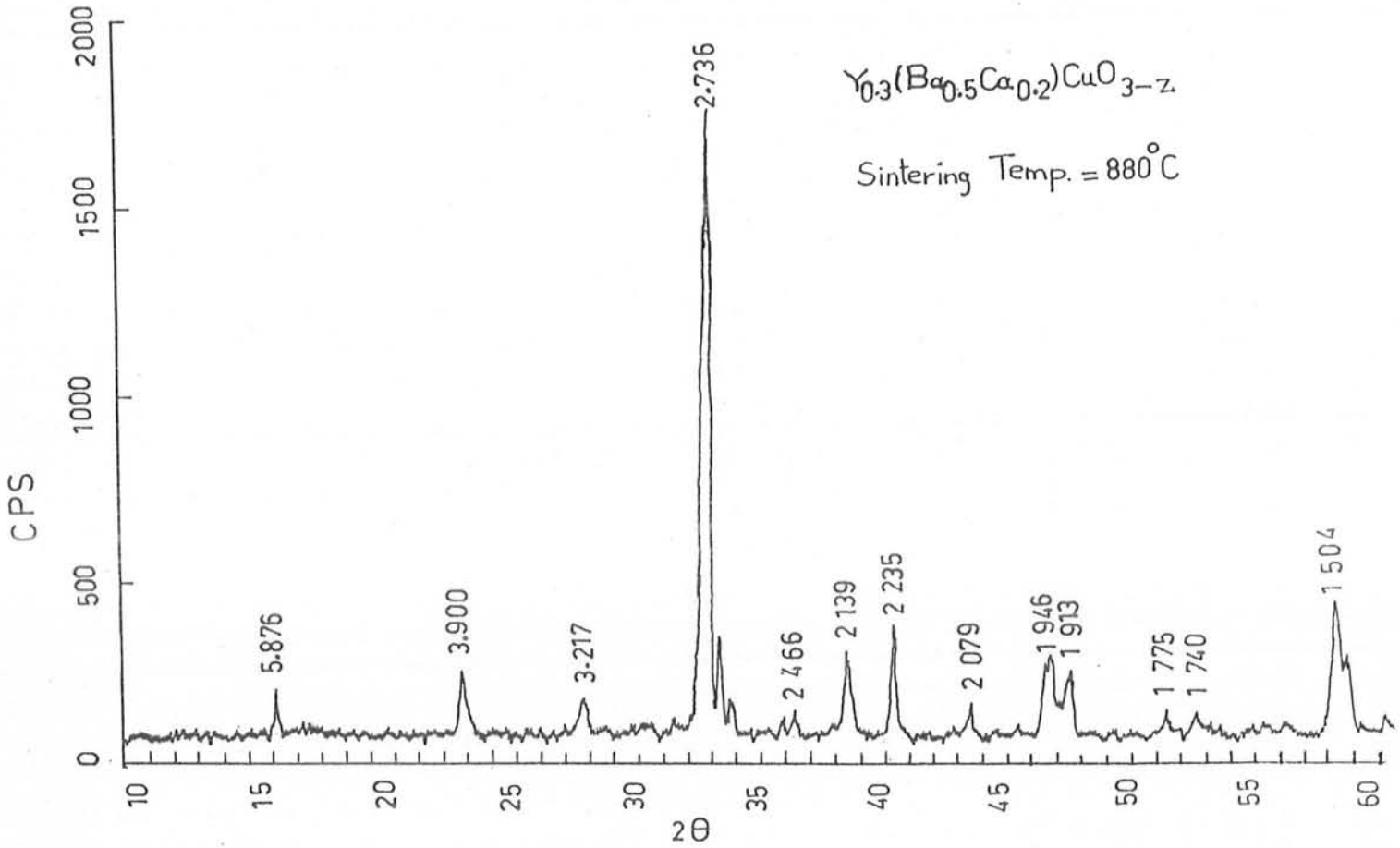
$Y_{0.3}(Ba_{0.5}Ca_{0.2})CuO_{3-z}$
Sintering Temp. = 880°C
CPS
2Θ
5.876
3.900
3.217
2.736
2 466
2 139
2 235
2 079
1 946
1 913
1 775
1 740
1 504

FIG. 4.6

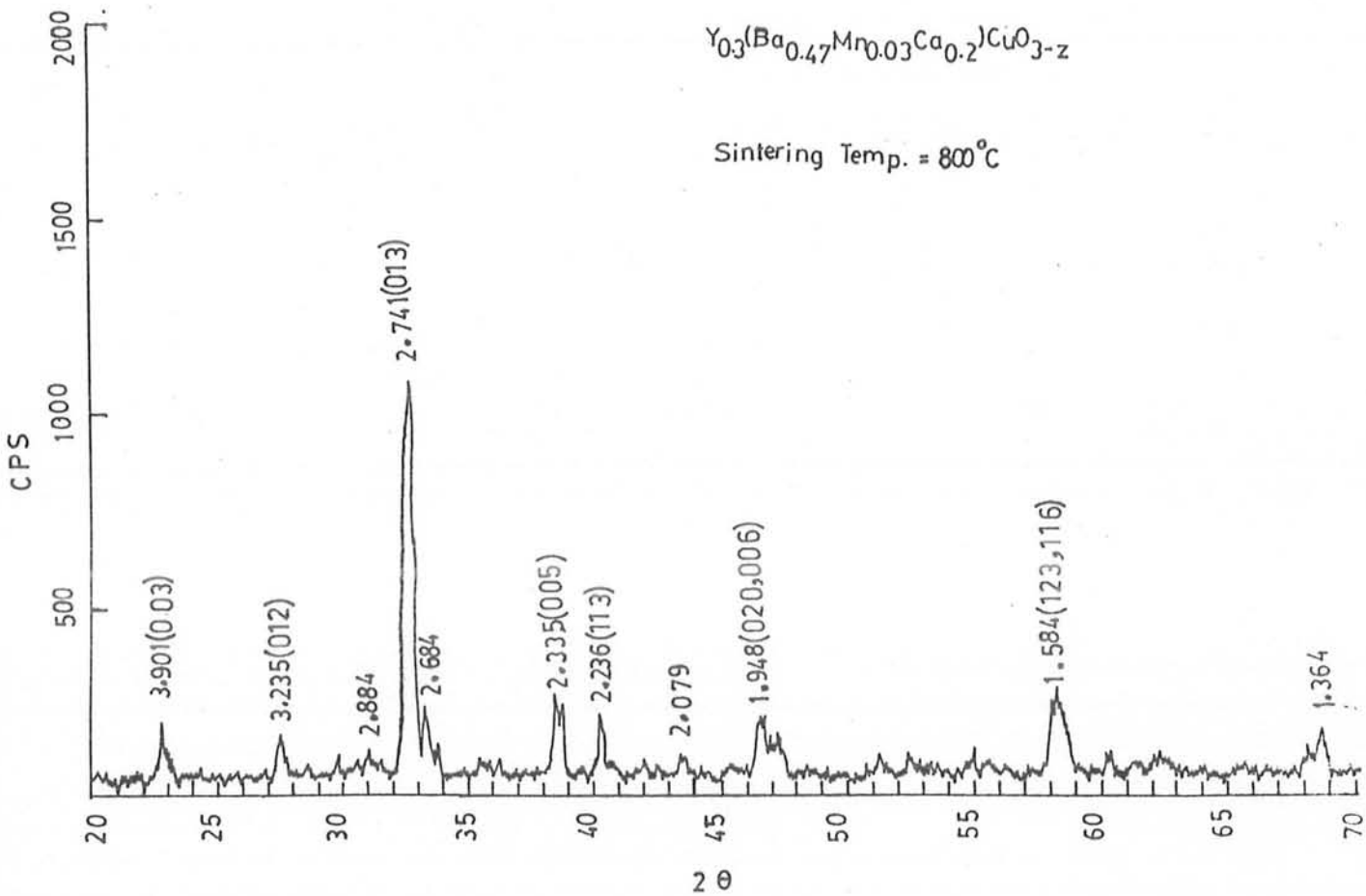
$Y_{0.3}(Ba_{0.47}Mn_{0.03}Ca_{0.2})CuO_{3-z}$
Sintering Temp. = 800°C
CPS
2000
1500
1000
500
3.901(003)
3.235(012)
2.884
2.741(013)
2.684
2.335(005)
2.236(113)
2.079
1.948(020,006)
1.584(123,116)
1.364
20
25
30
35
40
45
50
55
60
65
70
2θ

FIG. 4.7

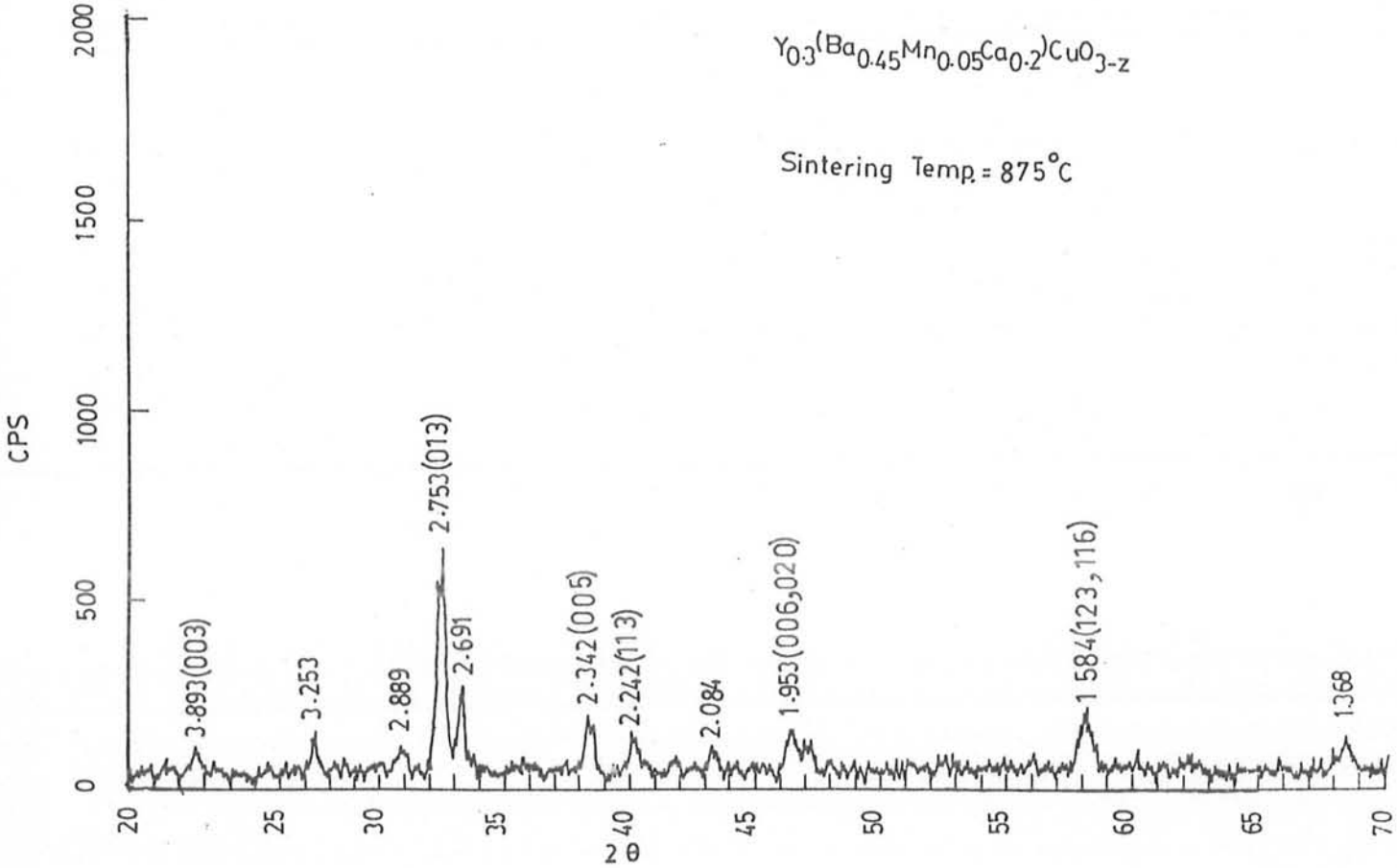
$Y_{0.3}(Ba_{0.45}Mn_{0.05}Ca_{0.2})CuO_{3-z}$
Sintering Temp. = 875°C
CPS
2θ
3.893(003)
3.253
2.889
2.753(013)
2.691
2.342(005)
2.242(113)
2.084
1.953(006,020)
1.584(123,116)
1.368

FIG. 4.8-A

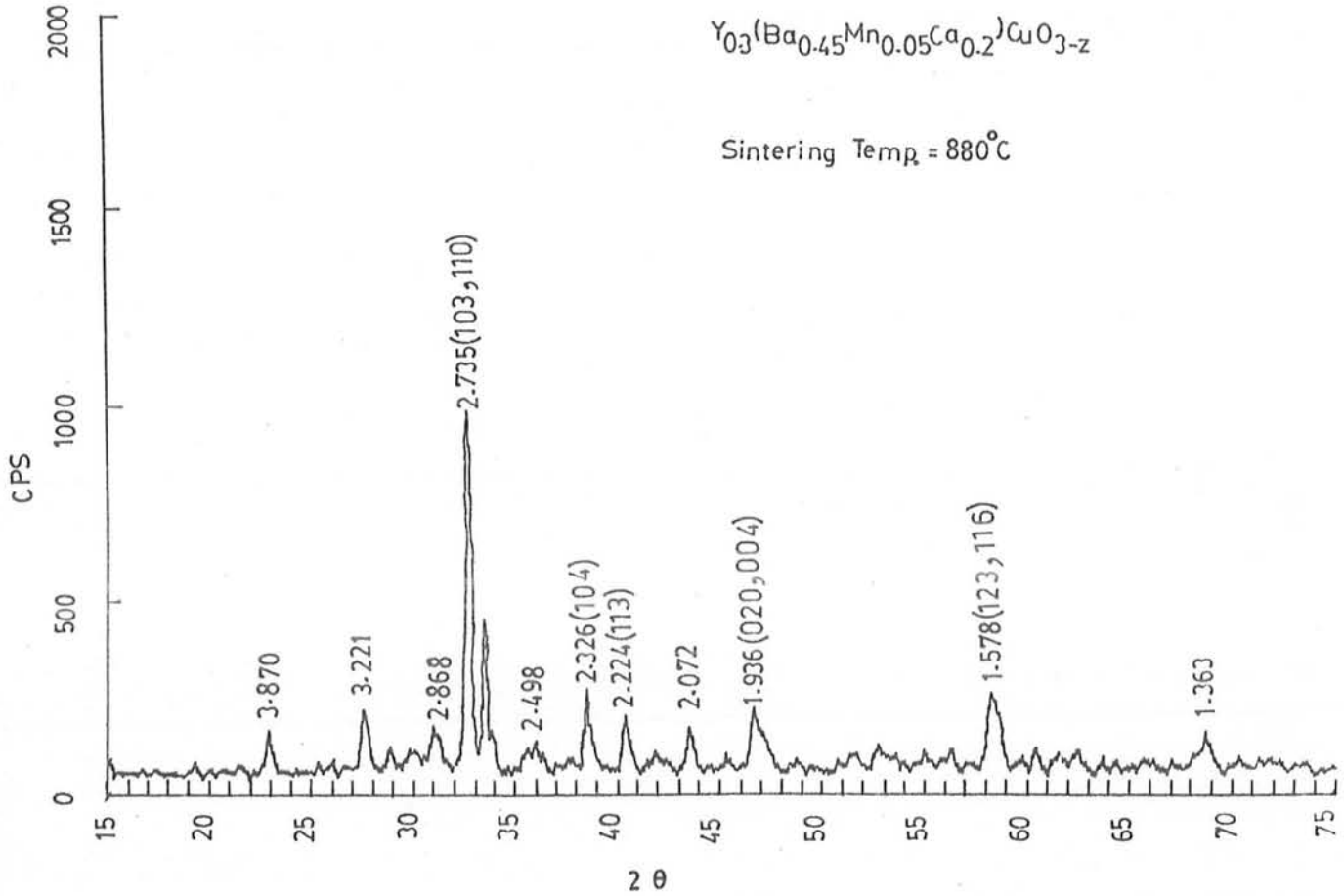
$Y_{03}(Ba_{0.45}Mn_{0.05}Ca_{0.2})Cu_{3-z}$
Sintering Temp. = 880°C
CPS
0
500
1000
1500
2000
3·870
3·221
2·868
2·735(103,110)
2·498
2·326(104)
2·224(113)
2·072
1·936(020,004)
1·578(123,116)
1·363
15
20
25
30
35
40
45
50
55
60
65
70
75
2θ

FIG. 4.8-B

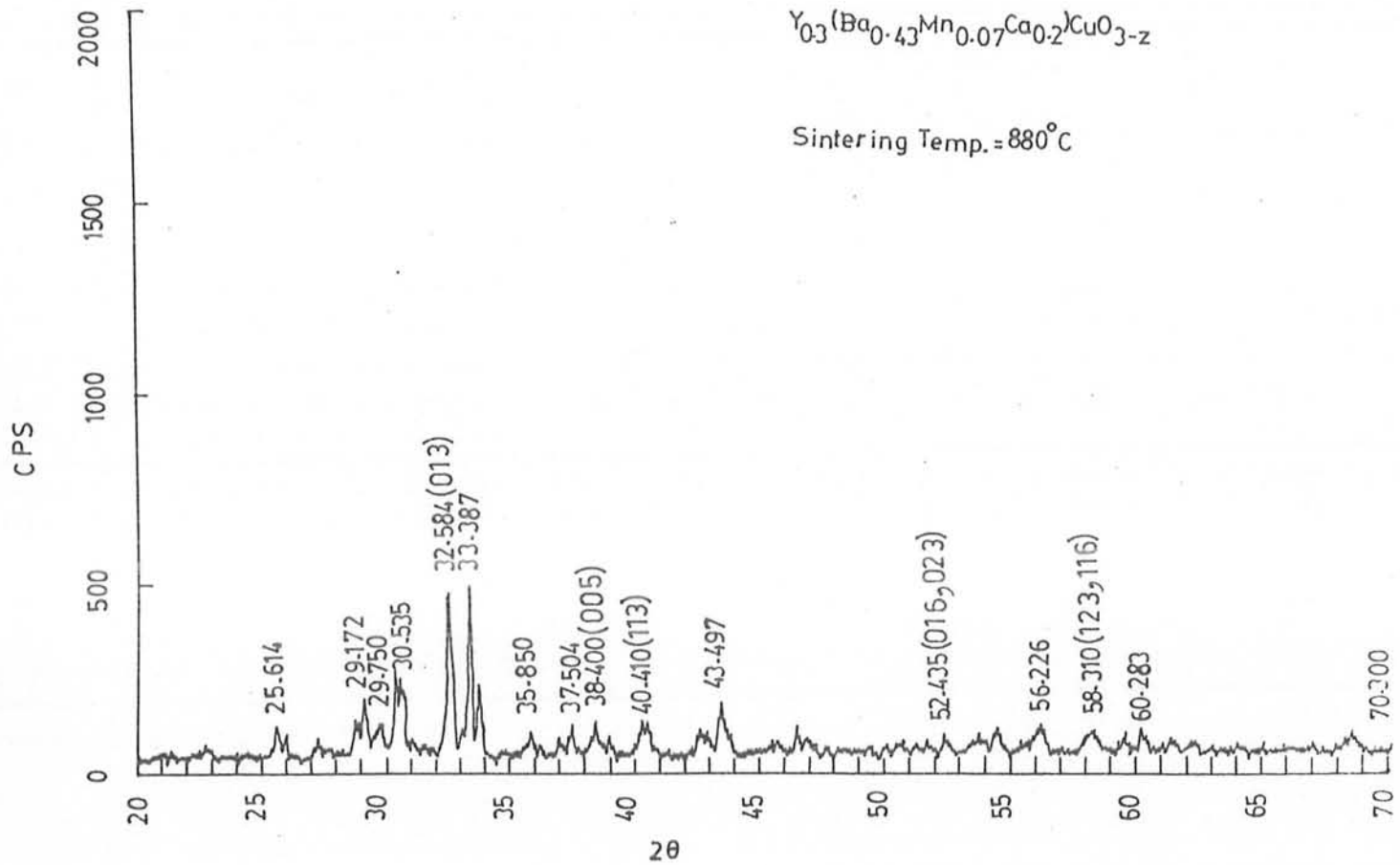
$Y_{0.3}(Ba_{0.43}Mn_{0.07}Ca_{0.2})CuO_{3-z}$
Sintering Temp. = 880°C
CPS
2θ
25.614
29.172
29.750
30.535
32.584(013)
33.387
35.850
37.504
38.400(005)
40.410(113)
43.497
52.435(016,023)
56.226
58.310(123,116)
60.283
70.300

FIG. 4.9-A

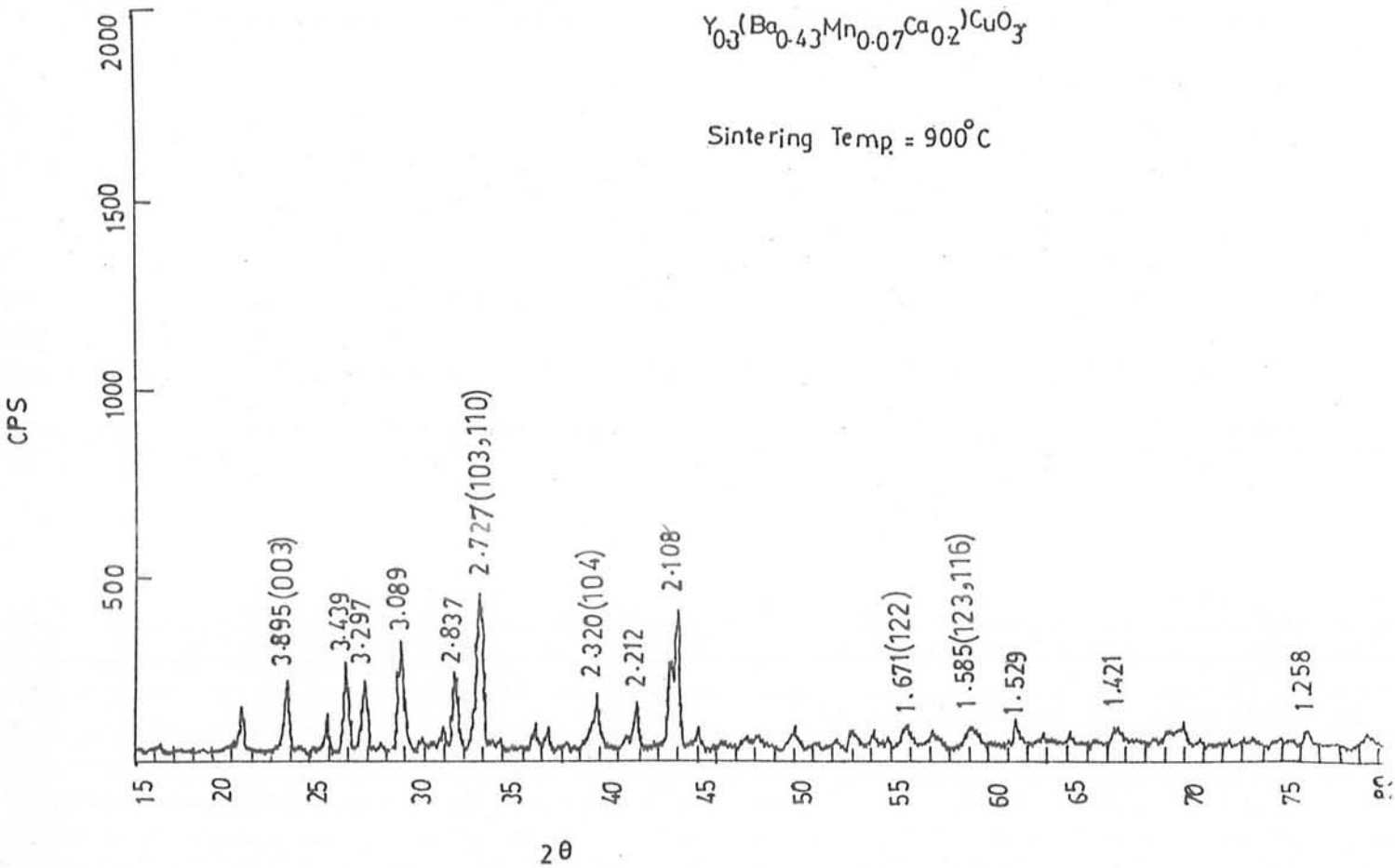
$Y_{03}(Ba_{0.43}Mn_{0.07}Ca_{0.2})CuO_3$
Sintering Temp. = 900°C
CPS
2000
1500
1000
500
3.895(003)
3.439
3.297
3.089
2.837
2.727(103,110)
2.320(104)
2.212
2.108
1.671(122)
1.585(123,116)
1.529
1.421
1.258
15
20
25
30
35
40
45
50
55
60
65
70
75
2θ

FIG. 4.9-B

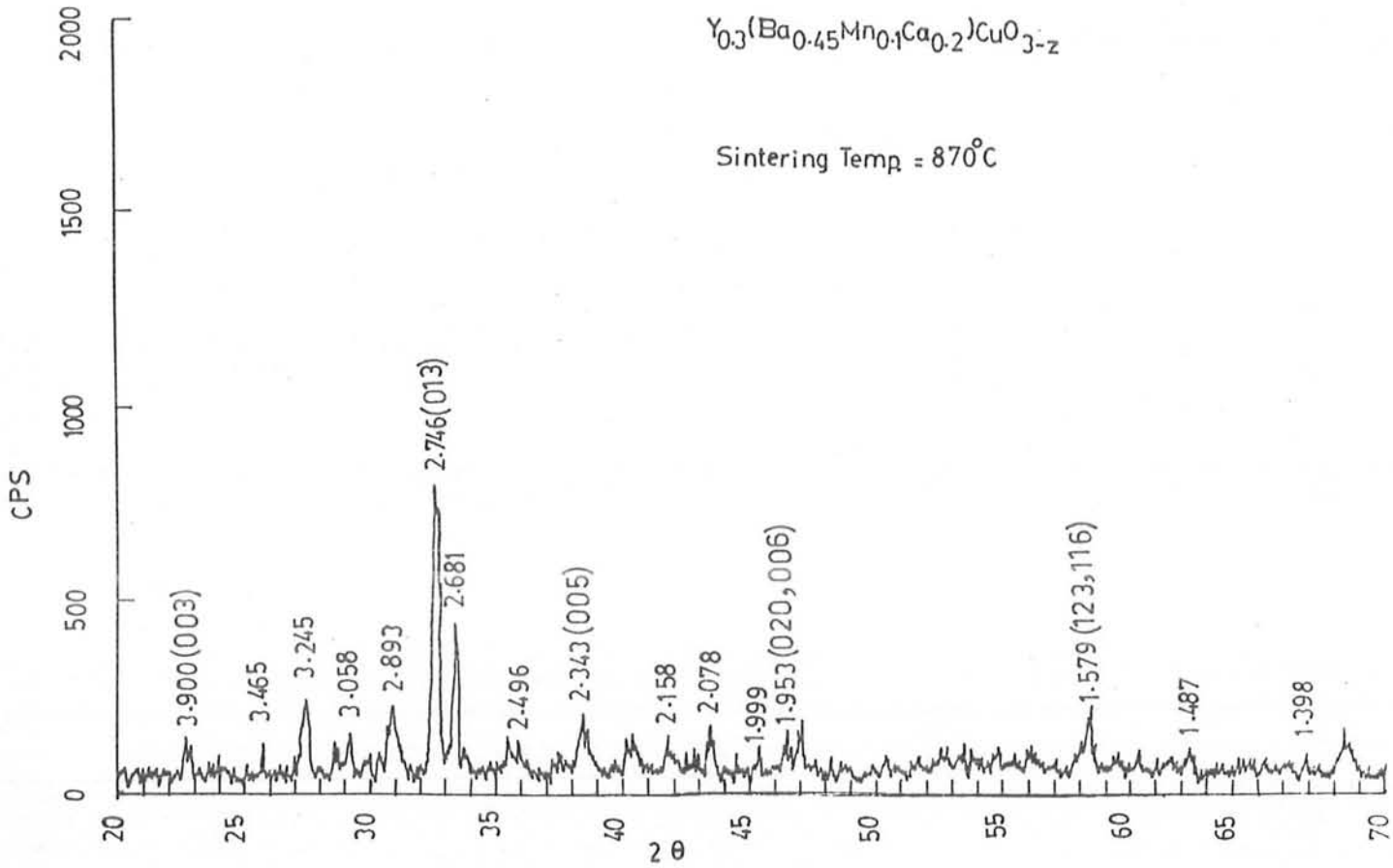
$Y_{0.3}(Ba_{0.45}Mn_{0.1}Ca_{0.2})CuO_{3-z}$
Sintering Temp = 870°C
CPS
2θ
3.900(003)
3.465
3.245
3.058
2.893
2.746(013)
2.681
2.496
2.343(005)
2.158
2.078
1.999
1.953(020,006)
1.579(123,116)
1.487
1.398

FIG. 4.10-A

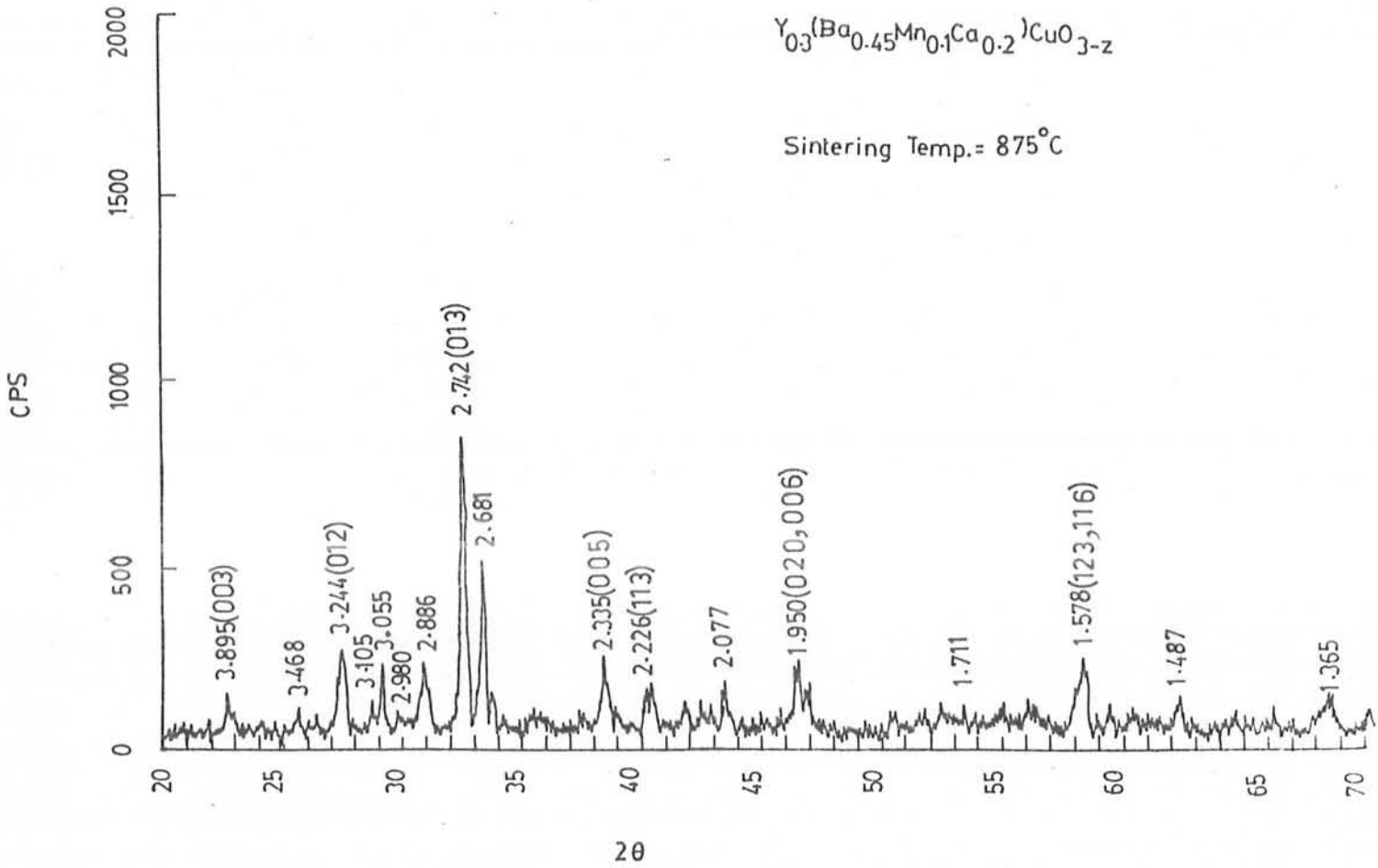
$Y_{0.3}(Ba_{0.45}Mn_{0.1}Ca_{0.2})CuO_{3-z}$
Sintering Temp.= 875°C
CPS
2θ
3.895(003)
3.468
3.244(012)
3.105
3.055
2.980
2.886
2.742(013)
2.681
2.335(005)
2.226(113)
2.077
1.950(020,006)
1.711
1.578(123,116)
1.487
1.365

FIG. 4.10-B

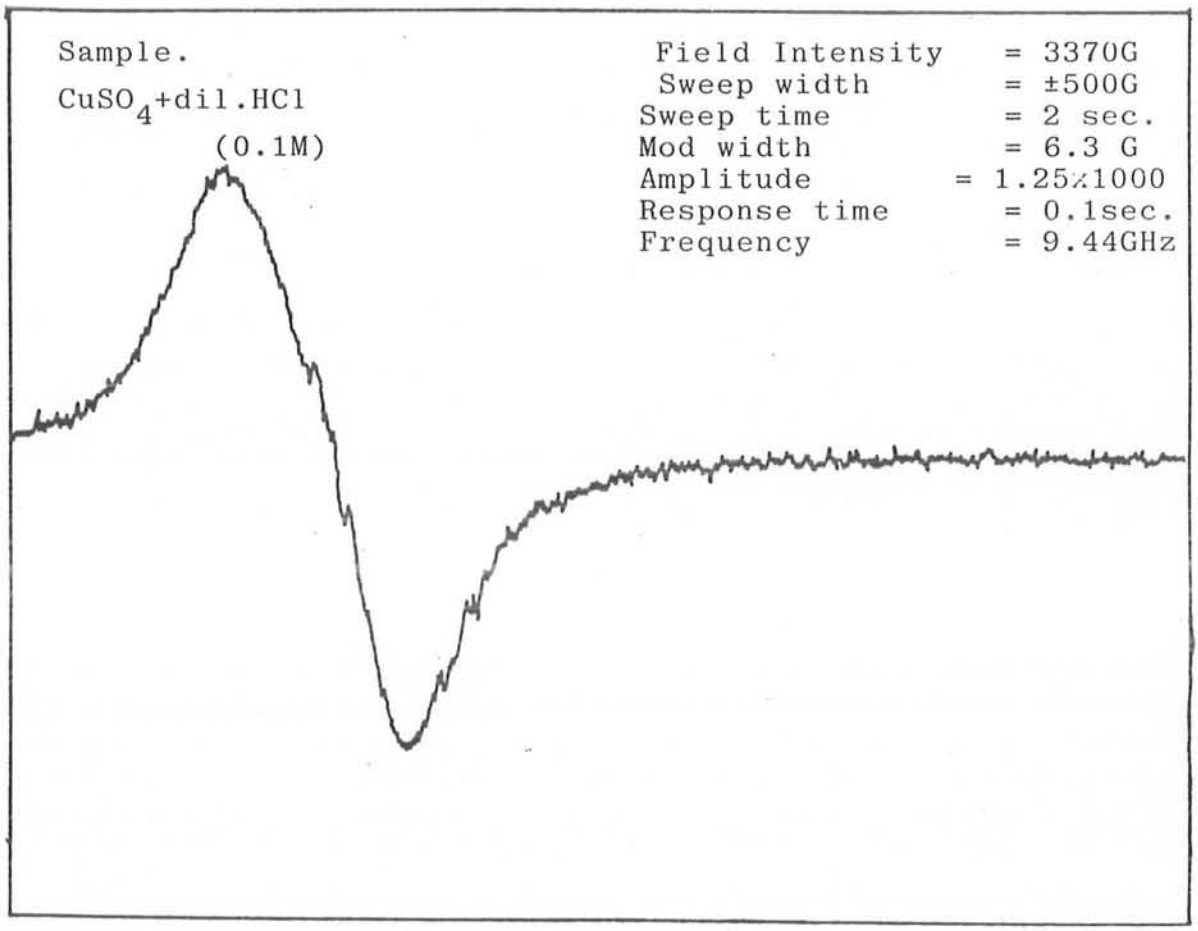
Sample.
$CuSO_4$+dil.HCl
(0.1M)
Field Intensity = 3370G
Sweep width = ±500G
Sweep time = 2 sec.
Mod width = 6.3 G
Amplitude = 1.25x1000
Response time = 0.1sec.
Frequency = 9.44GHz

FIG. 4.11

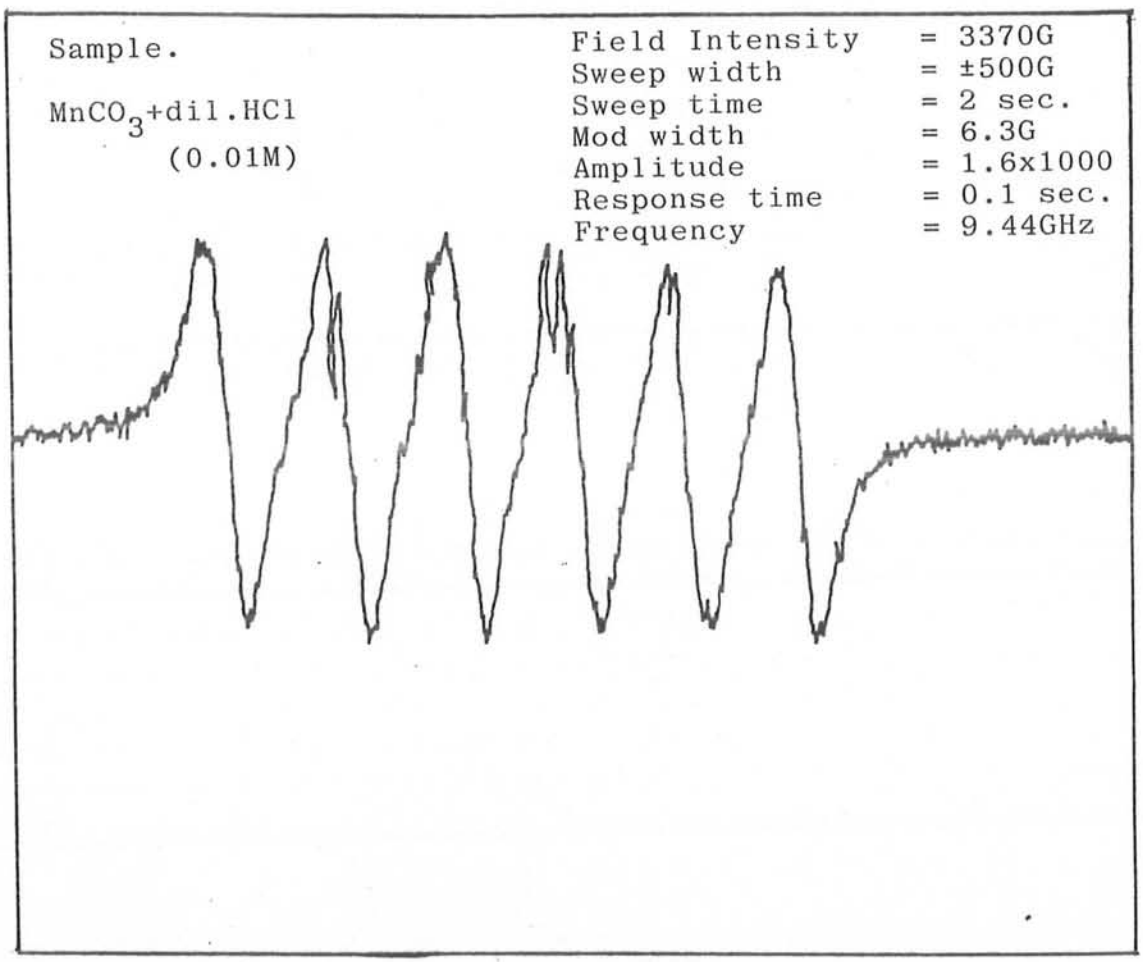
Sample.
$MnCO_3$+dil.HCl
(0.01M)
Field Intensity = 3370G
Sweep width = ±500G
Sweep time = 2 sec.
Mod width = 6.3G
Amplitude = 1.6x1000
Response time = 0.1 sec.
Frequency = 9.44GHz

FIG. 4.12

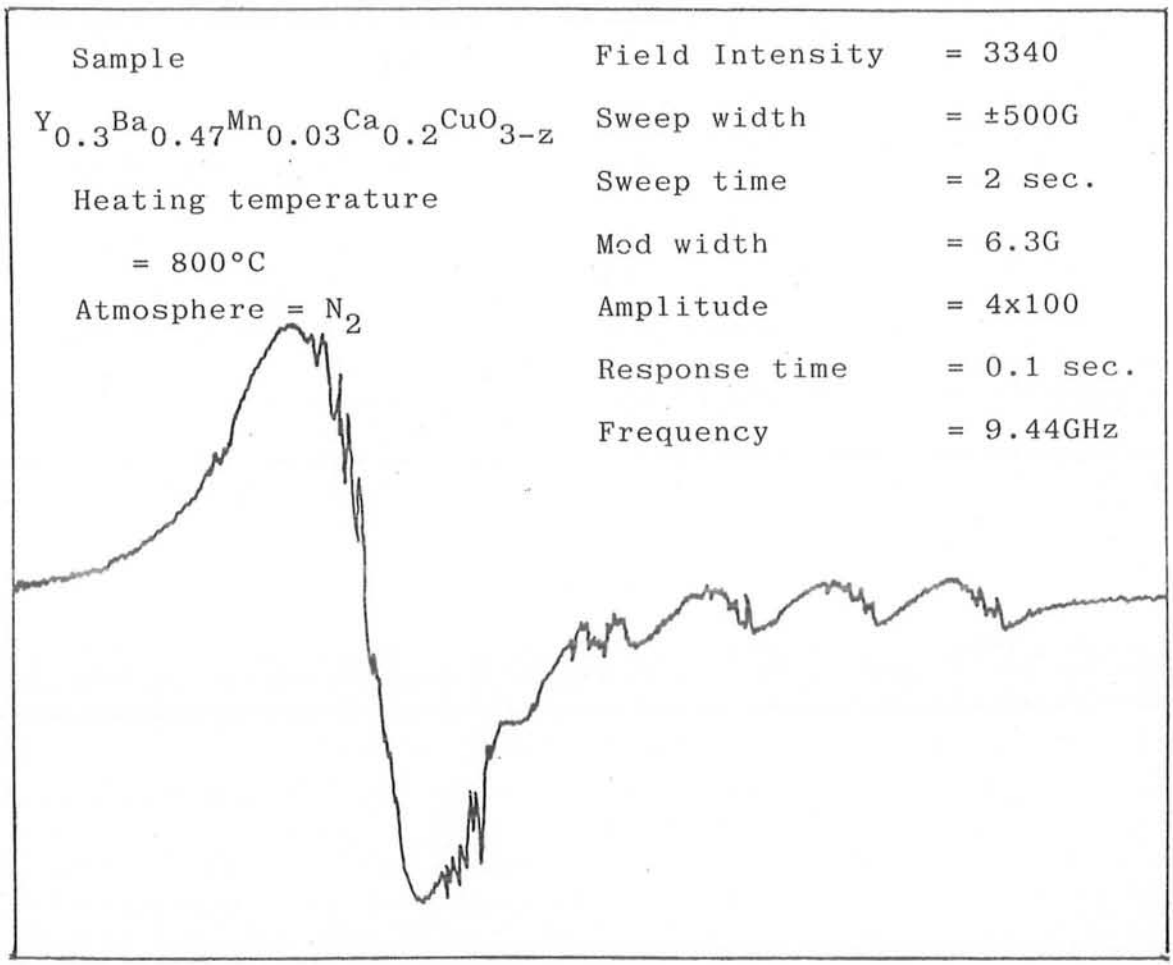
Sample
$Y_{0.3}Ba_{0.47}Mn_{0.03}Ca_{0.2}CuO_{3-z}$
Heating temperature
= 800°C
Atmosphere = N_2
Field Intensity = 3340
Sweep width = ±500G
Sweep time = 2 sec.
Mod width = 6.3G
Amplitude = 4x100
Response time = 0.1 sec.
Frequency = 9.44GHz

FIG. 4.13-A

Sample

$Y_{0.3}Ba_{0.47}Mn_{0.03}Ca_{0.2}CuO_{3-z}$

Temp.=820°C

Field Intensity = 3350G

Sweep width = ±500G

Sweep time = 2 sec.

Mod width = 6.3G

Amplitude = 2.5x100

Response time = 0.1 sec.

Frequency = 9.44GHz

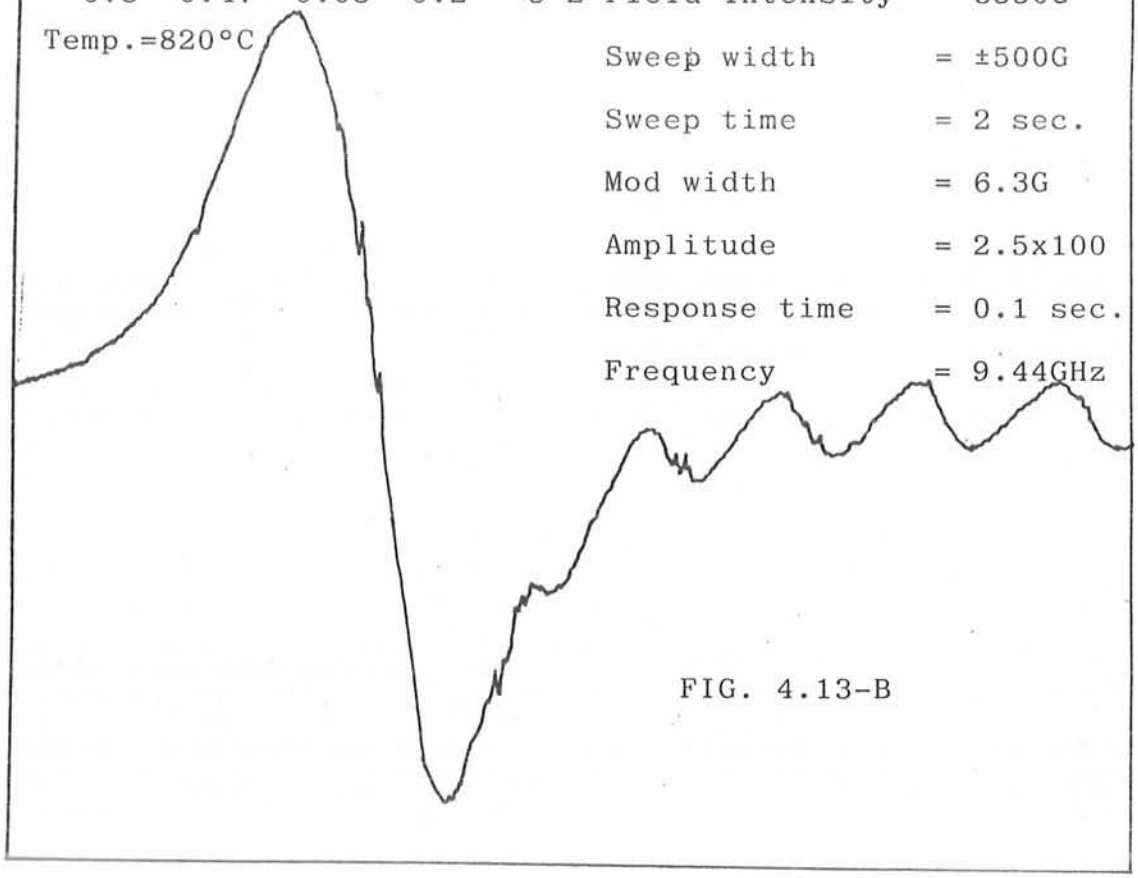

FIG. 4.13-B

Heating Temp. = 850°C

Field Intensity = 3370

a

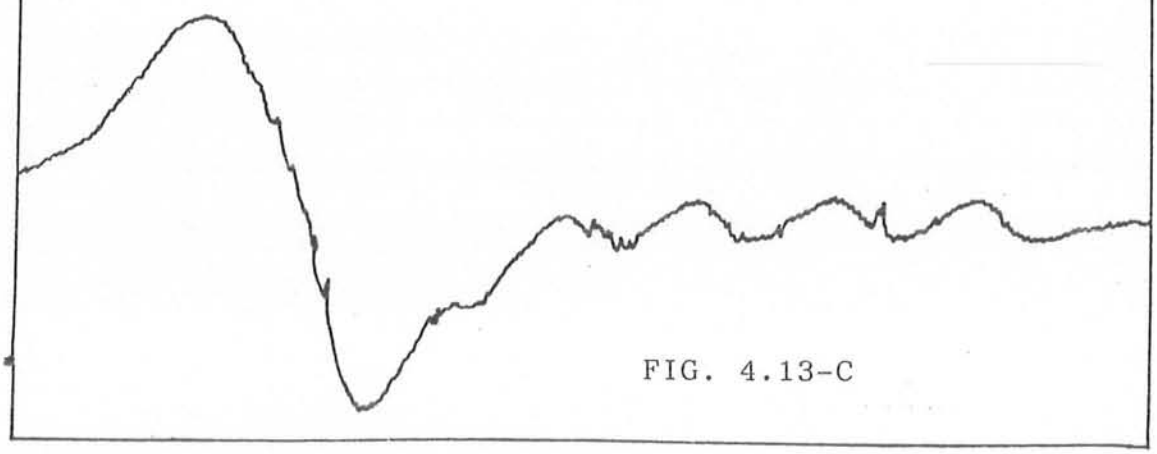

FIG. 4.13-C

a: same as above

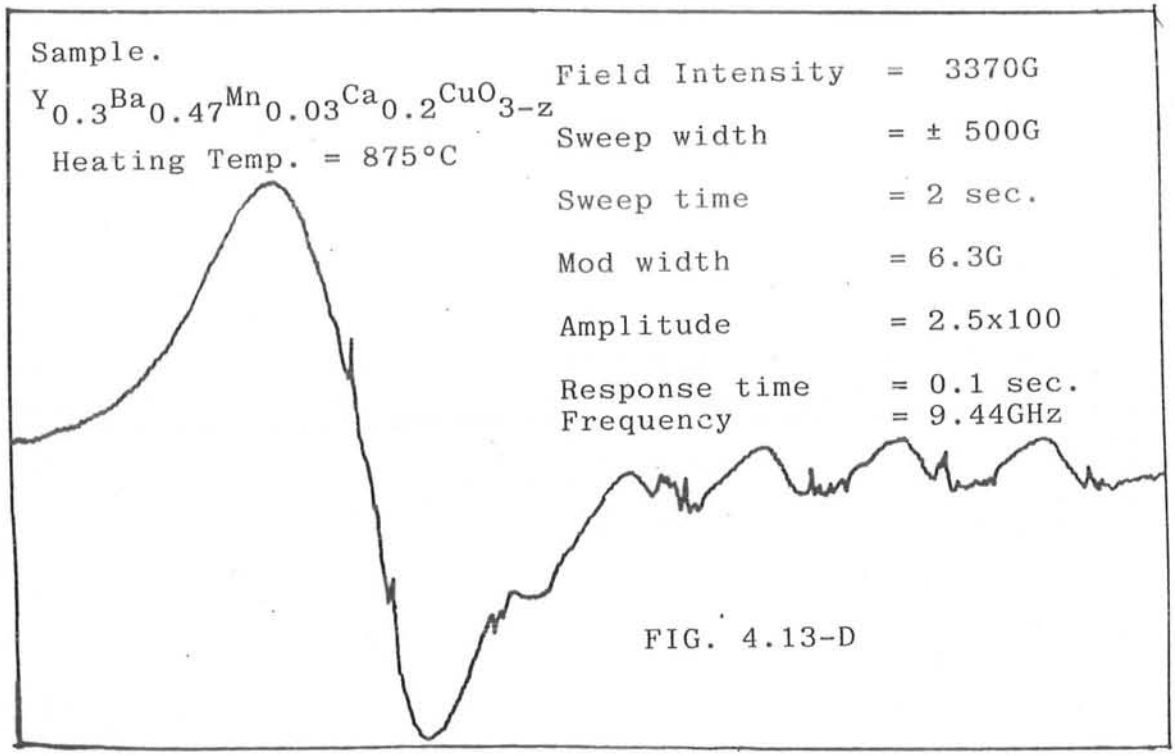

FIG. 4.13-D

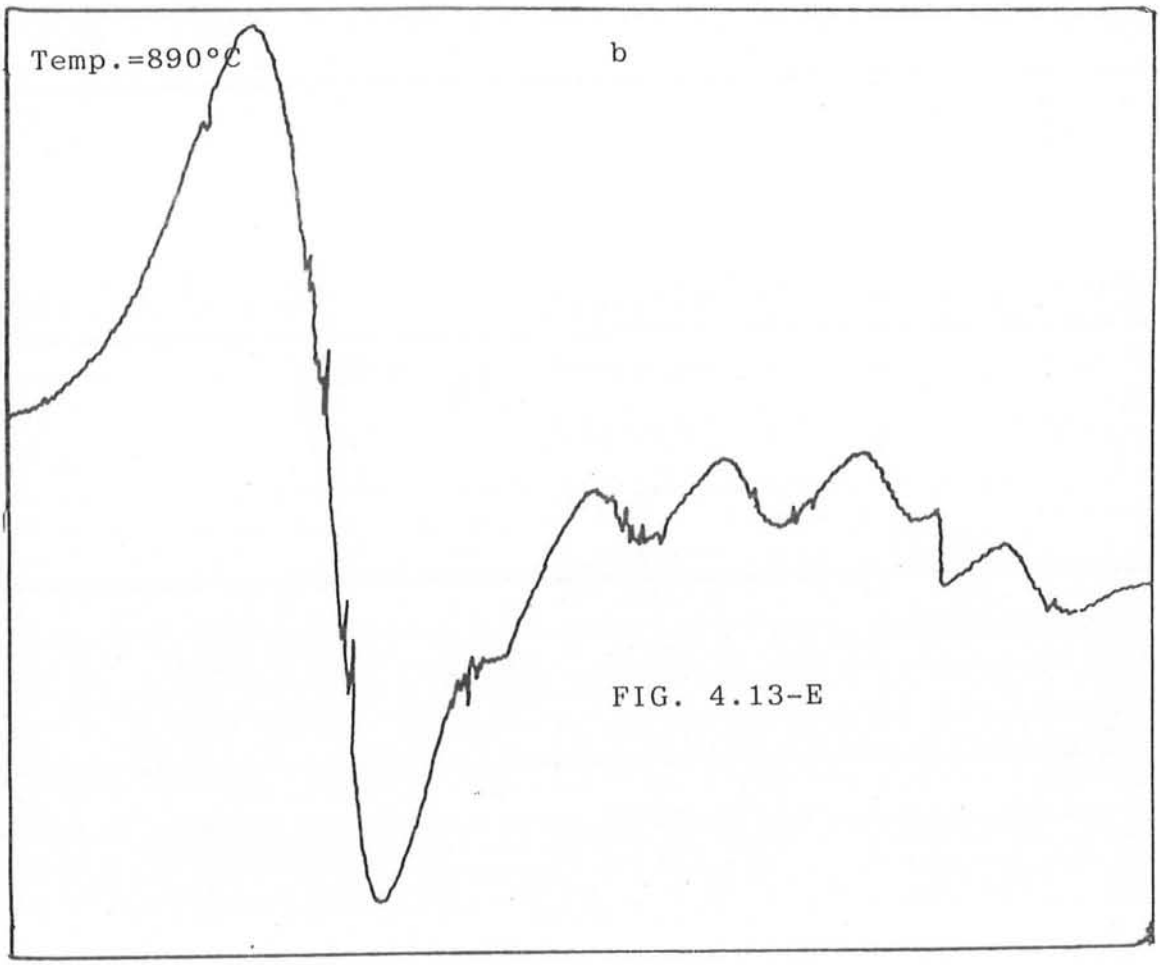

FIG. 4.13-E

b: same as above

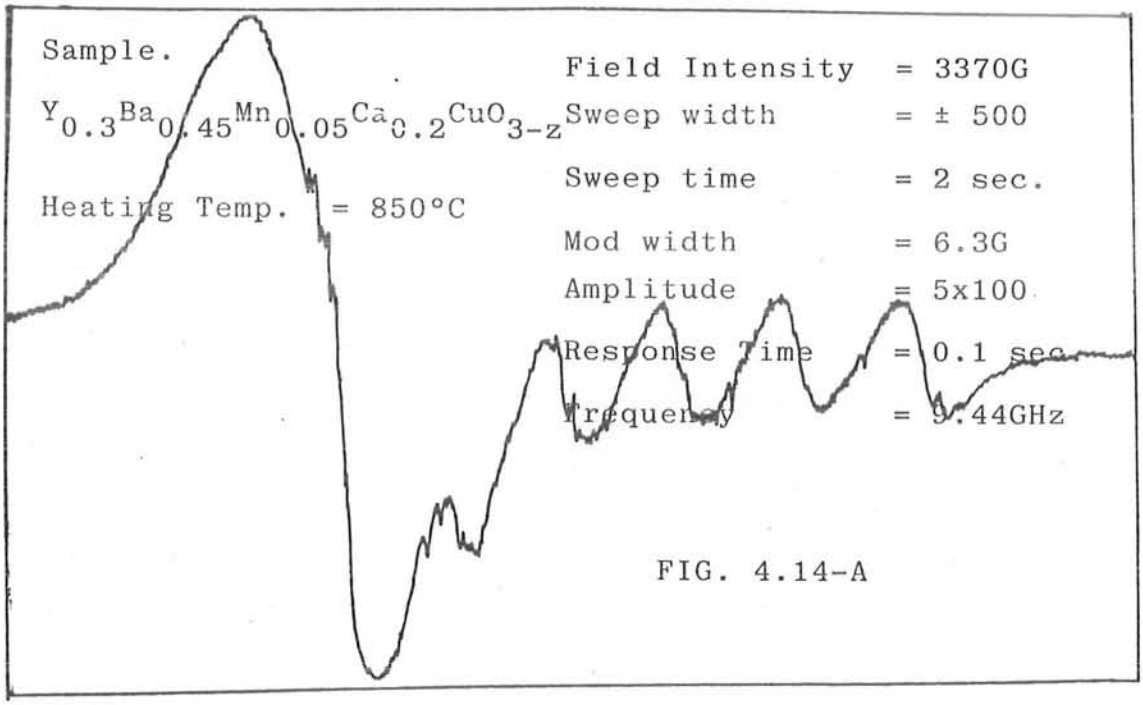

FIG. 4.14-A

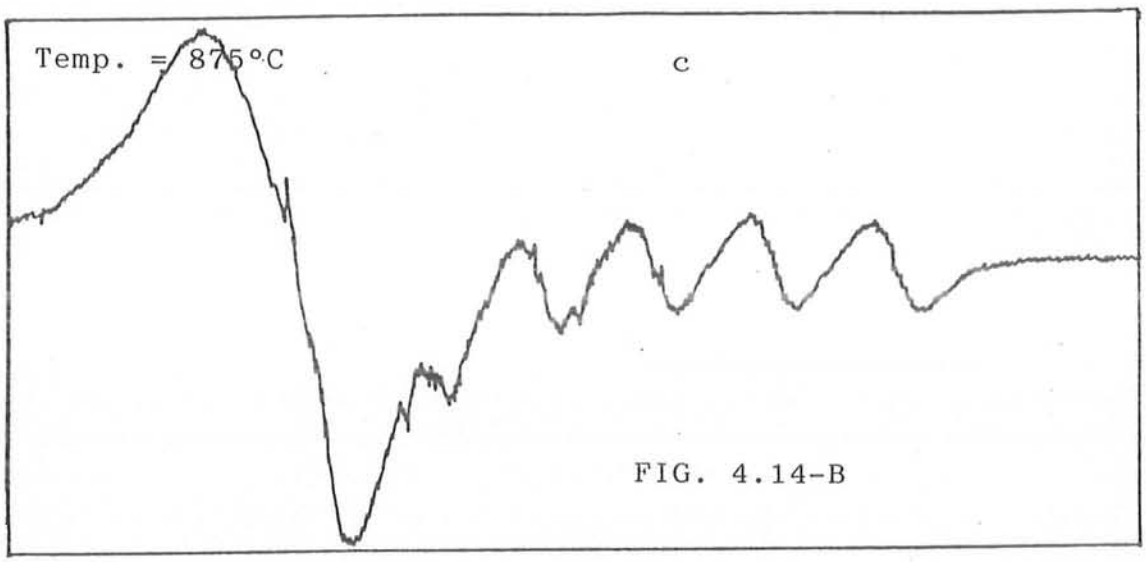

FIG. 4.14-B

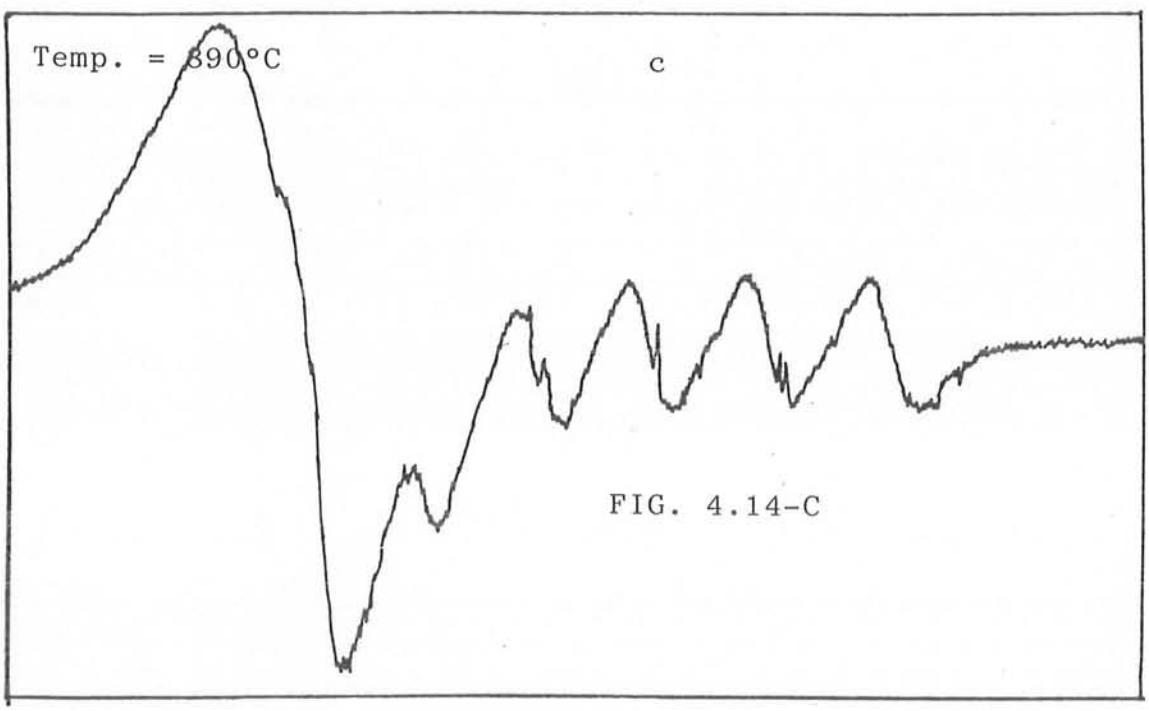

FIG. 4.14-C

c: same as above

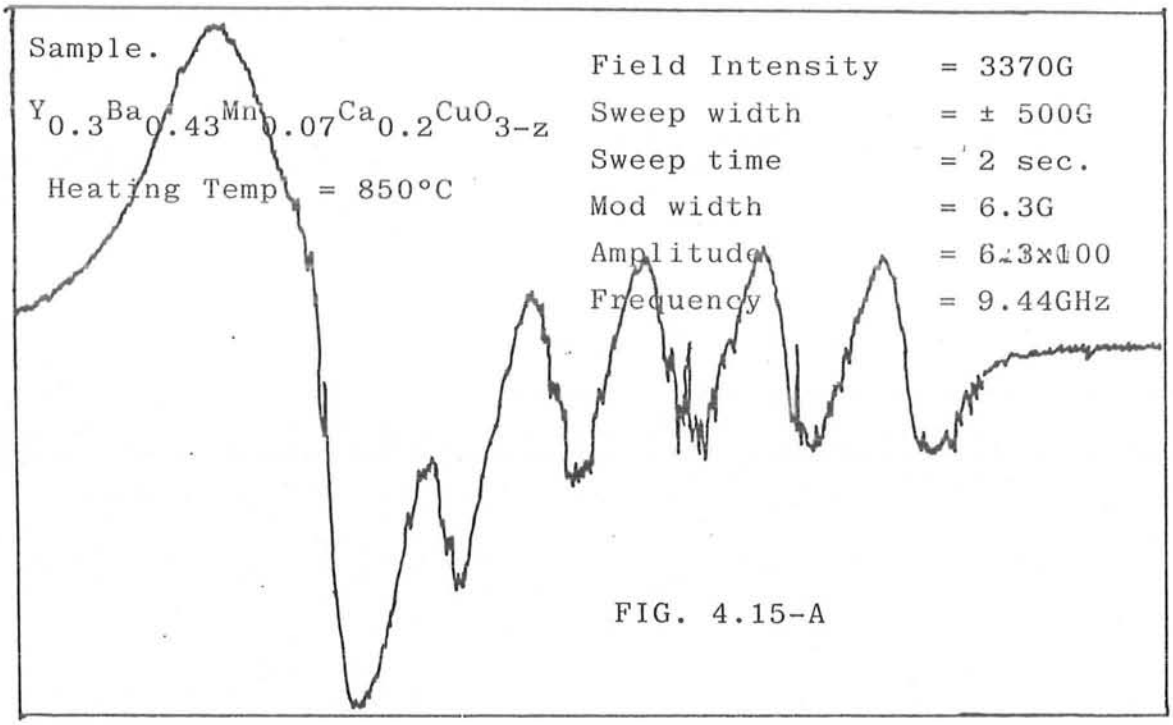

FIG. 4.15-A

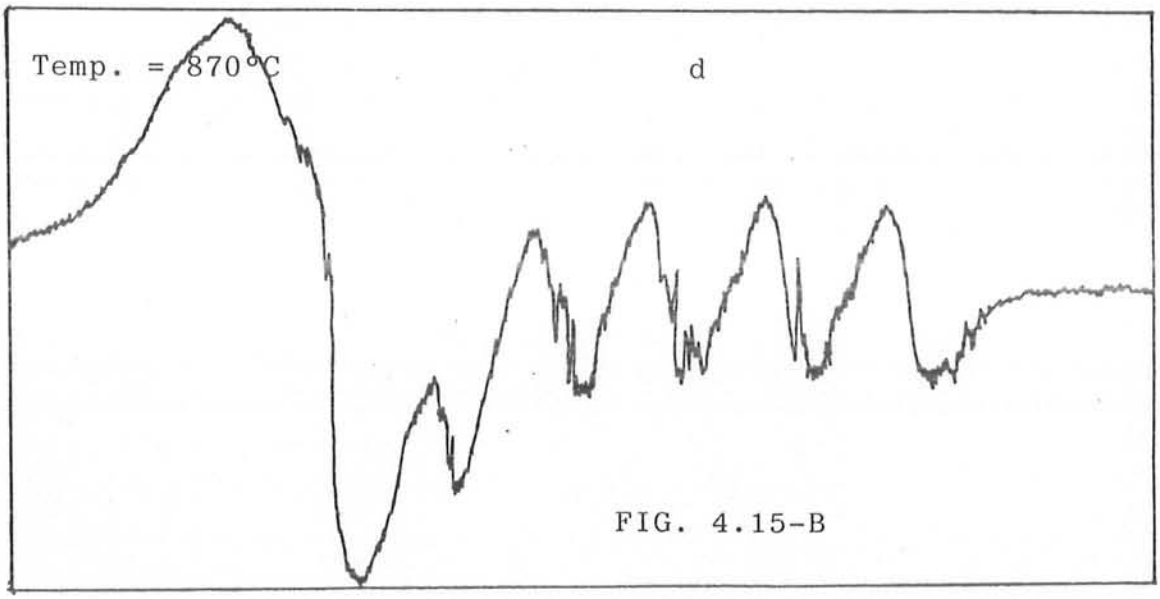

FIG. 4.15-B

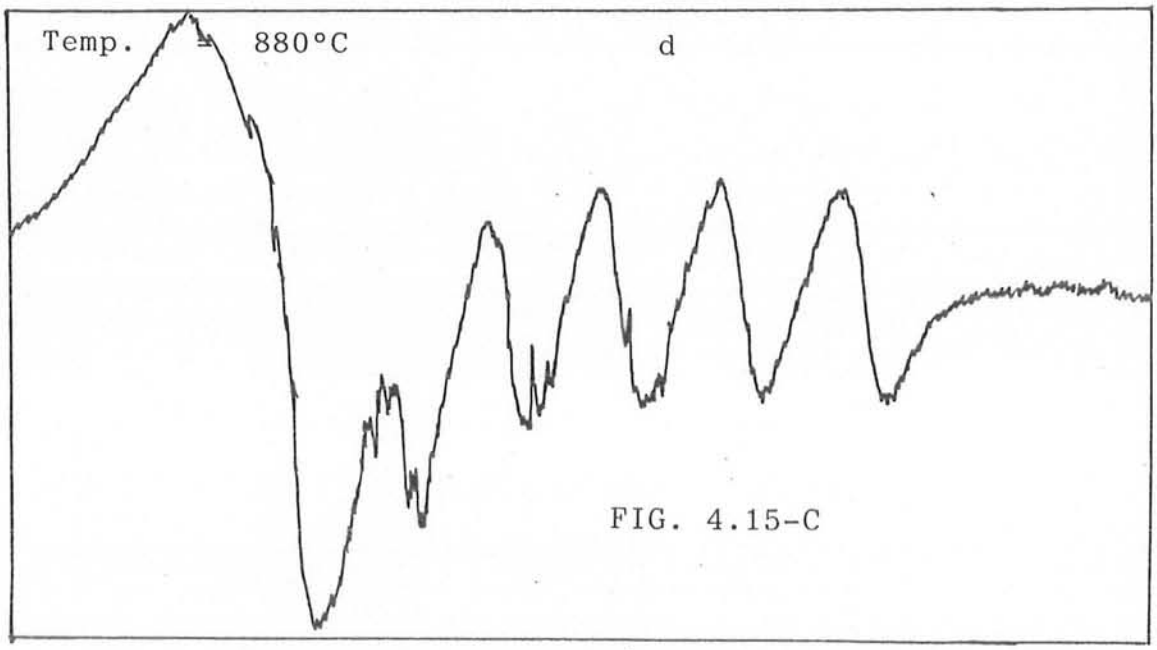

FIG. 4.15-C

d: same as above

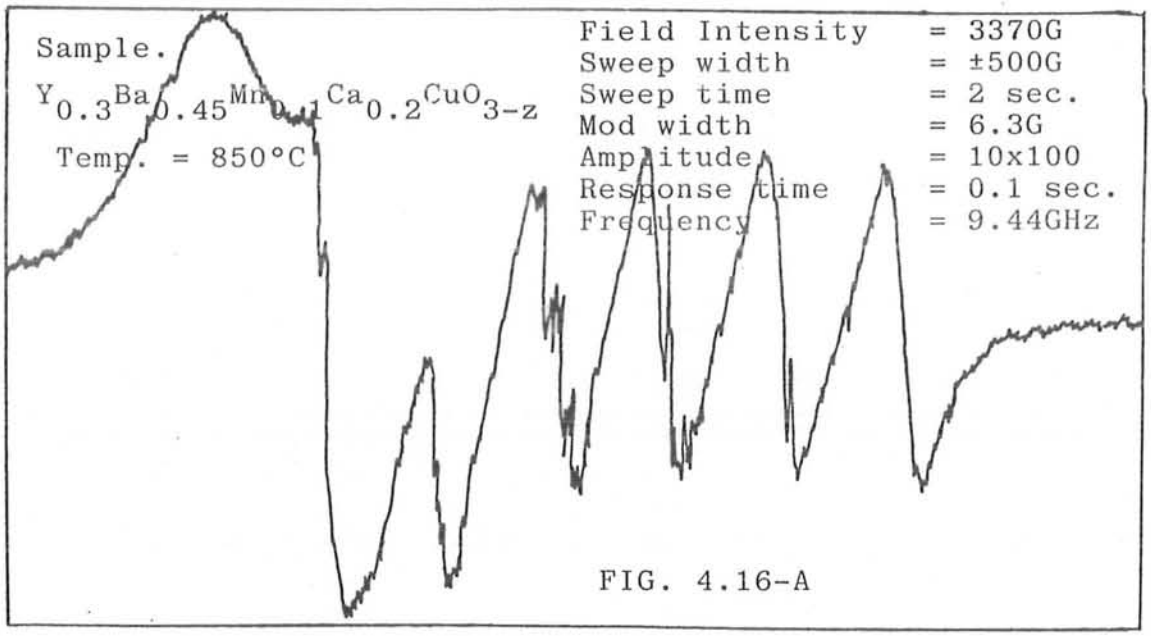

FIG. 4.16-A

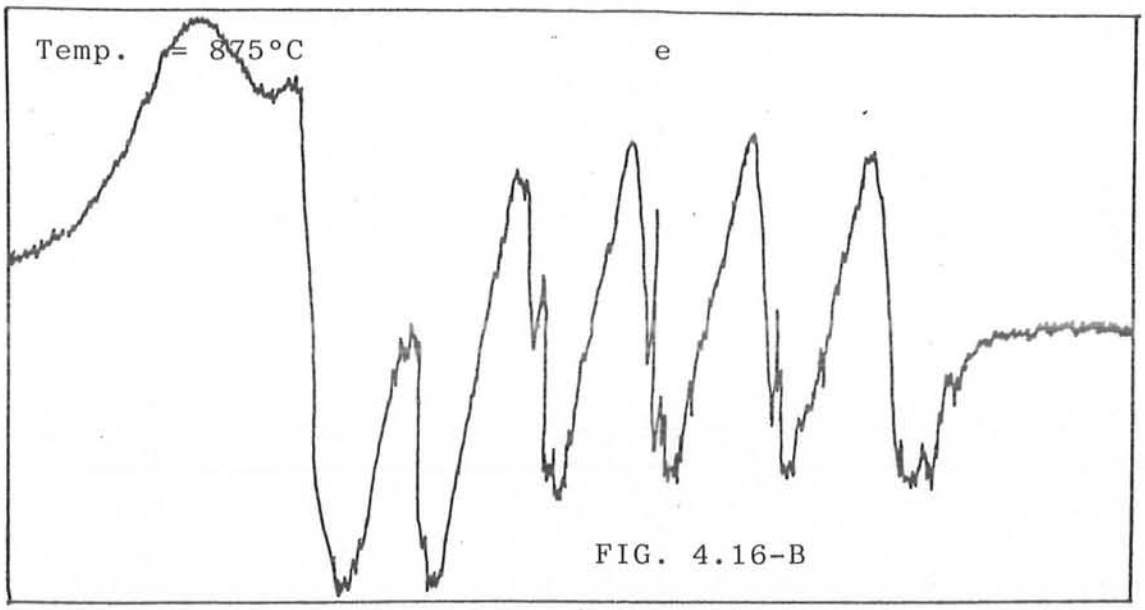

FIG. 4.16-B

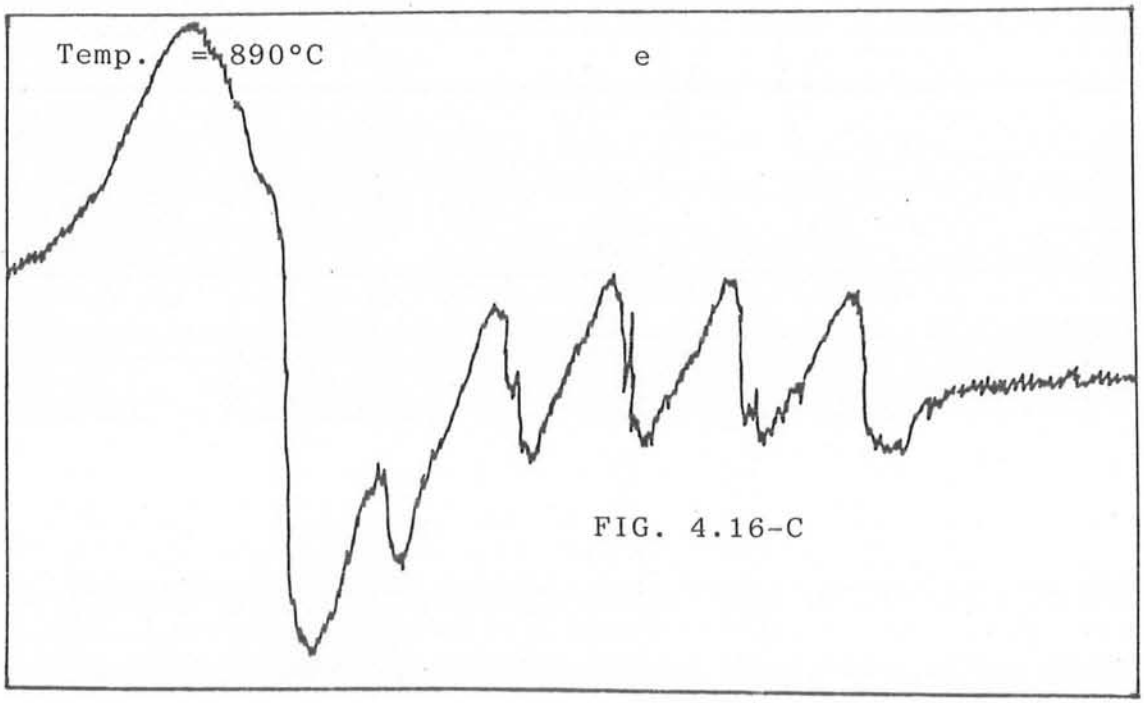

FIG. 4.16-C

e: same as above

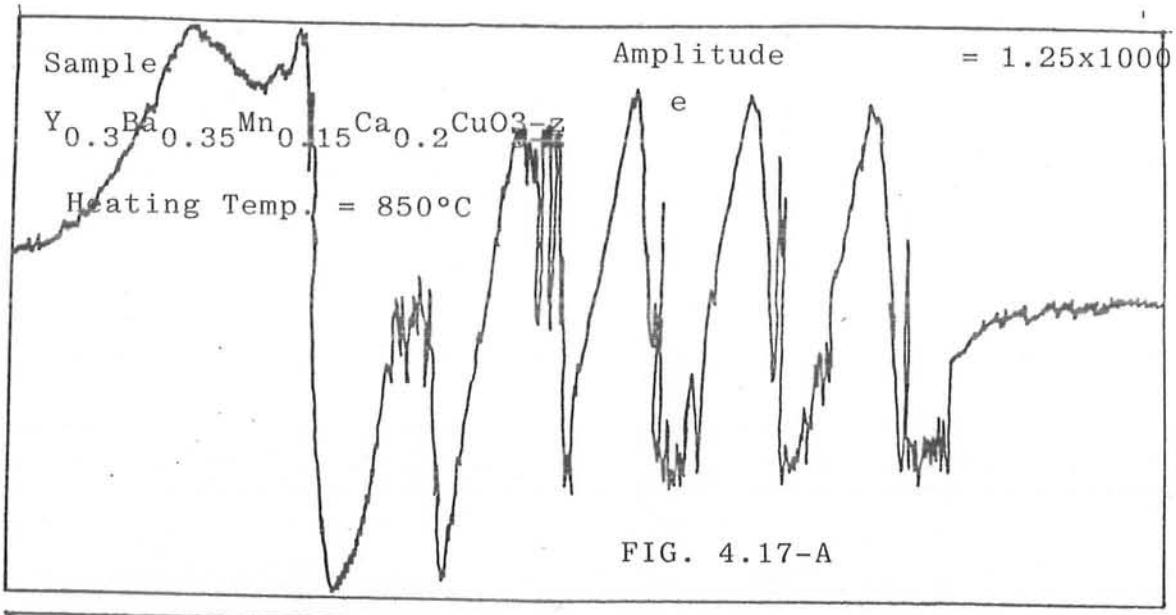

FIG. 4.17-A

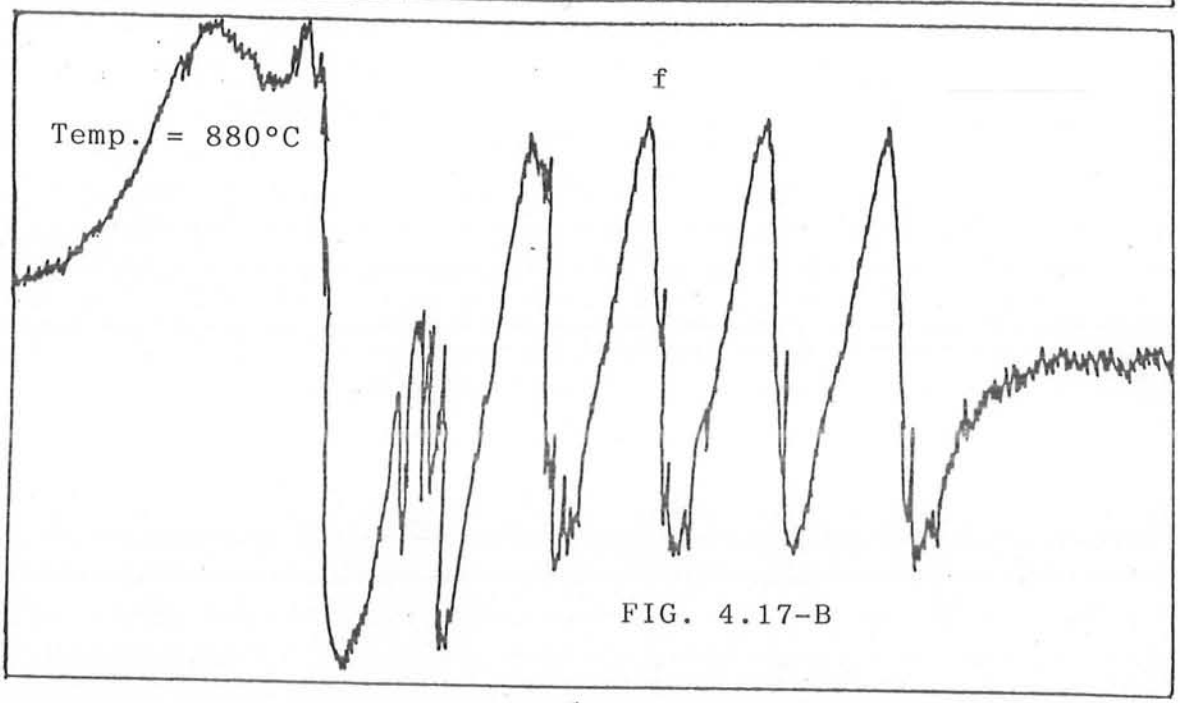

FIG. 4.17-B

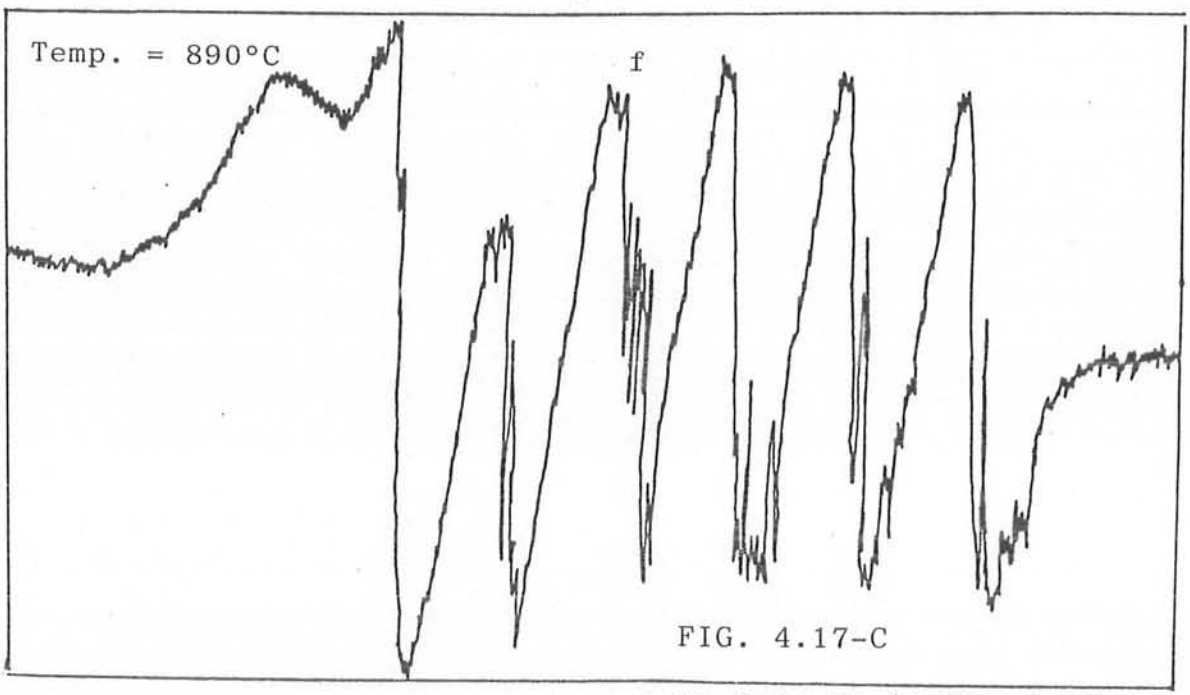

FIG. 4.17-C

e: same as in Fig.4.16-A
f: same as above.

REFERENCES

1. A.C. Rose Innes, E.H. Rhoderick, "Introduction to Superconductivity" Pergamon Press, 2nd Edition, Vol.6 (1987).
2. G. Chanin, E.A. Lynton and B. Serin, Phys, Rev. 114, 719 (1959).
3. B.T. Matthias, T.H. Geballe and V.B. Compton, Rev. Mod. Phys. 35, 1(1963).
4. Arai, Juichiro, Shimizu and Hajime, Physica C (Amsterdam) 162-164(Pt-II), 1295 (1989).
5. Tang, Weihua, Lin, Mingzhu, Meng and Xianren, Physica C (Amsterdam) 161(2), 257 (1989).
6. Xu, Youwen, Sabatini, R.L., Moodenbaugh, A.R., Zhu, Yimei, Shyu, S.G., Suenaga, M, Dennis, K.W., Mc Callum and R.W. Physica C (Amsterdam) 169(3-4), 205 (1990).
7. Imanaka, Nobuhito, Saito, Fumihiko, Imai, Hisao, Adachi and Gin Ya, Prog. High Temp. Supercond. 15, 73 (1989)
8. Ono, Akira, Uchida and Yoshishige, Jpn, J. Appl. Phys. Part 2, 29(4), L586 (1990).
9. Zhou, X.Y., Zhu, J.S., Zhang, H., Zhang and Q.R., Phys. Status Solidi A 123(1), K47(1991).
10. Muralidharan, P. Umadevi, Damodaran and A.D., Jpn. J. Appl. Phys. Part I, 30(2), 280 (1991).

11. T. Tsuneto, Prog. Theoret. Phys. 28, 857 (1962).

12. P.G. de Gennes et al., Phys. Condensed Matter 1, 176 (1963).

13. D. Markowitz and L.P. Kadanoff, Phys. Rev. 131, 563 (1963).

14. J.R. Schrieffer "Theory of Superconductivity" W.A. Benjamin Inc. (1964).

15. H. Shul and B.T. Matthias, Phys. Rev. 114, 977 (1959).

16. W Baltenspenger, Rev. Mod. Phys. 36, 157 (1964).

17. J.C. Phillips, Phys. Rev. Lett. 10, 96 (1963).

18. H. Suhl and D.R. Fredkin, Phys. Rev. Lett. 10(131), 268(1963).

19. A.A. Abrikosov and L.P. Gorkov, J. Exptl. Theoret. Phys. (USSR) 39, 1781 (1960).

20. F. Reif and M.A. Woolf, Phys. Rev. Lett. 9, 315 (1962).

21. J.G. Bednorz and K.A. Muller, Z. Phys. B64, 189 (1986).

22. A.W.B. Taylor "Superconductivity" Wykeham Publications (London) Ltd. (1970).

23. Ruth Jones, Peter P. Edwards, Martin R. Harrison, Thitinant Thanyasiri and Ekkehard Sinn., J. Am. Chem. Soc. 110, 6716 (1988).

24. P. Strobel, C. Paulsen and J.L. Tholence, Solid State Commun. 65(7), 585 (1988).

25. P. Umadevi Muralidharan, Phys. Stat. Sol. 123, 39 (1991).

26. Baldha, G.T., Jotania, R.B, Joshi, Pandya and Kulkarni, Solid State Commun. 71(10), 839(1989).

27. Yang, C.Y., Moodenbaugh, A.R., Wang, Xu, Youwen, Heald, S.M., Fischer and Kikland, Mater. Res. Soc. Symp. Proc. 169, 225 (1990).

28. Xu, Youwen, Moodenbaugh, A.R., Wang, Y.L., Suenaga, M., Sabatini and R.L., Mater. Res. Soc. Symp. Proc. 169, 221 (1990).

29. B.W. Veal, W.K. Kwok, A. Umezawa, G.W. Crabtree, J.D. Jorgensen, J.W. Downey, L.J. Nowicki, A.W. Mitchell, A.P. Paulikas and C.H. Sowers, Appl. Phys. Lett. 51(4), 279 (1987).

30. M. Mohammad, A.Y. Khan and Shahnaz Malik, J. Mater. Sci, Electronics 1, 209 (1990).

31. Sakov, D.M. Lipson, A.G., Saunin, E.I., Kuznetsov, V.A, Gromov, V.V., Toporov and Yu P., Zh. Fiz. Khim 65(5), 1214 (1991).

32. Rakvin B., Pozek, M., Dulcic and A., Springer. Ser. Solid. State. Sci. 99, 239 (1990).

33. Bur, Yakhtar, V.G., Loktev, V.M., Yablomskii and D.A., Fiz. Khim. Tekh. 2(1), 32 (1989).

34. Nagata, K. Saito, K., Egawa, Y., Liang R. Nakamura and T., J. Magn. Magn. Mater. 90-91, 649(1990).

35. Makarshin, L.L. Krivoruchko, O.P., Strpchenko, E.V., Luk' Yanova, O.V., Rudina, N.E., Moroz, E.M. and

Parmon, Sib. Khim. Zh. 2,43 (1991).

36. Kakihana et al., Phys. Mater. Sci. High. Temp. Supercond. 181, 581 (1991).

37. Hangyo M. Nakashima S., Nishiuchi M, Nii K and Mitsuishi, Solid State Commun. A67, 1171 (1988).

38. Akiro Moto, Akiharu Morimoto, Minoru Kumeda and Tatsuo Shimizu, Supercond. Sci. Technol 3, 579 (1990).

39. M.L. Cohen, Phys. Rev. 134, 511 (1964)

40. A 15 Compounds:-
"Conf. Proc. of low temperature Physics conference LT13" Editted by K.D. Timmerhans, W.J.O' Sullivan. E.F. Hammel, Plenum, New York. Vol. II, 3 (1974).

41. P.R. Wallace "Superconductinvity" Gordon and Breach, Science Publishers, New York. Vol.II (1969).

42. J.E. Crow and R.D. Parks, Phys. Lett. 21(4), 379 (1966).

43. Lynton, Serin and Zucker, J. Phys. Chem. Solids 3, 165 (1957).

44. A.A. Abrikosov and L.P. Gorkov, Soviet. Phys. JEPT 12(6), 1243 (1961).

45. Norman E. Philips and Matthias, Phys. Rev 137 (2A), 557A (1964).

46. Toshio Tsuzuki and Toshiko Tsumeto, Prog. Theor. Phys. 37(1), 1 (1967).

47. G. Roth, B. Renker, G. Heger, H. Hervieu, B. Domenges and R. Raveau, Z. Phys. B-condensed Matter 69, 53 (1987).

48. P.H. Hor., R.L. Meng, Y.Q. Wang, L. Gao, Z.J. H:uag, J Bechtold, K. Foster and C.W. Chu, Phys. Rev. Lett. 58(18), 1891 (1987).

49. M. Gasnier, M.O. O Ruault and Coworkers, Solid State Commun. 71 (6), 485 (1989).

50. Masaki, Kanai, Tamayi Kawai and Shichic Kawai, Appl Phys. Lett. 57(2), 198 (1990).

51. D.E. Moris, P. Narwanker, A.P.B. Sinha, K. Takano, B. Fayn and V.T. Shum, Phy. Rev. B 41(7), 4118 (1990).

52. Akira ONO and Uchida, Jpn. J. Appl. Phys. 29 (4), L586 (1990).

53. I. Felner and I. Nowik,, Phy. Rev. B 36 (7), 3923 (1987).

54. M. Mehbod and P. Wyder Phys. Rev. B-36(16), 8819 (1987).

55. C.Y. Yang, Y.L. Wang and their Coworkers, Phys. Rev. B24(4), 2231 (1990).

56. S. Gama, Lima and Tarriani, IEEE Trans, Magn. 25(2), 2307 (1989).

57. Takeyuki Suzuki, Tsuneto, Yamazaki, Ryuuta Sekine, Akinori Koukitu and Hisasi Seki, J. Mater. Sci. Lett. 8, 1271 (1989).

58. T. Bjornholna, T.K. Schuller, EArly and Maple, Phys. Rev B. 41(16), 11154 (1990).

59. Salamat Ali, M.Phil Thesis, Q.A.U. Islamabad (1990).

60. P.J. Wheatley "The determination of Molecular Structure" 2nd Edition, Oxford University Press, Ely House London W-1 (1968).

61. Mohammad Nasir Khan, M.Phil Thesis, Q.A.U. Islamabad (1990).

62. J.M. Tarascon, W.R. Mc Kinnow, L.H. Greene, G.W. Hull and E.M. Vogel, Phys. Rev. B. 36(1), 226 (1987).

63. R.F. Jardim, S. Gama, O.F. de Lima and I Thoriana, IEEE Trans. Magn. 25(2), 2307 (1989).

64. R.J. Cava, B. Batlog, R.B. Van Dover, D.W. Murphy and their coworkers, Phys. Rev. Lett. 58 (16), 1676 (1987).

65. Y. Khan et al. J. Mater Sci. 7, 321 (1988).

66. J.E. Wertz and James R. Bolton "Electron Spin Resonance Elementary Theory and Practical Applications" Ist Edition, Published in Great Britain by Chapman and Hall (1986).

67. JEOL ESR Manual, Chemistry Department, Q.A.U. Islamabad.

68. Malcolm Bersohn and James C. Baird "An Introduction to Electron Paramagnetic Resonance" W.A. Benjamin Inc. (1966).

69. Alexander J. Shuskus, Phys. Rev. 127(5), 1529 (1962).

70. Raymond S. Alger " Electron Paramagnetic Resonance, Techniques and Applications" Interscience Publishers (1968).